GEOHYDROLOGY, AQUEOUS GEOCHEMISTRY, AND THERMAL REGIME OF THE SODA LAKES AND UPSAL HOGBACK GEOTHERMAL SYSTEMS, CHURCHILL COUNTY, NEVADA

By F. H. Olmsted, Alan H. Welch, A. S. VanDenburgh, and S. E. Ingebritsen

---

U. S. GEOLOGICAL SURVEY

Water Resources Investigations Report 84-4054

Menlo Park, California

1984

CONTENTS

CONTENTS (Continued)

CONTENTS (Continued)

ILLUSTRATIONS

ILLUSTRATIONS (Continued)

TABLES

TABLES (Continued)

TABLES (Continued)

CONVERSION FACTORS AND ABBREVIATIONS

The metric system is used throughout this report, although some of the original measurements and data were reported in inch-pound units. Thermal parameters are given in the more familiar "working units" rather than in the now-standard International System of Units (SI). The table below lists metric and equivalent SI units for thermal properties, conversion factors for permeability units in common usage, temperature conversion for degrees Celsius to degrees Fahreheit, and water-quality units of measure used in this report.

Multiply metric units	By	To obtain inch-pound units
	Length	
millimeter (mm)	3.937×10^{-2}	inch (in)
meter (m)	3.281	foot (ft)
kilometer (km)	0.6214	mile (mi)
	Area	
square centimeter (cm^2)	0.1550	square inch (in^2)
square meter (m^2)	10.76	square foot (ft^2)
hectare (ha)	2.471	acre
square kilometer (km^2)	247.1	acre
	0.3861	square mile (mi^2)

Multiply metric units	By	To obtain inch-pound units
	Volume	
cubic centimeter (cm^2)	6.102×10^{-2}	cubic inch (in^3)
liter (L)	.2646	gallon (gal)
	3.531×10^{-2}	cubic foot (ft^3)
cubic meter (m^3)	35.31	cubic foot (ft^3)
	8.107×10^{-4}	acre foot (acre-ftt)
cubic hectometer (hm^3)	8.107×10^{2}	acre foot (acre-ft)
cubic kilometer (km^3)	.2399	cubic mile (mi^3)
	Fluid flow	
liter per second (L/s)	15.85	gallon per minute (gal/min)
	25.58	acre-foot per year (acre-ft/a)
cubic hectometer per year (hm^3/a)	8.107×10^{2}	acre-foot per year (acre-ft/a)
kilogram per second (kg/s)	7.938×10^{3}	pound per hour (lb/h)
	Mass	
gram (g)	3.528×10^{-2}	ounce (oz)
kilogram (kg)	2.205	pound (lb)

Multiply metric units	By	To obtain inch-pound units
Density		
gram per cubic centimeter (g/cm^3)	62.43	pound per cubic foot (lb/ft^3)

Thermal parameters		
Multiply "working units"	**By**	**To obtain SI units**
thermal-conductivity unit (tcu) (1 tcu = 1 10^{-3}mcal/cm x s x °C)	418.4	milliwatt per meter degree kelvin (mW/m x K)
calorie per gram per degree Celsius (cal/g °C)	4.184	joule per gram kelvin (J/g x K)
heat-flow unit (hfu) (hfu = 1μcal/cm^2 s)	41.84	milliwatt per square meter second (mW/m^2 x s)
calorie (cal)	4.184	joule (J)
calorie per second (cal/s)/	4.184	watt (W)

Conversion factors for permeability units in common usage are shown in the chart below.

PERMEABILITY

10^{-3} μm^2 / 10^{-15} m^2	millidarcy	[H_2O at 60°F (15.6°C)] Meinzer unit (gal/d ft^2)	ft/d	m/d
one	1.013	1.848×10^{-2}	2.471×10^{-3}	7.531×10^{-4}
0.987	one	1.824×10^{-2}	2.438×10^{-3}	1.432×10^{-4}
54.11	54.82	one	1.337×10^{-1}	4.075×10^{-2}
4.047×10^{2}	1.345×10^{3}	7.480	one	.3048
1.328×10^{3}	1.345×10^{3}	24.54	3.281	one

For temperature, degree Celsius (°C) is converted to degree Fahrenheit (°F) by the formula,

$$°F = [(1.8)(°C)] + 32$$

Water-quality units of measure used in this report are as follows: Concentrations of dissolved constituents are given in milligrams per liter (mg/L) and micrograms per liter (g/L), which are equivalent to parts per million (ppm) and parts per billion (ppb) for dissolved-solids concentrations less than about 7,000 mg/L. Specific conductance is given in micromhos per centimeter at 25°C (micromhos).

National Geodetic Vertical Datum of 1929 (NGVD of 1929): A geodetic datum derived from a general adjustment of the first-order level nets of both the United States and Canada, formerly called "Mean Sea Level." NGVD of 1929 is referred to as "sea level" in this report.

GEOHYDROLOGY, AQUEOUS GEOCHEMISTRY, AND THERMAL REGIME OF THE SODA LAKES AND UPSAL HOGBACK GEOTHERMAL SYSTEMS, CHURCHILL COUNTY, NEVADA

By F. H. Olmsted, Alan H. Welch, A. S. VanDenburgh, and S. E. Ingebritsen

ABSTRACT

The adjacent Soda Lakes and Upsal Hogback geothermal areas are in the west-central Carson Desert, about 100 kilometers east of Reno, Nev. Both areas represent the discharge parts of hydrothermal-convection systems in which rising thermal fluid is swept northeastward and northward in the direction of lateral ground-water flow within the uppermost 250 meters of nonmarine basin-fill sediments and, at Upsal Hogback, interbedded basalt flows, rather than emerging at land surface as thermal springflow.

The Soda Lakes thermal anomaly is strongly asymmetrical and elongated toward the northeast. Its hottest parts, near the southwest margin, probably coincide with the intersection of faults that trend north-northeast and northwest. The faults provide steeply inclined conduits for thermal fluids that may rise from depths of 3 to 7 kilometers within fractured Tertiary and (or) pre-Tertiary rocks. Some thermal fluid ascends to within about 20 meters of the land surface in the hottest parts of the anomaly, where near-surface heat flows exceed 300 heat-flow units. The Upsal Hogback anomaly is less asymmetrical than the Soda Lakes anomaly and is elongated toward the north rather than the northeast. Its hottest part appears to overlie a north-trending buried bedrock ridge where thermal fluid rises to a depth of about 245 meters, then moves laterally within a basalt flow dated at 4.5 million years by the potassium-argon method. Maximum near-surface heat flow within the anomaly is about 12 heat-flow units.

The dissolved-solids concentrations of undiluted thermal water in the Soda Lakes and Upsal Hogback systems are, respectively, about 4,000 and 6,500 milligrams per liter, dominated by sodium and chloride. These characteristics, along with stable-isotope data, suggest that the source of recharge to each hydrothermal system is ground water that (1) was subjected to considerable evaporation prior to deep percolation and (2) underwent only minor chemical modification--principally cation exchange and and an increase in silica concentration, but limited net transfer of mass to the aqueous phase--within the thermal aquifer.

Maximum temperatures measured within the Soda Lakes and Upsal Hogback

systems are respectively 199° and 78°C, at depths of 610 and 245 meters. Geothermometer calculations suggest reservoir temperatures of 186°-209°C and 120°C for the two systems.

Throughout the study area, most shallow ground water (less than 50 meters below the water table) having a temperature in excess of 20°C exhibits the geochemical imprint of one or more of the following processes, all of which post-date thermal upflow: Mixing of thermal and nonthermal water, conductive heating, steam loss, evaporation, and, near the Soda Lakes, acquisition of sulfate of apparently volcanic origin.

Total area occupied by the Soda Lakes system is estimated to be 370 to 640 square kilometers; the depth of circulation of thermal fluid, 3 to 7 kilometers; and the total volume, 1,100 to 3,800 cubic kilometers. The volume of the system above a depth of 3 kilometers having temperatures equal to or greater than 150°C is estimated to be 81 ± 24 cubic kilometers of which 3.4 ± 1.2 cubic kilometers represents effective pore space. The total heat content or reservoir thermal energy above 3 kilometers depth is estimated to be 7.0×10^{18} calories. Upflow of thermal water from the deep part of the system is estimated to be on the order of 1 million cubic meters per year, or 27 kilograms per second, which represents a heat discharge of 5.3 megacalories per second. Assuming steady-state conditions and once-through piston or displacement flow, the estimated period of circulation of thermal fluid through the system probably is within the range of 3,400 to 34,000 years.

The Upsal Hogback system occupies a total area of 140 to 230 square kilometers, and thermal water is known to circulate at a depth of 245 meters beneath the hottest part of the near-surface thermal anomaly. Upflow of 80°C water to a depth of 245 meters is estimated to be about 830,000 cubic meters per year, or 26 kilograms per second, which represents a heat discharge of 1.7 megacalories per second. Age of this water is about 25,000-35,000 years on the basis of a radiocarbon determination. Other features of the system are unknown because of the absence of test drilling below a depth of about 300 meters.

INTRODUCTION

Purpose of Present Study

This report summarizes the results of several years of intermittent field studies of two geothermal systems that were included in an earlier reconnaissance of selected hydrothermal systems in northern and central Nevada (Olmsted and others, 1975). The general objectives of the present study were to (1) describe the geology and hydrology of two geothermal systems in the western Carson Desert; (2) use information obtained from shallow drilling to provide semi-quantitative estimates of the pre-development flux of heat and fluid through the systems; and (3) incorporate available geophysical, geochemical, and deep and shallow drilling information into conceptual models of the systems. Much of the information used to accomplish the third objective was collected or became available since the report of Olmsted and others (1975). The present study uses analytical rather than digital-modeling techniques to accomplish the stated objectives. Although the present report represents a refinement of the earlier report by Olmsted and others (1975), the more recently obtained information permits a greater degree of confidence to be placed in the present models of the systems.

In essence, therefore, the present study represents an improvement and refinement of a part of the reconnaissance studies by Olmsted and others (1975). However, as in the earlier studies, the nature and configuration of the presumed deep geothermal reservoir remain largely speculative, although data recently made available from deep drilling and geophysical exploration by private industry (references UURI) permit more reasonable inferences about these features.

Regional Setting

The study area is in the west-central Carson Desert, about 100 km east of Reno, Nevada (fig. 1). The Carson Desert, an egg-shaped area 120 km long in a northeast direction by as much as 50 km wide, is the largest intermontane basin in Nevada. The Carson Sink in the northeastern part of the basin is barren, largely salt-encrusted, and nearly level. The surrounding lowlands consist of sparsely vegetated sand dunes, sandy plains, and clay flats with local relief of as much as 15 m. Present topography in large part is the result of wind scour since the final dessication of Lake Lahontan, a large intermontane

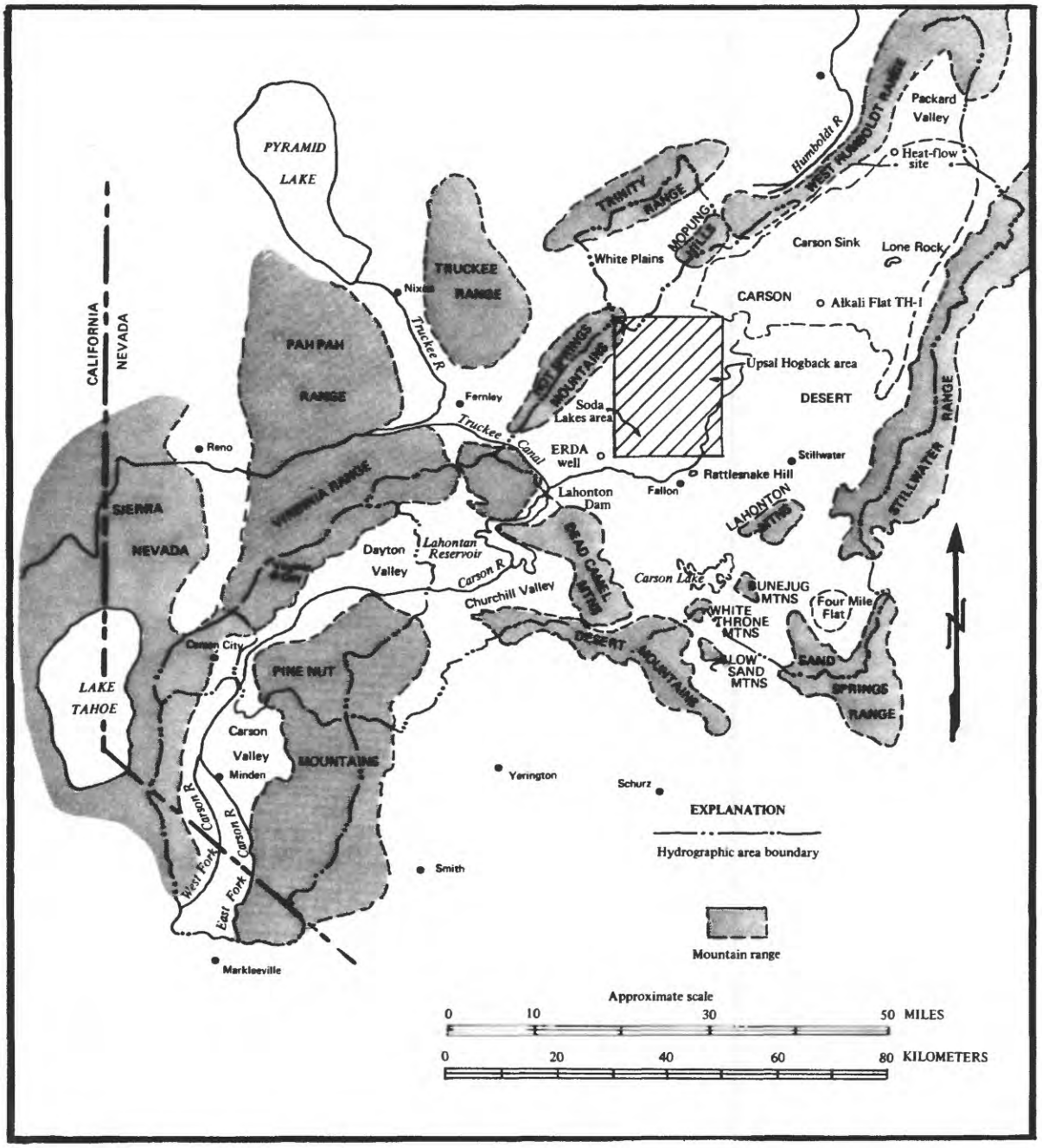

Figure 1. -- Location of the Soda Lakes and Upsal Hogback geothermal areas, in west-central Nevada.

lake that intermittently occupied much of northwestern Nevada during cooler and wetter stages of the late Pleistocene and early Holocene (Morrison, 1964). The Carson Desert is one of the deepest of the Lake Lahontan basins; the lowest part of Carson Sink, at an altitude of about 1,172 m above sea level, lies 160 m below the highest level reached by the lake.

Only deposits of Lake Lahontan and post-Lahontan age are exposed extensively on the basin floor. The basin is the terminal sink of the Carson and Humboldt Rivers, and, like the terminal basins of other large Great Basin rivers, it preserves a nearly complete sedimentary record of much of Quaternary time because no sediment is removed by exterior drainage.

The Carson Desert is rimmed for the most part by low, barren mountains. The highest range, the Stillwater Range on the east margin of the basin, reaches a maximum altitude of 2,679 m at Job Peak, about 1,500 m above the lowest part of the basin floor. The mountain ranges are composed of consolidated igneous, sedimentary, and metamorphic rocks ranging in age from Triassic to Quaternary (Willden and Speed, 1974). Similar rocks probably underlie the unconsolidated basin fill and young basaltic rock units of the basin floor.

Hot springs are absent in the Carson Desert, but there are other kinds of evidence of geothermal-resource potential within the basin. Basaltic rocks of Quaternary or probable Quaternary age occur at Lone Rock 58 km northeast of Fallon in the northeastern part of the Carson Sink, at Rattlesnake Hill 2 to 3 km northeast of Fallon, at Soda Lakes 10 to 12 km northwest of Fallon, and at Upsal Hogback 17 to 21 km north of Fallon. Lone Rock may be the remnant of a plug or neck (Garside and Schilling, 1979, p. 14); its age has not yet been established by radiometric dating. Rattlesnake Hill consists of a series of flows surrounding a central core of vent agglomerate (Morrison, 1964, p. 23). One of the flows has been dated by the potassium-argon method at 1.03$\pm$.05 m.y. (Evans, 1980, p. 20). Soda Lakes and Upsal Hogback both are much younger than Lone Rock and Rattlesnake Hill and are of explosive rather than flow or shallow-intrusive origin. Their nature and origin are discussed in a later section (p. 20).

Apart from Soda Lakes and Upsal Hogback, the only surface manifestation of hydrothermal activity within the last 30,000 years in the Carson Desert consists of a small tract of hydrothermally altered sand and clay and a few intermittently active fumarolic vents surrounding an old well that encountered steam and

boiling water at a depth of about 18 m (Morrison, 1964, p. 117; Garside and Schilling, 1979, p. 9). The site is 4 km north-northeast of Big Soda Lake and is the hottest near-surface part of the Soda Lakes geothermal area.

As established by shallow test drilling during this and earlier studies, the Soda Lakes geothermal area lies chiefly northeast of the old "steam" well, between Soda Lakes and Upsal Hogback; the Upsal Hogback geothermal area is largely east and north of the Hogback. Both thermal anomalies result from the convective upflow of hot water from depth into aquifers at shallow to moderate depths (20-245 m). A similar "hidden" hydrothermal convection system immediately north of the small community of Stillwater in the eastern Carson Desert has been described by Olmsted and others (1975, p. 87-98) and Morgan (1982). Future test drilling and geophysical exploration may confirm the presence of other such systems in the Carson Desert.

Climate and Vegetation

Lying in the rain shadow of the Sierra Nevada 100-150 km to west, the Carson Desert has a climate characterized by aridity and extremes of temperature, both diurnal and seasonal. Precipitation averages about 100 mm or less annually on Carson Sink and the immediately adjacent lowlands (Hardman, 1965). Average monthly temperature ranges from about 0°C in January to 23°C in July (National Oceanic and Atmospheric Administration, 1975). Native vegetation is sparse, consisting of perennial shrubs, many of which are phreatophytes, and annuals and grasses that grow in the spring. Irrigated crops, chiefly alfalfa, hay, and some grains, have been grown near Fallon and Stillwater since the early 1900's.

Previous Studies

Sources of data pertaining to the evaluation of the geothermal resources of Carson Desert were included in a tabulation by Olmsted and others (1973, p. 10-13) and are not listed here. Specific references to some of these sources are made later in this report. More recent papers on the geology, hydrology, and geophysics of the study area include Olmsted and others, (1975, p. 77-86; already alluded to), Glancy and Katzer (1975), Stanley and others (1976), Olmsted (1977), Evans (1980), and Stark and others (1980). Additional data are

available from open-file releases by the University of Utah Research Institute (UURI) [1979 a through k].

An earlier report by Olmsted and others (1975) summarized the information available at that time and presented a conceptual model for the geothermal system in the Soda Lakes area. Further work by Olmsted (1977) provided a more detailed study of the near-surface temperatures, allowing further definition of the extent of the thermal anomalies. The geologic structure has been studied using a variety of geophysical techniques, including gravity (UURI, 1979k), magnetic (UURI, 1979k), seismic (UURI, 1979d and e) and electrical (Stanley and others, 1976; UURI, 1979a-c; and Stark and others, 1980). Lithologic and temperature logs have also become available (UURI, 1979f-j). The data presented in these studies is discussed further in the appropriate sections of this report.

Methods of Investigation

The present study involved (1) the collection and analysis of existing data, (2) hydrogeologic mapping, (3) test drilling, (4) borehole geophysical logging of test wells, (5) measurements of temperature and temperature gradient, (6) water-level measurements, (7) description and analysis of lithologic samples from test wells, and (8) chemical analysis of water samples from test wells. Most of these methods were described in some detail by Olmsted and others (1975, p. 27-46). Instead of repeating all this material, the present discussion focuses on changes in and additions to the techniques described in the earlier report.

Existing data included the information summarized in the section "Previous Investigations". The open-file releases by the University of Utah Research Institute (1979a through j) were especially helpful in the later stages of the study. Much information, however, is of a proprietary nature and is still held in files of the energy-development companies that have prospected the area.

Hydrogeologic mapping consisted of the mapping of vegetation and soils by P. A. Glancy (written commun., 1979) of the Carson City office of the Geological Survey. Emphasis was placed on the identification of phreatophytes and the assessment of their density and vigor so as to provide estimates of ground-water evapotranspiration in the two geothermal areas.

Test drilling utilized the methods summarized by Olmsted and others (1975, p. 28-31), but with a few important differences.

First, shallow wells were installed at most of the sites at which deeper wells had been drilled in order to determine the position of the water table and to measure the vertical component of the hydraulic gradient. Some of these wells were finished with steel pipes fitted at the bottom with well-point screens like the earlier wells, but the rest were completed instead with polyvinyl chloride (PVC) casings of 51 mm inside diameter with slots cut near the bottom. Some of the deeper wells also were completed with PVC casings. At some sites, as many as four wells ultimately were installed in order to determine differences in water chemistry and vertical component of the hydraulic gradient between different depth zones.

Second, most of the later wells, particularly those in the lower-lying parts of the Upsal Hogback area, were completed by filling the annulus between the casing and the drill-hole walls with cement grout instead of the drill cuttings and surface material used in the earlier wells. This procedure minimized the possibility for upward or downward flow of water in the annulus and thereby assured more reliable measurements of temperature gradient and hydraulic head than were obtained in the earlier wells. Most of the cemented wells originally were fitted with steel caps at the bottom and filled with water to permit temperature measurements. In the later stages of the study, these capped wells were perforated near the bottom with explosive charges lowered on a wire, in order to open the well to aquifers for the purpose of obtaining water samples or water-level data, or both.

Finally, four of the later wells (Bureau of Reclamation wells 13B, 13C and 14A and Geological Survey well 64A) were drilled and completed to depths substantially greater than the 45-m limit for the other test wells, including those drilled for the earlier study (Olmsted and others, 1975, table 4). Bureau of Reclamation wells 13B and 14A in the Soda Lakes area were drilled and completed to a depth of about 150 m, and Geological Survey well 64A in the Upsal Hogback area was drilled and cased to a depth of about 305 m. All these wells provided exceedingly valuable information about the deeper subsurface temperature regime, geology, water chemistry, and hydraulic heads.

All the types of borehole geophysical logs described by Olmsted and others (1975, p. 32-36) were made in the later wells drilled in this study. Particular

emphasis was placed on the use of the gamma-gamma (density) and neutron (water-content) logs in interpreting lithology. Many lithologic logs of earlier wells were reinterpreted, using semi-quantitative analysis of these logs which permitted a more detailed and accurate analysis of the materials penetrated, especially with regard to their hydrologic properties.

Measurements of temperature and temperature gradient were made as described by Olmsted and others (1975, p. 37-39). In addition to the earlier temperature surveys at 1-m depth in the Soda Lakes area (Olmsted and others, 1975, p. 38), similar surveys were made of the Upsal Hogback geothermal area, as reported by Olmsted (1977). Measurements at 1 m were continued at four sites in the Soda Lakes area and at an increasing number of sites in the Upsal Hogback area. Ultimately, 40 sites were measured in the latter area, and mean-annual temperature at 1-m depth for 1977 was estimated for all these sites and, by correlation methods, for many of the earlier sites in the Soda Lakes area. All these data were used, together with bottom-hole temperatures in the deepest test wells at the same sites, to develop a more accurate estimate of near-surface conductive heat flow than was made by Olmsted and others (1975, p. 66-67), using a similar method.

Water-level measurements by the wetted-tape method were made in all the test wells at 6-month intervals from December 1973 to December 1979 and in many wells at more frequent intervals up to the spring of 1982. In the late stages of the study, beginning in the fall of 1981, hydraulic-head measurements were made with a pressure gage in the wells where water levels were above the top of the casing (the wells flow when uncapped).

Analysis of cores taken from test wells included (1) general classification and lithologic description, (2) mineral and clay-mineral identification by X-ray diffraction, (3) carbonate content by CO_2-absorbtion method, (4) particle-size distribution, (5) pore-size distribution, (6) vertical hydraulic conductivity, (7) thermal conductivity, (8) bulk density, and (9) grain density. In addition potassium-argon data were obtained for three samples of basaltic and andesitic rock from well 64A by E. H. McKee (written commun., 1981). Thermal conductivity was measured with needle-probe apparatus by Robert H. Munroe (written commun., 1973-78); and with steady-state comparator (divided-bar) apparatus by W. H. Somerton (written commun., 1978); the other analyses were made by the Hydrologic Laboratory of the U.S. Geological Survey, Lakewood,

Colorado.

The gathering of geochemical data consisted of the analysis of selected unstable constituents and properties in the field along with the collection of water samples that were sent to laboratories for analysis. Prior to sampling, each Geological Survey well was pumped or bailed several times over a period of several months. During the pumping and bailing effort, the volume of water removed was recorded and samples were collected for specific-conductance determination. These data were used to evaluate whether the water quality was reasonably constant after at least several well-bore volumes of water had been removed. Final sampling for laboratory analysis occurred only after the specific conductance in several successive samples was found to be virtually constant. Final samples were collected by bailing the wells.

Chevron Resources Co. well 1-29 was sampled during a flow test at the well. The sample was obtained from a side port on the discharge pipe. The water was routed through copper tubing immersed in cold water to condense the water vapor prior to sampling.

Field determinations were made of pH and alkalinity on all samples analyzed in 1978 and 1980 using the methods of Wood (1976, p. 12-18). The water was filtered through a 0.45-μm pore-size membrane (142-mm diameter) with acidification of samples collected for cation analysis. Unacidified, filtered samples were collected for anion and isotopic analysis. Samples for silica analysis were diluted with distilled water to prevent polymerization where oversaturation with respect to quartz was indicated by a preliminary field measurement of silica. All samples collected for chemical analysis were placed in plastic bottles that had been washed with acid. Glass bottles were used on samples collected for isotopic analysis.

Acknowledgments

This report benefitted from comments and suggestions by James R. Harrill, Robert H. Mariner, and John H. Sass. Assistance in various phases of the field studies was provided by Alan M. Preissler, F. E. Rush, Patrick A. Glancy and Rita L. Carman.

GEOLOGY

Stratigraphy

Rocks and deposits exposed in the Carson Desert range in age from Triassic to Holocene (Willden and Speed, 1974, pl. 1). Only deposits of late Quaternary age are exposed within the study area, except for a small area of Tertiary volcanic rocks in the eastern Hot Springs Mountains (pl. 1). Older rocks and deposits similar to those in the surrounding mountains have been penetrated by drilling, however. A nearly complete sequence was described by Horton (1978, Appendix A) from the ERDA Lahontan No. 1 well near the southwest corner of sec. 16, T. 19 N., R. 27 E., about 6 km southwest of Big Soda Lake. (See fig. 2.) A similar section was penetrated by Chevron Resources Soda Lake well 44-5 (pl. 1), 9 km northeast of the ERDA well. (See Sibbett, 1979, pl. 1).

Firm correlations of subsurface and exposed units are not possible on the basis of present information: The stratigraphic interpretations made herein and shown in figure 2 must therefore be regarded as tentative. A substantially different interpretation was made by Sibbett (1979, pl. 1) and Sibbett and Blackett (1982), as will be discussed in the following pages.

Pre-Tertiary Rocks

Pre-Tertiary rocks include chiefly clastic sedimentary rocks and minor carbonate and volcanic rocks of Triassic and Jurassic age exposed in the Stillwater and West Humboldt Ranges and plutonic rocks of Jurassic and Cretaceous age exposed in the Hot Springs Mountains as well as in the other two ranges just mentioned (Willden and Speed, 1974). In the subsurface, the dacite porphyry below a depth of 2,369 m in the ERDA Lahontan No. 1 well may be pre-Tertiary (Horton, 1978, pl. 1); alternatively, the top of the pre-Tertiary section may be at a depth of 2,554 m, where rocks described by Horton as meta-andesite and granite porphyry were encountered (see fig. 2) Sibbett and Blackett (1982, p. 8), on the other hand, suggested that the dacite porphyry in Lahontan No. 1 could be part of the Truckee Formation of Tertiary age; according to this interpretation, pre-Tertiary rocks probably were not penetrated by the Lahontan No. 1 well and presumably lie at much greater depths than those yet penetrated by any drill holes in the western Carson Desert.

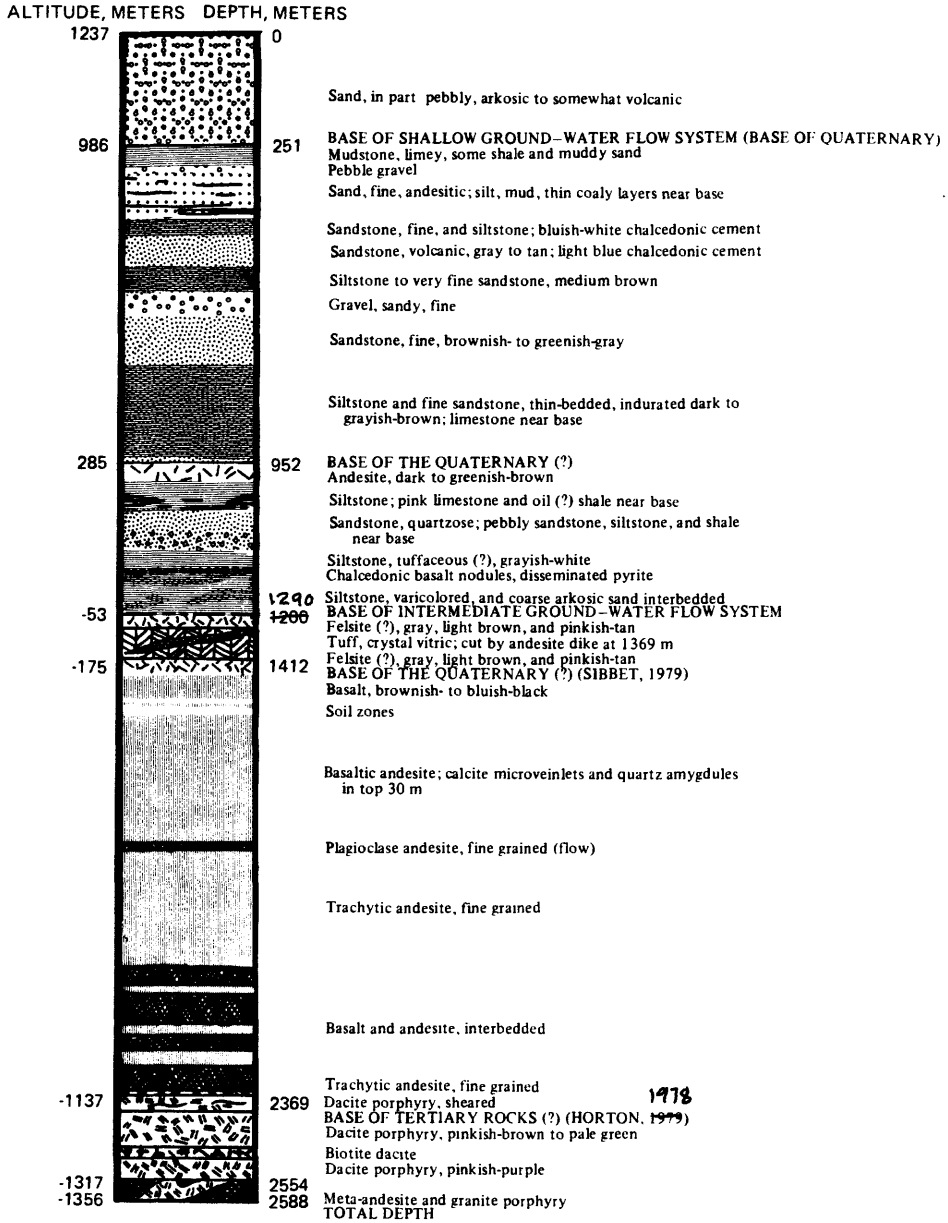

Figure 2. -- Generalized columnar section of rocks and deposits penetrated by by ERDA Lahontan No. 1 test well.

Tertiary System

The Tertiary rocks of the southern Carson Desert were assigned to five major rock-stratigraphic units by Morrison (1964) on the basis of field studies in the Carson Lake quadrangle and the eastern Desert Mountains. Rocks of similar age in the Hot Springs Mountains were assigned to eight map units in a reconnaissance by Voegtly (1981). Table 1 presents a summary of all these units and their inferred correlation.

Radiometric dating of volcanic rocks in the region suggests that some of the age assignments by Morrison (1964) may require modification. Evans (1980, p. 70) reported a potassium-argon age of 6.96±0.42 m.y. (whole-rock) for a basalt sample from the Carson Desert. According to Evans (oral commun., 1982), the sample came from the Dead Camel Mountains, about 19 km southwest of Soda Lakes, and was interpreted to be correlative with the Bunejug Formation, as mapped by Morrison (1964) in the Carson Lake quadrangle to the east. If the inferred correlation is correct, the Bunejug Formation would be, at least in part, of late Miocene age, rather than the Pliocene and Pleistocene age assigned by Morrison (1964), and the age of the underlying Truckee Formation presumably would be Miocene rather than Miocene and Pliocene.

In the absence of radiometric dates and sequences of rock types that can be clearly related to those mapped by Morrison (1964) and Voegtly (1981), the age and stratigraphic assignment of the rocks penetrated by the ERDA Lahontan No. 1 well (fig. 2) are unknown. Sibbett (1979, pl. 1) placed the top of the Bunejug Formation at the top of a basalt sequence at a depth of about 1,400 m in the Chevron Resources Soda Lake 44-5 well (which corresponds to a depth of 1,412 m in the Lahontan No. 1 well--fig. 2) and assumed that all the overlying rocks and deposits (chiefly sedimentary) were Quaternary. However, Sibbett's interpretation apparently was based on an assumed Pliocene and Pleistocene age of the Bunejug; if in fact the Bunejug is much older, then the top of the Tertiary system must be at a much shallower depth in those wells.

Although not penetrated in the ERDA Lahontan No. 1 well, intercepts of basalt or "basaltic crystal ash" were penetrated at depths of 430-600 m in Chevron Resources Co. Soda Lakes wells 44-5, 1-29, 11-33 and 63-33 (Sibbett, 1979, pl. 1). Sibbett described the basalt intercepts as dikes which presumably intrude the Quaternary deposits. An alternative interpretation, however, is that the basalt intercepts represent flows or perhaps sills rather than dikes:

Table 1. -- Major rock stratigraphic units in the southern Carson Desert and Hot Springs Mountains, western Carson Desert. [Modified from Morrison (1964) and Voegtly (1981)].

Southern Carson Desert				Hot Springs Mountains and western Carson Desert	
Period	Epoch	Unit and description	Maximum exposed thickness (m)	Unit and description	Maximum exposed thickness (m)
Quaternary	Holocene	Fallon Formation: Post-Lake Lahontan lacustrine and subaerial sediments	11	Hot-Spring sinter Wind-blown sand Alluvium Deposits of Soda Lakes Deposits of Upsal Hogback	70
	Pleistocene	Lahontan Valley Group: lacustrine and subaerial sediments	100		
		Paiute Formation: Fangravel and colluvium	12		
		Basalt of Rattlesnake Hill: Flows and agglomerate. Age 1.03 ± .05 m.y.(Evans, 1980)	60		
		////// Unconformity ? ///////			
		Pre-Lake Lahontan lacustrine sediments	6		
	?	/////// Unconformity ? /////		//////Unconformity///////	
Tertiary	Pliocene	Bunejug Formation: Basaltic flows and tuff in upper part, andesitic to basaltic flows in lower part; some dacite and mafic to silicic tuff.K-Ar date of basalt from Dead Camel Mountains 6.96±0.42 m.y. (Evans, 1980, p. 20)	200	Welded tuff: Ash flow of dacite or andesitic composition. Age (K-Ar) most likely 4.6 m.y. (F. K. Miller, written commun., 1978)	100
	Miocene	///Local Unconformity/////		Younger basalt. Dates (K-Ar) 9.6 m.y. and 11.2 m.y. (B. Myers and E.S. Sims Written commun., 1978)	100

Table 1. -- Major rock stratigraphic units in the southern Carson Desert and Hot Springs Mountains, western Carson Desert. (Continued).

Southern Carson Desert				Hot Springs Mountains and western Carson Desert	
Period	Epoch	Unit and description	Maximum exposed thickness (m)	Unit and description	Maximum exposed thickness (m)
Tertiary	Miocene and Pliocene	Truckee Formation: Silicic to mafic tuff, tuffaceous sandstone and gravel, diatomite and limestone ///Local Unconformity////	150	Truckee Formation: Lacustrine deposits composed chiefly of diatomite but containing also pumice, tuffaceous sandstone, pebble conglomerate, limestone, coquina, and basalt	1,100
		Eagles House Rhyolite: Rhyolite to dacite flows /// Unconformity///////	120	Older basalt: Chiefly flows; some dikes, sills, tuff beds, interbedded silicified lacustrine shale. Roughly equivalent to Desert Peak Formation of Axelrod (1956)	700
	Miocene and older	Dacite of Rainbow Mountain: Mostly dacitic flows /// Unconformity////////	60	Andesite	120
		Basalt of Rainbow Mountain and some andesitic flows; some tuff. Much folded and generally altered. Base not exposed	210	Siliceous shale: Some interbedded sandstone and basaltic dikes, sills, and flows. K-Ar date of 13.9 m.y. (Evernden and James, 1964). Roughly equivalent to the Chloropagus Formation of Axelrod, 1965) /// Unconformity////////	700

Table 1. -- Major rock stratigraphic units in the southern Carson Desert and Hot Springs Mountains, western Carson Desert. (Continued)

Southern Carson Desert				Hot Springs Mountains and western Carson Desert	
Period	Epoch	Unit and description	Maximum exposed thickness (m)	Unit and description	Maximum exposed thickness (m)
Tertiary	Miocene and older	Basalt of Rainbow Mountain: Basaltic and some andesitic flows; some tuff. Strongly faulted and generally altered. Base not exposed	210?	Dacite: Underlies andesite in northeast part of mountains. Tuff: May be equivalent to Chloropagus Formation of Axelrod (1956) ///// Unconformity///////	60
Pre-Tertiary				Diorite: Dark green, fine-grained. Altered along faults to chlorite and sericite	

They are petrologically similar and occur at similar depths in all the wells (Sibbett, 1979, pl. 1), and the underlying sediments are highly tuffaceous and apparently somewhat consolidated, as is characteristic of the Truckee Formation elsewhere in the Carson Desert area (see Morrison, 1964; Voegtly, 1981; Willden and Speed, 1974). In any case, it seems likely that a substantial thickness of the section above a depth of 1,400 m--perhaps several hundred meters--is Tertiary, not Quaternary, in age.

Further evidence for placing the Tertiary-Quaternary boundary at a shallower depth than interpreted by Sibbett (1979) is the presence of the basalt of Ratttlesnake Hill at a depth of 150-180 m approximately 7 km east of the Chevron Resources Soda Lake well 63-33 (Glancy, 1981) and basalt at a depth of 115 m in well 64A, 2 km east of Upsal Hogback. The basalt of Rattlesnake Hill has been dated by the potassium-argon (whole-rock) method as 1.03±0.05 m.y. (Evans, 1980, p. 20); this age corresponds to middle Pleistocene according to most presently accepted time scales. There is no evidence to suggest the abrupt westward thickening of the Quaternary section between Fallon and the Soda Lakes area that would be required if the base of Quaternary were as deep as 1,400 m at Chevron Resources well 63-33.

The basalt in well 64A yielded a K-Ar age of 4.7±1.0 m.y.for a core sample from 122.8 m depth (E. H. McKee, written commun., 1981). The basalt overlies predominantly sand, clay, and minor basalt layers to a depth of 260 m, where andesite or basaltic andesite was penetrated. Samples of the latter from depths of 262 and 263 m gave K-Ar ages of 4.7±1.6 m.y. and 4.4±2.0 m.y. (E. H. McKee, written commun., 1981). Below the andesite are layers of tuff, mudstone, and basaltic sandstone. The basalts and andesites may be correlative with the Bunejug Formation, as suggested by the similarity in the sequence of rock types (see fig. 2).

In summary, rocks of Tertiary age beneath the Soda Lakes geothermal area, as indicated by the log of ERDA Lahontan No. 1 well, consist essentially of a lower section composed primarily of volcanic rocks and an upper section composed chiefly of sedimentary rocks. The base of the lower section (top of pre-Tertiary rocks) cannot be identified with certainty on the basis of present information. It may lie at the top of a sheared dacite porphyry at a depth of 2,369 m. Alternatively, it may be at the top of a section composed of meta-andesite and granite porphyry at a depth of 2,554 m. Still another possibility

is that the base of the Tertiary was not penetrated by the ERDA well and thus lies at a depth greater than 2,588 m. The base of the predominantly sedimentary section can be identified with more assurance as being at a depth of 1,290 m. The upper boundary of the Tertiary sedimentary rocks is uncertain, however. It could be as shallow as 251 m, at the top of a laterally extensive thick bed of limy mudstone, or as deep as 952 m, at the top of a bed of andesite (see fig. 2).

Quaternary System

The Quaternary System within the study area comprises lacustrine, deltaic, fluvial, and eolian sediments, and basaltic deposits of pyroclastic origin. Morrison (1964, p. 18) subdivided the upper part of this sequence (the late Pleistocene and Holocene sediments) into three major rock-stratigraphic units--Paiute Formation, Lahontan Valley Group, and Fallon Formation (see table 1). The Paiute Formation, which consists of pre-Lake Lahontan subaerial deposits, is not exposed within the study area but may be present in the subsurface. The Lahontan Valley Group, a sequence of intertonguing deep-lake, subaerial, and shallow-lake sediments, comprises in generally ascending order the Eetza, Wyemaha, Sehoo, Indian Lakes, and Turupah Formations (Morrison, 1964, p. 28). Only the Wyemaha Formation--a subaerial unit consisting of interbedded sand, silt, and clay (the last locally organic-rich), and the Sehoo Formation--a lacustrine unit--are exposed extensively within the study area (pl. 1). The Eetza Formation may occur in the subsurface, and the Turupah Formation probably is present as older dune deposits but was not differentiated by Morrison (1964) from the sandy upper member of the Sehoo Formation in the area shown on plate 1. The Fallon Formation consists of alluvial, eolian, and shallow-lake sediments of Holocene age and is the youngest unit exposed within the study area. The Fallon was differentiated by Morrison (1964) from older formations in the eastern part of the Upsal Hogback area but not in the Soda Lakes geothermal area (pl. 1).

Other Quaternary units exposed within the study area (pl. 1) consist of the basaltic tuff of Upsal Hogback, which is coeval with the Wyemaha Formation, and the volcanic-sand complex of the Soda Lake which is generally coeval with the Sehoo Formation but may include deposits as old as the Eetza Formation in the lower part (Morrison, 1964, p. 38, 72).

No attempt was made to assign deposits below the Wyemaha Formation to particular formations or stratigraphic units in the logs of the test wells. Most of the test wells 45 m deep or less probably do not penetrate beds below the Wyemaha. The most consistent marker is the lower, clay member of the Sehoo Formation, which was penetrated in most USGS test wells and lies at or near the land surface over much of the study area (pl. 2). The coarser deposits tend to occur as lenticular or ribbonlike bodies; the finer deposits, as exemplified by the lower member of the Sehoo Formation, tend to be more continuous laterally. (See pl. 2) In addition to the lower member of the Sehoo Formation, an undated bed having very high natural gamma radiation--possibly a silicic ash or tuff--could prove to be an excellent time-stratigraphic marker in the Upsal Hogback geothermal area (pl. 2).

As discussed previously, the subsurface boundary between the Tertiary and Quaternary Systems cannot be defined within narrow limits with data presently at hand. In the ERDA Lahontan No. 1 well it probably lies somewhere between depths of 251 and 972 m (see fig. 2). In test well 64A east of Upsal Hogback, it can be no deeper than 115 m, the depth to the top of the basalt dated at 4.7±1.0 m.y. (E. H. McKee, written commun., 1981), and it may be much shallower. Assuming a uniform rate of deposition, the 150-180-m depth of the top of the million-year-old basalt of Rattlesnake Hill 7 km east of Chevron Resources well 63-33 (pl. 1) suggests a thickness there of about 300-360 m for Lake Lahontan and post-Lake Lahontan sediments.

Structure

The Carson Desert is in the western part of the Basin and Range province. This region is characterized by generally east-west crustal extension and associated normal faulting (Stewart, 1971). Present topography in the Carson Desert reflects displacements along northwest- to northeast-trending high-angle normal faults, modified by deposition of sedimentary and volcanic rocks that partly fill the basin.

Although early Tertiary deformations in the region were mostly compressional, high-angle-normal faulting related to extensional strain has dominated during the last 17 m.y. (Stewart, 1971, p. 1036). Tertiary rocks beneath the Soda Lakes geothermal area are transected by high-angle normal faults, as indicated by seismic data (University of Utah Research Institute, 1979d). This

style of deformation is consistent with that seen in other parts of the Carson Desert. The degree of deformation of Tertiary rocks increases with age, and several episodes of Tertiary faulting are indicated (Morrison, 1964, p. 15, 16).

A complex configuration of the present buried bedrock surface within the study area is indicated by the results of gravity, seismic, magneto-telluric, and resistivity surveys. Reflection-seismic gravity, and ground-magnetic data (UURI, 1979d and k) indicate a set of concealed northwest-trending faults beneath the Soda Lakes anomaly. Gravity data (UURI, 1979k) indicate the presence of a north-trending bedrock ridge in the vicinity of well 64A, the location of the hottest known part of the Upsal Hogback thermal anomaly, although the ground-magnetic data do not definitely indicate a ridge. If the ridge reflects the presence of buried normal faults like those beneath the Soda Lakes thermal anomaly, rising thermal water may be localized in fault zones having high vertical permeability.

The north-northeast alinement of Soda Lakes, Upsal Hogback, and the intervening Soda Lakes thermal anomaly may indicate a concealed fault or fault zone having this orientation (Olmsted and others, 1975, p. 104). Linear features mapped by Sibbett (1979, fig. 2) are consistent with this trend. The hottest part of the Soda Lakes thermal anomaly therefore may coincide with the intersection of faults that trend north-northeast and northwest.

Except for several northeast- to north-trending high-angle faults of small apparent displacement mapped by Morrison (1964) at Soda Lakes and at or near Upsal Hogback, the exposed deposits of the Lake Lahontan deposits in the study area do not appear to be transected by faults. Bedding in these deposits is nearly horizontal, although some horizons, such as the contact of the Wyemaha and the Sehoo Formations, appear to dip slightly northeast, toward the Carson Sink. Some of the dip may indicate syndepositional topography, but at least part probably is the result of post-depositional downwarp caused by differential compaction.

Physiography

The Soda Lakes and Upsal Hogback geothermal areas lie in the west-central Carson Desert, about 15-30 km northwest and north of Fallon (fig. 1). The two areas are named for the most prominent physiographic features in this part of

the Carson Desert.

Soda Lake (or Big Soda Lake as it is sometimes called), about 1.1 by 1.5 km across and 63 m in maximum depth, and Little Soda Lake, just south of Big Soda Lake and 0.3 km in diameter and 17 m in maximum depth (Rush, 1972), occupy craters formed by repeated explosive eruptions. The eruptions deposited a rim of loose to semi-consolidated basaltic and nonvolcanic debris on all sides of the craters except the southwest, presumably the direction of the prevailing winds during the eruptions. The rim is roughly oval, 2-4 km across, and has a maximum altitude of 1,251 m--35 m above the present level of the lakes--on the northeast side. The outside of the rim, which has an average slope of about 0.08 (4-5°), appears to be unmodified by shoreline processes that would be associated with former stages of Lake Lahontan above the 1,220-m altitude of the base of the cone. This evidence suggests that the most recent eruptions that formed the present cone took place within the last 6,900 years (Garside and Schilling, 1979, p. 14).

Upsal Hogback, 10-15 km north-northeast of Soda Lakes, is a group of overlapping low, broad cones composed of moderately to highly indurated basalt cinder tuff formed by multiple explosive eruptions. Included in the tuff are accidental blocks as much as 1 m in diameter of basalt, andesite, and welded tuff similar to rocks of Tertiary age mapped by Voegtly (1981) in the Hot Springs Mountains to the northwest. Four to possibly as many as seven vents are evident (Morrison, 1964, p. 38). The youngest and best defined vent is at the northern end of the Hogback. Its crater is nearly circular and 800 m in diameter. The highest point on the Hogback, 1,267 m above sea level and about 60 m above the flanks and 47 m above the present floor of the crater, is on the northern rim of a cone at the south end. The older, less well-preserved cones are on the west flank of the Hogback, where their shapes and stratigraphic relations with adjacent sedimentary deposits are obscured by erosion and subsequent lacustrine deposition.

The tuff beds dip radially outward from the craters at angles ranging from 2 to 15 degrees on the flanks and at steeper angles toward the vents (Morrison, 1964, p. 38). Most of the dips are steeper than the present slopes, which have been subsequently modified greatly by shoreline processes during high stands of Lake Lahontan. The eruptions occurred during a time when the lake was dry or possibly at a lower level, as indicated by intertonguing of the basalt tuff with

nonvolcanic sediments of the Wyemaha Formation, a subaerial deposit (Morrison, 1964, p. 38). Evidence presented by Morrison (1964, p. 38, pl. 10) indicates the eruptions that formed the Hogback took place during the interval 30,000 to 45,000 years ago. Basaltic debris in the lower part of the Sehoo Formation, which overlies the Wyemaha, suggests an age of 25,000-30,000 years for the latest eruptions (Garside and Schilling, 1979, p. 14; Berkeland, Crandall, and Richmond, 1971: Quaternary Research VI, no. 2, p. 208-277.)

The landforms surrounding Soda Lakes and Upsal Hogback are largely products of eolian processes. Wind scour and deposition have created a landscape of undrained depressions and intervening sandy flats locally mantled with small dunes.

The depressions are crudely semicircular to irregular in plan, range upward to 2 km in maximum dimension (most commonly oriented easterly or east-northeasterly), and have floors as much as 12 m below the level of the adjacent sandy flats. Most of the depressions are floored by clay or silt of the Sehoo Formation (p. 18), but a few deeper ones expose sand of the underlying Wyemaha Formation (see pl. 1). Because of the rise in the water table following the advent of irrigation to the south and east in the early 1900's, many of the deeper depressions now contain small perennial or seasonal lakes and ponds. In the Soda Lakes area, the sandy flats between the depressions define a nearly plane original surface, formed on the upper sand member of the Sehoo Formation, which slopes north-northeastward from an altitude of about 1,220 m near Big Soda Lake in the southwestern corner of the study area to about 1,210 m above sea level at the southern end of Upsal Hogback. This surface generally is absent in the Upsal Hogback area, where, apart from the Hogback itself, most exposures are of the stratigraphically lower Wyemaha Formation. In the northeastern part of the Upsal Hogback area, the exposures of Wyemaha stand 1-2 m below adjacent terrace-like remnants of the Sehoo Formation. The exposures of Wyemaha Formation are at altitudes as low as 1,179 m above sea level at the northeastern corner of the study area. A few exposures of clay and silt of the lower member of the Sehoo Formation north of Upsal Hogback rise as much as 4 m above adjacent exposures of the Wyemaha Formation (pl. 2).

Sand dunes, most of which overlie the sandy flats described above, but some of which occupy parts of the depressions, range from irregular small mounds and ridges 1 m or less in height to elongate features as much as 6 m in height. The long axes of these larger features are oriented roughly east-northeast, presumably parallel to the former prevailing wind direction that shaped them. Most of the dunes are presently inactive and are mantled with perennial shrubs.

GEOHYDROLOGY

Regional Hydrologic Setting

The Carson Desert is the undrained depression that forms the sump for the Carson River and, at times, the Humboldt River by way of overflow from the Humboldt Sink through the White Plains hydrographic area (fig. 1). The major source of ground-water recharge in the Carson Desert is water from the Carson River. Since 1906, the flow of the Carson River downstream from Lahontan Reservoir has been augmented by water from the Truckee River diverted by way of the Truckee Canal. Before irrigation development in the early 1900's, recharge from the Carson River to the ground-water system took place by seepage through channel bottoms of its natural distributory system and by overbank flooding. Today, most Carson River water, along with the imported Truckee Canal water, is used for irrigation. Ground-water recharge takes place largely by percolation of applied irrigation water to the saturated zone and by leakage from unlined irrigation canals. Irrigation is concentrated largely in the Fallon and Stillwater areas, generally south and east of the study area. Since extensive irrigation began about 1906, ground-water levels have risen as much as 18 m near Soda Lakes (Rush, 1972).

Ground-water recharge from local precipitation on the Carson Desert is believed to be small. Average annual precipitation ranges from less than 100 mm on the Carson Sink in the lowest part of the basin to more than 400 mm on the summits of the Stillwater Range (Hardman, 1936; Hardman and Mason, 1949). In the lower parts of the basin, potential evapotranspiration may exceed precipitation by a factor of 10 or more. Little precipitation infiltrates to the saturated zone except where the water table is within 1 or 2 m of the land surface and the capillary fringe extends at times to the surface. In addition to the areas of shallow water table, ground-water recharge probably takes place in the higher parts of the mountains and also near the apexes of alluvial fans, where ephemeral streams debouch onto coarse permeable fan deposits.

Glancy and Katzer (1975), using an empirical method developed by Eakin and Maxey (1951), estimated potential recharge from local precipitation at approximately 1.6×10^6 m^3/a, or only about 0.2 percent of the total precipitation

on the Carson Desert. By comparison, recharge from excess applied irrigation water and flow of Carson River may exceed one half of the approximately 480 x 10^6 m^3/a average annual release from Lahontan Reservoir (Olmsted and others, 1975, p. 80). The estimate of Glancy and Katzer (1975) for local recharge may be low, however; their estimate did not include potential recharge in areas of shallow water table.

Because of the absence of surface drainage from the Carson Desert and of the probable absence of thick sequences of permeable consolidated rocks in the mountains, ground-water movement out of the basin is believed to be negligible. Almost all water entering the basin is discharged eventually by evapotranspiration. Evaporation takes place from ponds, lakes, reservoirs, and other bodies of surface water and from areas of bare soil. Phreatophytes and irrigated crops transpire large volumes of water. Important areas of natural ground-water discharge are Carson Sink, Carson Lake, and Four Mile Flat (fig. 1).

Large-scale lateral movement of ground water in the Carson Desert is toward the areas of natural discharge mentioned above. Sand aquifers within a few tens of meters of the land surface probably transmit ground water most rapidly. Water at greater depths moves more slowly. Near areas of ground-water discharge, confined ground water at depth moves upward across confining beds of clay and silt. In recharge areas, especially in the irrigated lands, the vertical component of ground-water flow is mainly downward.

Subdivisions of the Ground-Water System

The ground-water system beneath the study area is herein subdivided into shallow, intermediate, and deep subsystems on the basis of differences in the hydrologic properties of the geologic materials and inferred differences in the ground-water-flow regime. The scanty data available from deep test drilling suggest that the subsystem boundaries are locally difficult to define or gradational and probably will require revision as new data are acquired. The inferred thermal and hydrologic properties of the three subsystems, the four major geologic units that they comprise, and the approximate average depths to major boundaries in the Soda Lakes area, are summarized in table 2. A brief description of each subsystem follows.

The shallow subsystem generally is coextensive with the Quaternary System discussed in the preceding section on geology. These fluvial, lacustrine, and

Table 2. -- Inferred thermal and hydrologic properties of shallow, intermediate, and deep ground-water subsystems in the Soda Lakes geothermal area

Depth (km)	Subsystem	Major geologic unit	Thermal conductivity (thermal conductivity unit)	Effective porosity (percent)	Nature of pore space
0-0.25	Shallow	Quaternary deposits	3.5	15	Intergranular
0.25-1.3	Intermediate	Tertiary and Quaternary sedimentary rocks	4.0	10	Chiefly intergranular; some fractures
1.3-2.5	Deep	Tertiary volcanic rocks	5.0	5	Chiefly fractures; some intergranular (?)
2.5-4.0		Pre-Tertiary rocks	6.0	2	Fractures; solution channels
4.0-6.0			8.0	1	

eolian deposits generally are unaltered and unconsolidated. Maximum thickness is uncertain because of the uncertain or gradational boundary with the underlying intermediate subsystem but probably is less than 400 m. The average thickness may be about 250 m in the Soda Lakes geothermal area (table 2) and somewhat less in the Upsal Hogback area. Ground water moves chiefly through intergranular pores in the shallow deposits, and the directions and approximate rates of movement generally are well understood.

The intermediate subsystem consists predominantly of slightly to moderately consolidated sediments of Tertiary (?) age with minor intercalated basalt, probably in the form of flows but possibly including sills or dikes (Sibbett, 1979, p. 8). The sediments are distinguishable from the overlying deposits of the shallow subsystem by their somewhat indurated and altered character and by the abundance of ash, tuff, and diatomite. The intermediate subsystem probably averages slightly more than 1,000 m in thickness beneath the Soda Lakes area (table 2); beneath the Upsal Hogback area the thickness is unknown. As in the shallow subsystem, ground water presumably moves chiefly through intergranular pores, but average permeability probably is substantially less than that of the shallow subsystem, owing to the somewhat indurated and altered character of the deposits. Fractures may form locally important flow channels, especially in the more indurated zones. The direction of ground-water flow in the intermediate subsystem is poorly known because of the general absence of hydraulic-head data from test drilling.

The deep subsystem is composed predominantly of volcanic rocks of presumed Tertiary age and pre-Tertiary igneous, metamorphic, and sedimentary rocks. Owing to their low primary porosity and their highly indurated character, these rocks are hydrologically distinct from those of the overlying two subsystems. Ground-water flow probably takes place primarily in fractures and other secondary openings related to cooling, faulting, or dissolution of rock by ground water. Information on ground-water flow in the deep sub-system is limited. Water levels in the ERDA Lahontan no. 1 well indicate a head of 1,173.59-1,173.80 m above sea level (U.S. Geological Survey, unpub. data, 1977-1981) for the perforated interval 1,434-1,437 m below land surface. This apparently indicates a deep potential gradient away from the Carson Sink as a well drilled in the sink (T.C.I.D. No. 1) drilled to a depth of 1,145 m below land surface flows at the surface (Garside and Schilling, 1979, p. 17). Using the surface elevation

as a minimum head for the T.C.I.D. well (1,181 m above sea level), then there is approximately a 7 m hydraulic potential to the southwest--away from the sink. This apparent reversal in hydraulic potential from that seen in the shallow subsystem over a distance of about 50 km is one indication that ground-water flow in the deep subsystem probably is complex and largely not understood at this point. A potential for flow toward Dixie Valley to the east is indicated by the fact that the land surface in the lowest part of that valley is about 150 m lower than the lowest part of the Carson Sink. However, as stated earlier (p.24), the thick sequences of permeable consolidated rocks that would transmit such flow probably are absent.

Occurrence and Movement of Ground Water in the Shallow Subsystem

The unconsolidated deposits of the shallow ground-water subsystem throughout the study area are saturated with ground water below depths ranging from less than 1 m in the floors of undrained depressions and the lowest lying playas to more than 70 m beneath the higher parts of Upsal Hogback. At most places within the Soda Lakes area, the depth to the water table ranges from about 1.5 to 11 m; in the Upsal Hogback area, outside the Hogback itself, the depth ranges from about 0.5 to 20 m. Seasonal fluctuations in the water table from place to place range from less than 0.1 m to about 1 m. No definite long-range trend upward or downward has been noted in recent years, although since the early 1900's, when irrigation began in the Carson Desert, the water table has risen by as much as 18 m in the southwest part of the study area, as indicated by the reported rise in stage of Soda Lakes from 1906 to 1930 (Rush, 1972).

Confined conditions exist throughout most of the saturated deposits. However, unconfined conditions are present to depths as much as several meters below the water table where the water table is in coarse-grained deposits. The confined potentiometric surface is above the water table in or adjacent to areas of ground-water discharge by evapotranspiration, indicating an upward component of the hydraulic gradient. The reverse is true in or adjacent to areas of ground-water recharge.

Directions of ground-water movement in the shallow ground-water subsystem may be inferred from observed lateral and vertical components of the hydraulic gradient.

Lateral hydraulic gradients are defined by the configuration of potential surfaces represented by altitudes of water levels in the test wells. At most test-well sites, some degree of confinement at depths more than a few meters below the water table is indicated by the presence of laterally extensive thick fine-grained beds and by upward or downward vertical components of the hydraulic gradient. Therefore, the configurations of potential surfaces vary with the depth of the aquifers in which the wells are screened, and lateral hydraulic gradients at different depths are correspondingly variable.

The configuration of the water table in mid-December 1979, as indicated in very shallow piezometer wells screened just below the water table, is shown in figure 3. The altitude of the water table at each well site was computed by adjusting the measured water level in the shallowest test well for difference in head between the depth of the center of the screen in that well and the water table, using the vertical component of the hydraulic gradient indicated by measurements in the shallowest and the next deeper well at the site.

In constructing the water-table contours depicted in figure 3, account was also taken of the fact that, in some undrained depressions and low-lying playas where the water table is within about 2 m of the land surface, its configuration is analogous to a seepage surface, except that the water discharges by evapotranspiration instead of by seepage. Where evaporation and transpiration rates are insufficient to maintain the water table below the land surface, free-water surfaces of small lakes and ponds indicate its position.

As shown in figure 3, the direction of the lateral gradient of the water table is generally northeastward, and the gradient generally decreases in that direction. There are, however, significant departures from that generalization, chiefly related to the topographic influences described above. The water-table configuration, therefore, is an unreliable guide to the directions and rates of lateral ground-water flow at appreciable depths below the water table. For this reason, in order to calculate the average direction and rate of ground-water flow through the zone from the water table to a depth of 45 m below land surface, water levels representing a depth of 30 m below land surface were selected, as discussed below.

Configuration of the confined potentiometric surface representing a depth of 30 m below land surface in mid-December 1979 is shown in figure 4. Because

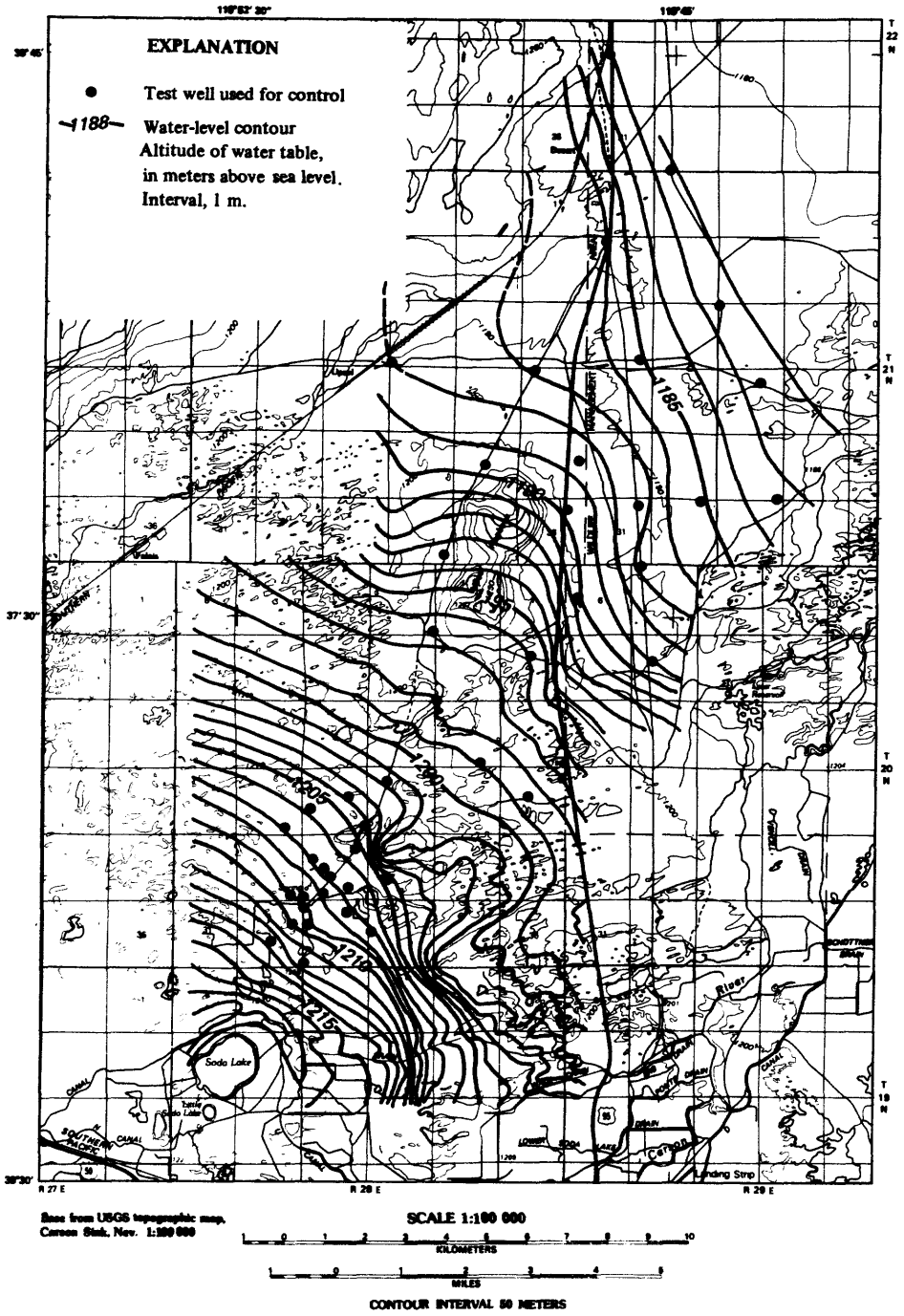

Figure 3. -- Altitude of water table, December 1979, Soda Lakes and Upsal Hogback geothermal areas.

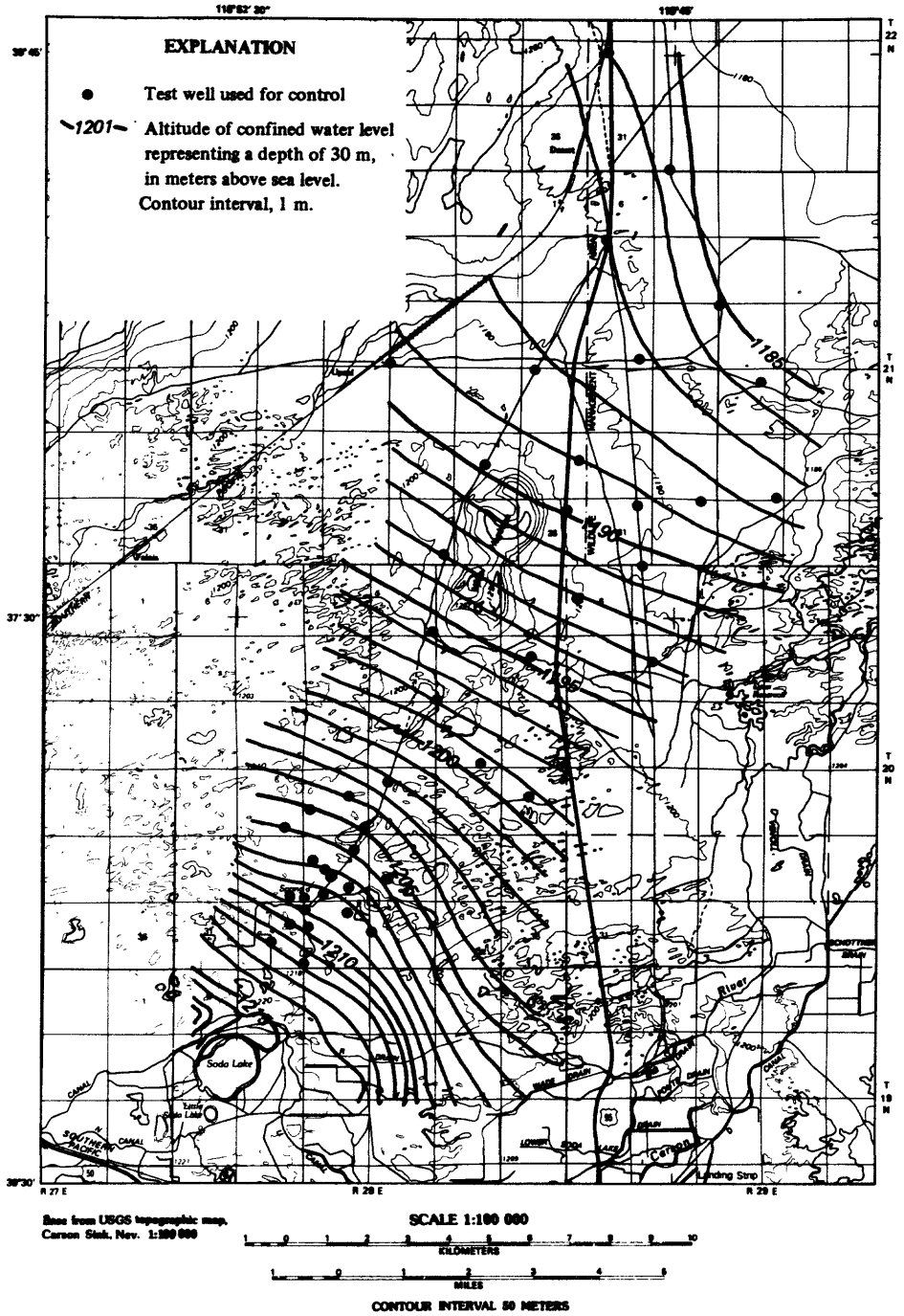

Figure 4. -- Altitude of confined water level representing a depth of 30 m, December 1979, Soda Lakes and Upsal Hogback areas.

most of the test wells are not screened at a depth of exactly 30 m, water levels measured in those wells were adjusted to levels representing a depth of 30 m by computing the difference in head between the depth of the center of the well screen and a depth of 30 m, using the vertical component of the hydraulic gradient at the site. At some well sites, measured vertical hydraulic gradients were adjusted for the "short-circuit" effect of vertical flow of water through the annulus outside the well casing above the screen at the bottom of the well. Adjustments were made where low-density material near the bottom of the well was indicated by the gamma-gamma log and where confined water levels representing a depth of 30 m obviously were anomalous in comparison with levels from adjacent sites at which annular flow is believed to be insignificant. The magnitude of the effect of annular flow on the vertical hydraulic gradient at each well site is indicated by the ratio of the hydraulic gradient interpolated from the maps of the unconfined and confined water levels (figs. 3 and 4) to the gradient actually measured in the wells at each site. This ratio, termed herein the "gradient adjustment factor", is discussed later in the section on estimates of vertical ground-water flow (p. 41).

Like the water table, the direction of the confined hydraulic gradient is northeastward, and the gradient decreases in that direction, but the configuration of the confined potentiometric surface is much more regular than that of the water table. The confined potentiometric surface is thus much less affected by topographic irregularities than is the water table.

Ground-Water Budget

One of the principal objectives of the study was to derive a water budget or budgets for the portion of the shallow ground-water subsystem having data available from test drilling. The primary purpose of the ground-water budget was to provide estimates of the rate of discharge of thermal water from a deep source or sources. A secondary purpose was to estimate vertical ground-water flow rates between a depth of 45 m and the water table in order to provide a comparison with rates calculated from measured vertical hydraulic conductivities. The "best estimates" of vertical ground-water flow rates (specific discharge or recharge) were then used to adjust estimated conductive heat flows in this depth interval for convective effects, using a method given by Lachenbruch and Sass (1974, p. 641-643).

The budget involves estimates of annual rates of ground-water flow, both lateral and vertical, through a prism of sediments between the water table and a depth of 45 m below the land surface, for convenience termed the "budget prism". The width of the prism was constrained by the lateral limits of reasonably adequate water-level control in the southwest part of the Soda Lakes geothermal area, as shown in figure 5. The depth limit of 45 m was the approximate depth of most of the Geological Survey test wells. Obviously, this depth is substantially less than the total thickness of the shallow ground-water subsystem at most places within the study area, and estimated rates of lateral ground-water flow do not represent total lateral flow through the subsystem.

It would have been preferable, of course, to have used a particular aquifer or aquifer zone, rather than an arbitrary depth below land surface, for the base of the budget prism. However, as shown in the geologic sections (pl. 2), no such widespread aquifer exists. Also, the land surface is irregular in parts of the area, so that the base of the budget prism is not a plane surface. The saturated thickness of the prism therefore is not constant. However, the range in saturated thickness is not large, except under the higher parts of Upsal Hogback, where the depth to the water table actually exceeds 45 m. Beneath the Hogback, therefore, the base of the budget prism is considered to be at the same altitudes as on the flanks of the Hogback, rather than at a depth of 45 m.

Four sections, designated A-A', B-B', C-C', and D-D', were established across the budget prism; sections A-A' at the southwestern edge, D-D' at the northeastern edge, and the two ground-water flow lines that represent the limits of reasonably adequate water-level control, define the lateral limits of the budget prism (fig. 5). As thus defined, all lateral ground-water flow above a depth of 45 m is through the four sections (A-A' to D-D'); no flow occurs across the side boundaries of the prism.

Implicit in the budget estimates is the assumption of steady-state conditions. Conditions observed in 1979 were assumed to represent long-term average conditions so that net changes in ground-water storage in the prism were zero--annual rates of ground-water outflow were equal to annual rates of inflow. Lateral ground-water flow through each of the three budget subprisms delineated by the sections was estimated, as described below.

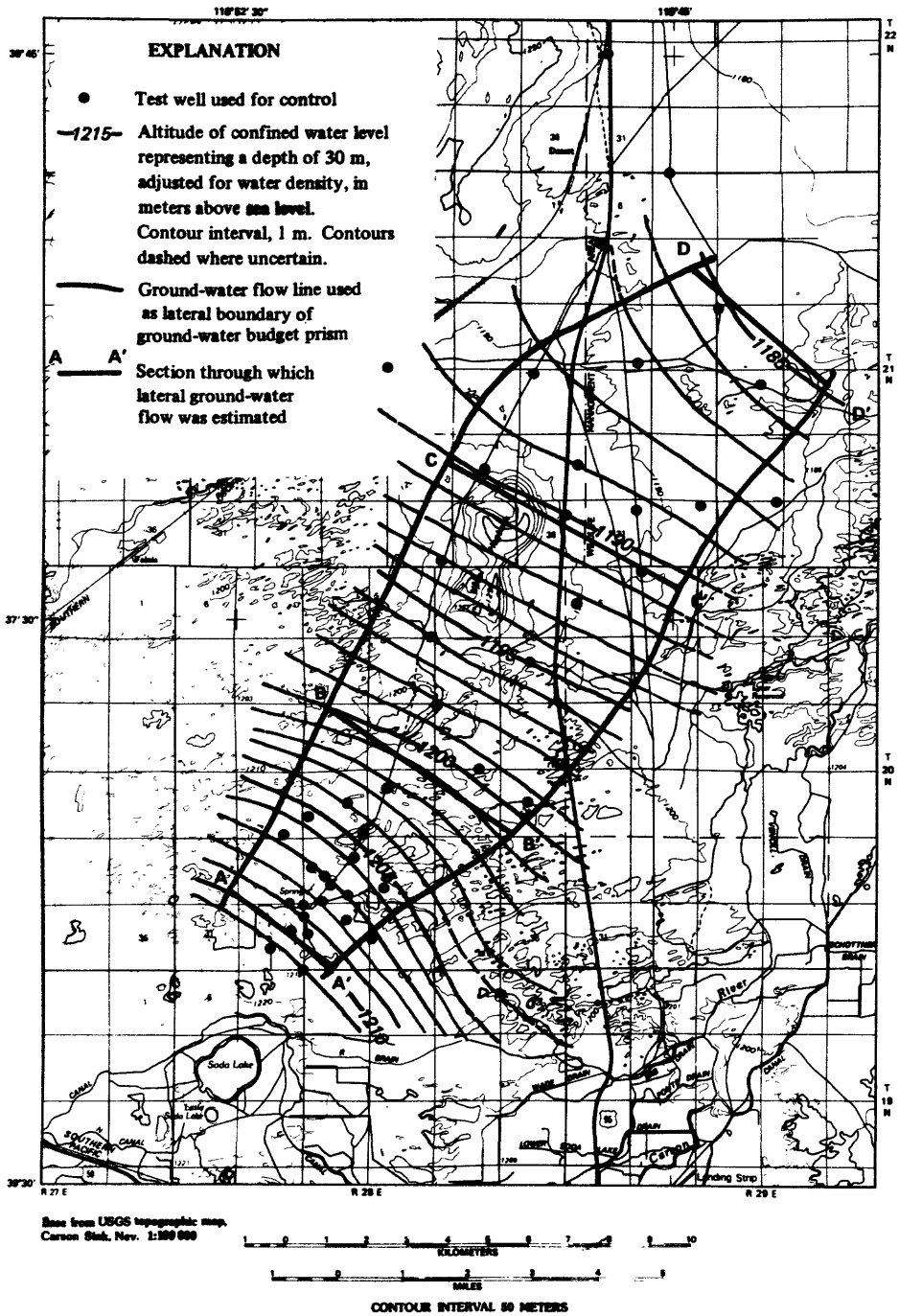

Figure 5. -- Ground-water budget prism and altitude of adjusted confined water level representing a depth of 30 m, December 1979, Soda Lakes and Upsal Hogback geothermal areas.

Estimates of Lateral Ground-Water Flow

The lateral component of ground-water flow through each of the four sections across the the budget prism, for convenience abbreviated hereinafter as lateral ground-water flow, was computed as the product of the saturated thickness, the width of the section, the average lateral hydraulic conductivity, and the average lateral hydraulic gradient perpendicular to the section.

Lateral hydraulic gradients in mid-December 1979 representing a depth of 30 m below the land surface (fig. 4) were discussed in an earlier section (p. 31). These gradients do not, however, represent actual pressure gradients at depth and therefore were not used to estimate rates of lateral ground-water flow. In order to derive the pressure gradients required to estimate rates of lateral ground-water flow, the altitudes of the confined water levels were adjusted for density of the water. Temperature is the only factor that significantly affects water density within the study area; the effect on water density of differences in dissolved-solids concentration is negligible.

An integrated-average water density was computed using observed temperature-depth relations at each well site. The adjusted altitude of the confined water level was then computed by multiplying the observed height of the water level above the mid-depth of the well screen at the bottom of the well by the integrated-average density of the water and adding the product to the altitude of the mid-depth of the screen. The resultant altitude was then adjusted for the observed vertical hydraulic gradient in the confining beds (silt or clay) between the depth of the well screen and a depth of 30 m. The altitudes thus derived were used to define the adjusted confined potentiometric surface shown in figure 5; the slope of this surface was used to estimate the average lateral hydraulic gradient normal to each of the four sections.

The average lateral hydraulic conductivity of the deposits between the water table and a depth of 45 m at each of the four sections was determined from a map showing areal variations in this quantity based on estimates at individual well sites (fig. 6).

The average lateral hydraulic conductivity at each well site was estimated using the values of lateral intrinsic permeability for unconsolidated aquifer materials listed in table 3. A weighted-average lateral intrinsic permeability for the saturated materials penetrated by the well was calculated from the

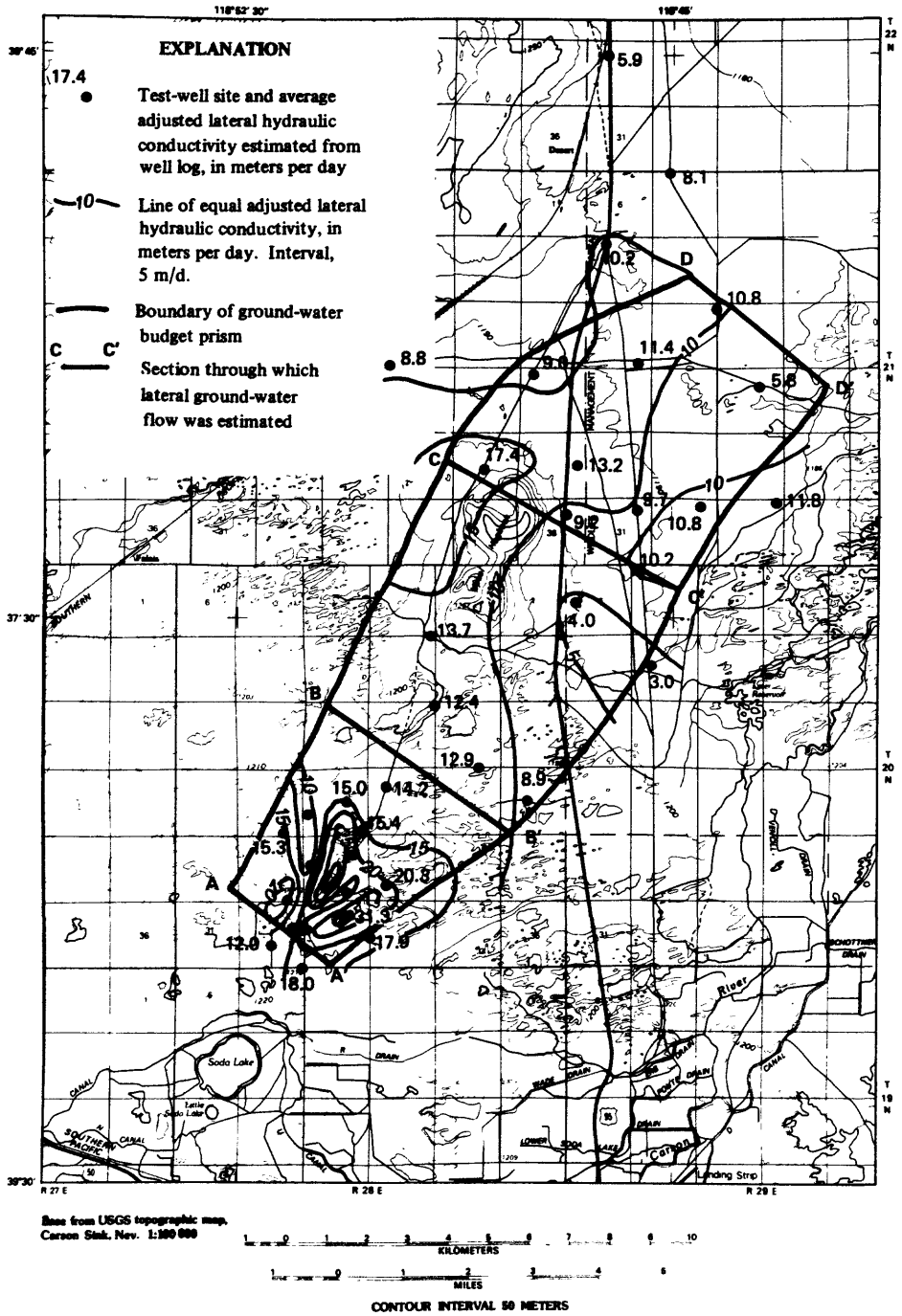

Figure 6. -- Ground-water budget prism showing average adjusted lateral hydraulic conductivity of deposits between the water table and a depth of 45 m.

Table 3. -- Values of intrinsic permeability and thermal conductivity assigned to materials classified in lithologic logs of test wells

Materials	Intrinsic permeability ($\times 10^{-15}$ m^2)		Thermal conductivity (thermal conductivity unit)
	Lateral	Vertical	
Gravel and sand; sand and gravel; pebbly sand; coarse sand; medium to coarse sand.	64,000	300	4.7
Medium sand; fine to medium sand; sand; coarse sand with silt	16,000	100	4.2
Fine sand; silty sand; sand and silt; clay and gravel; clay and coarse sand		30	
Silt and fine sand; clay and sand	0	10	3.2
Silt; sandy clay; clay and fine sand; pebbly clay		3	
Clayey silt; silty clay and fine sand		1	2.2
Clay; sity clay		.3	

values given in table 3 and the bed thicknesses reported in the lithologic log. Beds of silt and finer particles were assumed for practical purposes to have zero lateral permeability. Finally, the weighted-average lateral hydraulic conductivity at the site was calculated by converting the intrinsic permeability to hydraulic conductivity, converting units from 10^{-15} m^2 to meters per day (m/d), and adjusting the hydraulic conductivity for the difference in kinematic viscosity between water at standard temperature of 15.6°C and the integrated-average temperature from the water table to a depth of 45 m at the site.

Values of lateral intrinsic permeability in table 3 are based primarily on values reported by Bedinger (1961) for fluvial sands of the Arkansas River Valley of Colorado and by Remson (written commun., 1978) for shallow brine-bearing sands just east of the Upsal Hogback area. These values are corroborated in a general way by results of specific-capacity tests of 24 wells in the Schurz area, about 60 km south of Fallon (fig. 1), reported by Schaefer (1980).

Using the average lateral hydraulic conductivity, the average lateral hydraulic gradient, and the cross-section area (product of length and saturated thickness), the lateral ground-water flow through sections A-A', B-B', C-C', and D-D' was estimated as shown in table 4. The estimated flow increases northeastward, down the hydraulic gradient, from 1,200,000 m^3/a entering the budget prism at section A-A'to 1,800,000 m^3/a at section B-B', northeast of the hottest near-surface part of the Soda Lakes geothermal area. The flow then decreases to an estimated 1,000,000 m^3/a at section C-C' at Upsal Hogback, and, finally, to an estimated 370,000 m^3/a at section D-D' at the northeastern end of the budget prism. The increase in flow between sections A-A' and B-B' probably is due to the upward inflow of thermal water within this subprism. Subsequent decreases in lateral flow rate reflect the net discharge (upward flow) by evaporation and transpiration from the water table in the two downgradient subprisms. The significance of these estimates and their relation to other estimates of vertical inflow or outflow of water in the three budget subprisms are discussed farther on in the section, "Summary of ground-water budget estimates".

Table 4. -- Lateral ground-water flow above a depth of 45 m through sections A-A', B-B', C-C', and D-D', December 1979

[See figure 9 for location of sections]

Section	Length (m)	Average thickness (m)	Average lateral hydraulic gradient (m/km)	Average lateral hydraulic conductivity (m/d)	Lateral ground-water flow (m^3/d)	Lateral ground-water flow (m^3/a)
A-A'	3,100	38	2.2	12.7	3,300	1,200,000
B-B'	5,600	38	1.8	12.5	4,800	1,800,000
C-C'	6,800	36	1.0	11.6	2,800	1,000,000
D-D'	4,500	44	.6	8.6	1,000	370,000

Estimates of Vertical Ground-Water Flow

In addition to the lateral ground-water flow component discussed above, a vertical flow component, for convenience referred to as vertical ground-water flow, exists throughout most of the ground-water budget prism. Four kinds of evidence for vertical ground-water flow are: (1) Differences in lateral flow through the budget prism, as discussed in the preceding section and shown in table 4; (2) vertical hydraulic gradients observed at most test-well sites; (3) the presence of phreatophytic vegetation and soil-salts accumulation, which indicate ground-water discharge by evaporation and transpiration (evapotranspiration); and (4) change in vertical conductive heat flow with depth in the test wells.

Two methods, based on the second and third kinds of evidence listed above, were used to estimate rates of vertical ground-water flow in the study area: (1) the "hydraulic" method, and (2) the "vegetation" method. In principle, a method based on the fourth kind of evidence--the change in vertical conductive heat flow with depth--also could have been used. However, its use would have required more precise estimates of vertical conductive heat flow at different depths than were possible using only estimated rather than measured values of vertical thermal conductivity. (See discussion on p. 98-104.) The "hydraulic" and "vegetation" methods are described in the following paragraphs.

The "hydraulic" method estimates average rate of vertical ground-water flow through the budget prism as the product of the average vertical component of the hydraulic gradient between a depth of 45 m and the water table and the harmonic-mean vertical hydraulic conductivity of the deposits at the temperatures prevailing for this interval.

The vertical component of the hydraulic gradient at each test-well site was determined by water-level measurements in pairs of wells of different depths. The shallower well is screened a short distance below the water table; the deeper well at most sites is screened at depths ranging from about 30 to 45 m. The gradient was computed as the difference in depth to water from land-surface datum in the two wells divided by the difference in depth between the bottom of the screen in the shallower well and the top of the screen in the deeper well. Where the depth to water in the shallower well was greater than that in the deeper well, the gradient was assigned a positive value (upward component); where the reverse was true, the gradient was assigned a negative value (downward

component).

Throughout the study area, the budget prism from the water table to a depth of 45 m (or, roughly, for the depth interval between the shallower and deeper well at each site) comprises several horizontally stratified layers of extremely variable vertical intrinsic permeability. The harmonic-mean vertical intrinsic permeability, k_n, of a series of n layers is

$$k_n = \frac{z_t}{\sum_{i=1}^{n} z_i/k_i}$$

where z_i equals the thickness of layer i; k_i equals the vertical intrinsic permeability of layer i; and z_t equals the total thickness.

In the equation above it is apparent that the layers of low permeability have a dominant effect on the harmonic mean. The accuracy of the estimate of vertical ground-water flow clearly is dependent on the accuracy of the thickness of confining layers reported in the lithologic log of the test well and, especially, on the validity of the value of vertical intrinsic permeability assigned to each of these layers.

Values of vertical intrinsic permeability were assigned to materials classified in lithologic logs of test wells, as given in table 3. The lowest value in table 3, $0.3 \times 10^{-15} m^2$ for clay or silty clay, is the geometric mean average of values of $0.1 \times 10^{-15} m^2$ for clay given by Morris and Johnson (1967, table 12) and $1 \times 10^{-15} m^2$ for silty clay interpolated from Morris and Johnson (1967, tables 5 and 12). The value for fine sand and related materials in table 3, $30 \times 10^{-15} m^2$, actually is based on the average value of $32 \times 10^{-15} m^2$ for silt given by Morris and Johnson (1967, table 5). The reason for the application of this value to materials coarser than silt is that the lithologic logs of the test wells generally are not sufficiently detailed to indicate the presence of thin beds of finer materials within thick sequences described as fine sand or related deposits of similar hydrologic character. Such beds, whose abundance is indicated in cores from several test wells, tend to control the vertical permeability of the zones in which they occur. Similarly, values indicated in table 3 for medium sand and coarser materials reflect the presence of thin beds of finer materials. For practical purposes, however, these materials were assumed

to have infinite vertical permeability because of their negligible effect on the calculated harmonic mean.

Estimates of specific discharge or recharge (vertical Darcian velocity) by the "hydraulic" method are presented in table 5. As in the estimates of lateral ground-water flow rates, the average values of vertical intrinsic permeability were adjusted for integrated-average (by depth) temperature (which affects the kinematic viscosity of the water) to derive the adjusted average vertical hydraulic conductivity used in the calculations. Because the vertical hydraulic gradients upon which the estimates are based change with time, many measurements over a period of several years were averaged to obtain reasonable estimates of long-term average gradients at almost all the test-well sites. The approximate amplitude of the variation in depth to water table, vertical hydraulic gradient, and specific discharge or recharge is indicated by the plus or minus values in table 5, which represent two standard deviations from the long-term mean values.

The gradient-adjustment factor, defined earlier (p. 31) and listed in table 5, was used to adjust measured vertical hydraulic gradients for wells having significant annular flow immediately above the well screen. At a few locations, notably USGS sites 10, 27, and 34, the adjustment factors are large, which indicates high rates of flow. At several other sites (USGS sites 33, 36-39, and 54, and USBR site 10), measured vertical hydraulic gradients were not available, and the gradients listed in table 5 are based entirely on the gradients interpolated from figures 3 and 4.

The "vegetation" method derives an indirect estimate of vertical ground-water flow in the budget prism by calculating annual rates of ground-water evapotranspiration on the basis of empirical values assigned to various types of phreatophytes and soil conditions. These empirical values, listed in table 6, have been used successfully in ground-water budgets for hydrographic areas in Nevada in numerous ground-water reconnaissance studies by the Geological Survey. (See summary in Nevada Division of Water Resources, 1971.) The evapotranspiration data, along with a pheatophyte and surface-conditions map of the study area, were provided by P. A. Glancy (written commun., 1979).

The estimates of vertical ground-water flow (specific discharge or recharge) by the two methods described above are summarized in table 7. As indicated in table 7, the estimates by different methods differ substantially at many well sites. In part, the differences reflect the fact that the values represent different depth intervals, but a large part of the difference is a result of

Table 5. -- Specific discharge or recharge at test-well sites estimated by "hydraulic" method

[Positive values indicate discharge (upward flow); negative values, recharge (downward flow); plus or minus values indicate two standard deviation (approximately equal to the amplitude of variation); gradient adjustment factor is ratio of interpolated to measured vertical hydraulic gradient, as explained in text]

Test well site	Date or period of measurement	Depth interval (m)	Vertical intrinsic permeability ($\times 10^{-15} m^2$)	Integrated average temperature (°C)	Adjusted vertical hydraulic conductivity (mm/d)	Depth to water table (m)	Gradient adjustment factor	Vertical hydraulic gradient	Specific discharge (+) or recharge (-) (mm/a)	Footnotes
U.S. Geological Survey wells										
1	82 05 19	2.01- 6.16	4.8	15.6	3.8	2.01	1.0	-0.020	-28	1/
2	1974-82	10.39-25.91	2.7	28	2.7	9.61 ± .07	1.5	+0.023 ± .007	+23 ± 7	2/
3	1974-82	7.91-43.56	2.7	22.5	2.4	2.33 ± .19	1.0	+0.0036 ± .0036	+ 3.2 ± 3.6	3/
8	1974-82	3.63-37.95	1.7	17	1.4	3.29 ± .25	1.0	-0.063 ± .006	-32 ± 3	4/
9	1975-82	10.18-39.32	2.2	18.0	1.7	9.13 ± .09	1.0	+0.018 ± .003	+11 ± 2	5/
10	1975-82	3.86-32.31	3.2	19	2.6	2.83 ± .04	4.3	+0.046 ± .033	+44 ± 31	6/
12	1974-82	14.60-21.46	1.7	17.5	1.4	10.03 ± .09	1.0	-0.068 ± .009	-35 ± 5	7/
13	1975-82	4.83-21.18	2.4	20.7	2.1	3.07 ± .15	1.2	+0.038 ± .008	+29 ± 6	8/
17	1974-82	6.56-8.99	3.0	65	5.7	2.93 ± .39	1.0	-0.017 ± .032	-35 ± 67	9/
18	1974-82	5.33-41.15	4.5	16.7	3.5	4.60 ± .76	1.0	-0.0087 ± .019	-11 ± 24	10/
27	1975-82	4.97-44.07	2.2	31	2.4	4.52 ± .35	3.3	+0.044 ± .021	+39 ± 18	11/
29	1975-82	6.68-43.95	2.6	25.5	2.4	6.19 ± .32	1.5	+0.035 ± .010	+31 ± 9	12/
30	1974-82	3.17-39.93	1.7	80	4.0	1.78 ± .42	1.0	+0.021 ± .006	+19 ± 5	13/
32	1975-82	7.19-44.33	3.1	41	1.7	6.88 ± .26	1.0	-0.0077 ± .0050	- 4.8 ± 3.1	14/

Table 5. -- Specific discharge or recharge at test-well sites estimated by "hydraulic" method (Continued)

[Positive values indicate discharge (upward flow); negative values, recharge (downward flow); plus or minus values indicate two standard deviation (approximately equal to the amplitude of variation); gradient adjustment factor is ratio of interpolated to measured vertical hydraulic gradient, as explained in text]

Test well site	Date or period of measurement	Depth interval (m)	Vertical intrinsic permeability ($\times 10^{-15} m^2$)	Integrated average temperature (°C)	Adjusted vertical hydraulic conductivity (mm/d)	Depth to water table (m)	Gradient adjustment factor	Vertical hydraulic gradient	Specific discharge (+) or recharge (-) (mm/a)	Footnotes
U. S. Geological Survey wells										
33	79 12 13	5.3 -30.0	2.1	70	4.3	5.3	---	+0.025 -----	+39	15/
34	1974-82	7.50-44.44	1.4	24	1.3	7.21 ± .12	4.9	+0.028 ± .019	+13 ± 9	16/
35	1974-82	2.59-20.06	2.4	31.5	2.6	1.67 ± .18	1.3	+0.021 ± .006	+20 ± 6	17/
36	79 12 14	8.7 -20.7	1.3	25.7	1.3	8.68	---	+0.014 -----	+ 6.6 --	15/
37	79 12 13	5.4 -13.6	2.6	50	4.0	5.38	---	+0.028 -----	+41 --	15/
39	79 12 13	6.5 -30.0	9.9	17.8	7.9	6.5	---	+0.017 -----	+49 --	15/
41	1975-81	11.81-41.85	2.6	18.7	2.1	9.34 ± .08	1.3	+0.017 ± .005	+10 ± 3	18/
46	1981-83	1.55-25.66	2.4	15.6	1.8	1.12 ± .18	1.9	+0.046 ± .011	+30 ± 7	19/
	1981-83	16.54-25.66	9.6	16.7	7.5	1.12 ± .18	1.9	-0.030 ± .053	-84 ±146	9/
	1975-83	4.54-16.08	1.6	15.6	1.2	1.13 ± .15	1.9	+0.118 ± .044	+51 ± 19	
	1975-83	1.55-3.93	30	15.6	23	1.13 ± .15	1.0	+0.0047 ± .039	+38 ±330	20/
48	1975-83	4.57-30.94	2.6	22	2.3	2.19 ± .25	1.2	+0.057 ± .006	+48 ± 3	21/
49	1976-82	4.84-31.55	2.0	17	1.6	1.05 ± .07	1.1	+0.140 ± .020	+82 ± 12	22/
	1976-81	1.85- 4.84	5.7	16	4.4	1.00 ± .18	1.0	+0.046 ± .040	+74 ± 64	
50	1975-82	2.53-19.29	1.5	15.6	1.1	1.59 ± .66	1.1	+0.142 ± .049	+57 ± 22	23/
51	1975-82	12.41-43.91	1.1	17.5	0.88	11.79 ± .35	1.9	+0.106 ± .019	+34 ± 6	24/

Table 5. -- Specific discharge or recharge at test-well sites estimated by "hydraulic" method (Continued)

[Positive values indicate discharge (upward flow); negative values, recharge (downward flow); plus or minus values indicate two standard deviation (approximately equal to the amplitude of variation); gradient adjustment factor is ratio of interpolated to measured vertical hydraulic gradient, as explained in text]

Test well site	Date or period of measurement	Depth interval (m)	Vertical intrinsic permeability ($x10^{-15} m^2$)	Integrated average temperature (°C)	Adjusted vertical hydraulic conductivity (mm/d)	Depth to water table (m)	Gradient adjustment factor	Vertical hydraulic gradient	Specific discharge (+) or recharge (-) (mm/a)	Footnotes
U.S. Geological Survey wells										
52	1975-82	20.32-44.81	6.6	20	5.6	17.45 ± .12	1.0	+0.0032 ± .0044	+ 6.5 ± 9.1	9/
53	1975-82	10.97-41.92	5.0	22.5	4.5	9.67 ± .14	2.1	+0.017 ± .011	+28 ± 17	25/
54	79 12 13	2.20-30.0	2.5	17.7	2.0	2.2	----	+0.129	+94	15/
55	1981-83	2.55-42.22	4.2	20	3.5	1.26 ± .17	1.0	+0.072 ± .009	+92 ± 12	26/
	1978-83	1.40-2.32	1.0	16	.76	1.31 ± .22	1.0	+0.221 ± .370	+61 ±103	9/
56	1981-83	4.51-42.46	2.1	17.6	1.6	3.38 ± .13	1.0	+0.120 ± .013	+70 ± 8	26/
	1975-83	4.51-22.81	1.7	17.0	1.3	3.38 ± .11	1.0	+0.079 ± .007	+37 ± 3	27/
	1981-83	23.27-42.46	2.8	19.1	2.1	3.38 ± .13		+0.167 ± .029	+130 ± 22	28/
57	83 03 05	6.16-41.35	2.6	16.5	2.0	1.06 ± .38	1.7	+0.102 ± .012	+74 ± 8	29/
	1975-82	1.73-5.71	1.2	15.5	0.90	1.06 ± .35	1.0	+0.215 ± .051	+71 ± 17	
58	1981-83	3.08-42.08	3.7	14.6	2.7	.79 ± .12	1.0	+0.096 ± .018	+95 ± 10	30/
	1975-83	1.02-2.63	10	15.5	7.5	.75 ± .21	1.0	+0.032 ± .032	+88 ± 88	20/
59	1975-82	6.85-45.10	3.9	24	3.7	4.47 ± .19	1.7	+0.018 ± .006	+25 ± 8	31/
60	1982-83	3.11-41.51	3.8	18.5	3.1	1.90 ± .17	1.0	+0.079 ± .009	+89 ± 10	26/
	1975-83	3.11-30.22	3.2	18.0	2.6	1.94 ± .13	1.0	+0.096 ± .008	+91 ± 8	
	1982-83	30.68-41.51	6.3	20.4	5.3	1.90 ± .17	1.0	+0.043 ± .024	+85 ± 46	
63	1975-80	9.81-29.09	3.2	17.6	2.6	9.10 ± .20	1.0	+0.054 ± .009	+51 ± 9	32/

Table 5. -- Specific discharge or recharge at test-well sites estimated by "hydraulic" method (Continued)

[Positive values indicate discharge (upward flow); negative values, recharge (downward flow); plus or minus values indicate two standard deviation (approximately equal to the amplitude of variation); gradient adjustment factor is ratio of interpolated to measured vertical hydraulic gradient, as explained in text]

Test well site	Date or period of measurement	Depth interval (m)	Vertical intrinsic permeability ($\times 10^{-15} m^2$)	Integrated average temperature (°C)	Adjusted vertical hydraulic conductivity (mm/d)	Depth to water table (m)	Gradient adjustment factor	Vertical hydraulic gradient	Specific discharge (+) or recharge (-) (mm/a)	Footnotes
U.S. Bureau of Reclamation wells										
10	79 12 14	7 - 50.2	3.8	53	6.1	7	---	+0.017	+40	15/
13	1975-82	10.00- 66.14	3.9	19.2	3.2	5.15 ± .45	1.0	-0.037 ± .004	-43 ± 5	
	1978-82	67.06-152.40	.84	53	75	5.23 ± .30	1.0	+0.0037 ± .0008	+ 1.0 ± 0.2	
14	1975-82	12.65-158.96	1.11	132.7	4.2	6.18 ± .90	1.0	+0.024 ± .007	+37 ± 11	

Footnotes:

1/ Water table defined by water surface in nearby drain.
2/ Slow upflow in annulus above well screen.
3/ Slow upflow in annulus but well screen appears to be isolated.
4/ No significant flow in annulus.
5/ Lateral flow of cool water at about 30 m; possibly also at 20 m.
6/ Strong upflow in annulus; possible lateral flow of cool water at 28 m.
7/ Well screens appear to be isolated.
8/ Some upflow in annulus; possible lateral flow of warm water
9/ Gradient reverses at times.
10/ Lateral flows of cool and warm water at several depths; gradient reverses at times.
11/ Upflow in annulus; probable lateral flow of cool water at 36 m.
12/ Upflow in annulus, mostly above about 28 m.
13/ Lateral flow of warm water at 18 m.
14/ Lateral flow of cool water 37 m.
15/ Based on interpolated gradient.
16/ Lateral flow of cool water at 37 m; upflow below 37 m.
17/ Possible lateral flow of warm water at 12 m.
18/ Slow upflow in annulus; lateral flow of cool water at about 34 m.
19/ Upflow in annulus; especially upper part.
20/ Gradient reverses abruptly after intense precipitation events
21/ Slow upflow in annulus.
22/ Upflow in annulus, but well screen appears to be almost isolated.
23/ Slow upflow in annulus, chiefly above 17 m.
24/ Position near edge of terrace results in a larger vertical hydraulic gradient than normal at this depth for water table.
25/ Upflow in annulus, especially above about 20 m.
26/ Annulus cemented.
27/ Annulus of deeper well not cemented; may be some upflow.
28/ Annulus of shallower well not cemented.
29/ Annulus cemented but seal apparently incomplete.
30/ Annulus cemented; only site having reverse temperature gradient.
31/ Upflow in annulus, especially between 16 and 32 m.
32/ Vertical intrinsic permeability poorly known.

Table 6. -- Estimated rates of evapotranspiration from ground water for various types of phreatophytes or surface conditions

(Data from P. A. Glancy, written commun., 1979)

Type of phreatophytes or surface conditions	Annual evapotranspiration rate (mm)
Perennially free water surface	1,200
Irrigated pasture or cropland; assumes 300 mm use per cutting of alfalfa	900-1,200
Seasonally free water surface	600
River-channel and riparian vegetation	450
Marsh grasses growing in a dominantly non-saline environment and (or) dense assemblage of salt cedar, greasewood, and salt grass	300
Salt grass dominant; locally includes minor amounts of greasewood and rabbitbrush	150
Greasewood dense or dominant, with or without rabbitbrush and (or) saltbrush with a thin understory of salt grass	100
Greasewood dominant but of moderate density; locally includes rabbit brush and (or) big sage and hairy horsebrush in sandy areas	60
Playa deposits containing scattered stands of pickleweed	45
Greasewood of low density and vigor; locally includes scattered rabbitbrush; playa deposits lacking vegetation	30
Greasewood of very low density and vigor	20
Area of deep water table lacking phreatophytes	0

Table 7 -- Summary of estimates of specific discharge or recharge at test-well sites

Test-well site	Long-term average depth to water table (m)	Estimates of specific discharge (+) or recharge (-) in mm/a: Hydraulic method	Vegetation method	Water-table depth relation (figure 8)	Value assigned for heat-flow
U.S. Geological Survey wells					
2	9.61	+23	+30	+22	+23
3	2.33	+ 3.2	+60	+67	+ 3.2
7	7.8	---	+30	+29	-15
8	3.29	-32	+60	+57	-32
9	9.13	+11	+30	+23	+11
10	2.83	+44	+30	+62	+44
11	11.5[1/]	---	0	+16	0
12	10.03	-35	0	+20	-35
13	3.07	+29	+30	+59	+29
17	2.93	-35	0	+61	-35
18	4.60	-11	+60	+47	-11
27	4.52	+39	+60	+48	+39
29	6.19	+31	+30	+37	+31
30	1.78	+31	+60	+73	+31
31	5.7	---	+60	+40	-15
32	6.88	- 5.9	+30	+33	- 5.9
33	5.3	+39	0	+42	+40
34	7.21	+13	0	+31	-45
35	1.76	+20	+30	+74	+20
36	8.6	+ 6.6	+30	+25	+ 6.6
37	5.4	+41	0	+41	+41

Table 7 -- Summary of estimates of specific discharge or recharge at test-well sites (Continued)

Test-well site	Long-term average depth to water table (m)	Estimates of specific discharge (+) or recharge (-) in mm/a: Hydraulic method	Vegetation method	Water-table depth relation (figure 8)	Value assigned for heat-flow
U.S. Geological Survey wells					
38	6.5	---	0	+35	-40
39	6.5	+49	+60	+35	+49
40	7.3	---	+30	+31	- 5
41	9.34	+10	+30	+23	+10
46	1.13	+30	+30	+80	+30
47	0.9	---	+30	+83	+85
48	2.19	+48	+60	+68	+48
49	1.00	+82	+30	+82	+82
50	1.59	+57	+30	+75	+57
51	11.79	+34	+20	+15	+34
52	17.45	+ 6.5	+20	+ 6.4	+ 6.5
53	9.67	+28	+20	+21	+28
54	2.2	+94	+60	+68	+94
55	1.32	+92	+30	+78	+92
56	3.38	+70	+45	+57	+70
57	1.06	+74	+30	+81	+74
58	.75	+95	+30	+85	+95
59	4.47	+25	+30	+48	+25
60	1.94	+89	+30	+71	+89
61	13.2	---	0	+12	0
63	9.10	+51	+30	+23	+25
64	3[1/]	---	+60	+60	+40

Table 7 -- Summary of estimates of specific discharge or recharge at test-well sites (Continued)

Test-well site	Long-term average depth to water table (m)	Estimates of specific discharge (+) or recharge (-) in mm/a: Hydraulic method	Vegetation method	Water-table depth relation (figure 8)	Value assigned for heat-flow
U.S. Bureau of Reclamation wells					
10	7[1/]	+ 40	0	+ 32	+ 40
13	5.15	- 43	+ 60	+ 43	- 43
14	6.18	+ 37	0	+ 37	+ 37

[1/] Estimated

inaccurate or uncertain data. Sources of error in the estimates and reasons for some of the variations are outlined in the following paragraphs.

In principle, the "hydraulic" method should provide a reliable estimate of specific discharge or recharge throughout the ground-water budget prism because the depth interval represented by most well pairs approaches the full thickness of the prism (water table to a depth of 45 m below land surface). However, application of this method involves two potentially serious sources of error: (1) The factor used to adjust measured vertical hydraulic gradients for the "short-circuit" effect of vertical flow of water in the annulus of the deeper well may be substantially in error; and (2) estimates of vertical hydraulic conductivity have a large range of uncertainty.

The "vegetation" method yields uncertain results because it is not based on actual hydraulic data. Moreover, the estimates by this method are not directly comparable with estimates by "hydraulic" method. The "vegetation"-method estimates represent only the rate of discharge from the uppermost part of the saturated zone, whereas the estimates by the "hydraulic" method represent all or most of the thickness of the ground-water budget prism. This fact accounts for the seemingly anomalous situation of consumptive use of water by phreatophytes (representing specific discharge) at sites where vertical hydraulic gradients recorded by well pairs indicate net specific recharge for all or most of the thickness of the budget prism. The data for USGS sites 8, 18, 32, and 34, and USBR site 13 all illustrate this case. At several other sites, the direction of vertical ground-water flow indicated by the two methods is the same, but the rates near the water table do not represent the rates at greater depth. However, in areas of major ground-water discharge by evapotranspiration, especially in the northern and eastern parts of the Upsal Hogback area, and in the wind-scoured depressions in the Soda Lakes area, ground-water discharge should, in principle, be roughly equal to the specific discharge through the entire ground-water budget prism.

The significant advantage of the "vegetation" method over the "hydraulic" method is that, for one of the two major purposes of the ground-water budget discussed in the next section, the specific discharge at the water table--ground-water evapotranspiration, not the specific discharge (or recharge) throughout the entire thickness of the budget prism, is the item of interest. (See p. 61).

Comparison of specific discharge with depth to the water table at selected test-well sites (table 7) indicates a fairly strong correlation. (See fig. 7.) The sites (most of which are in the Upsal Hogback area) were selected so as to

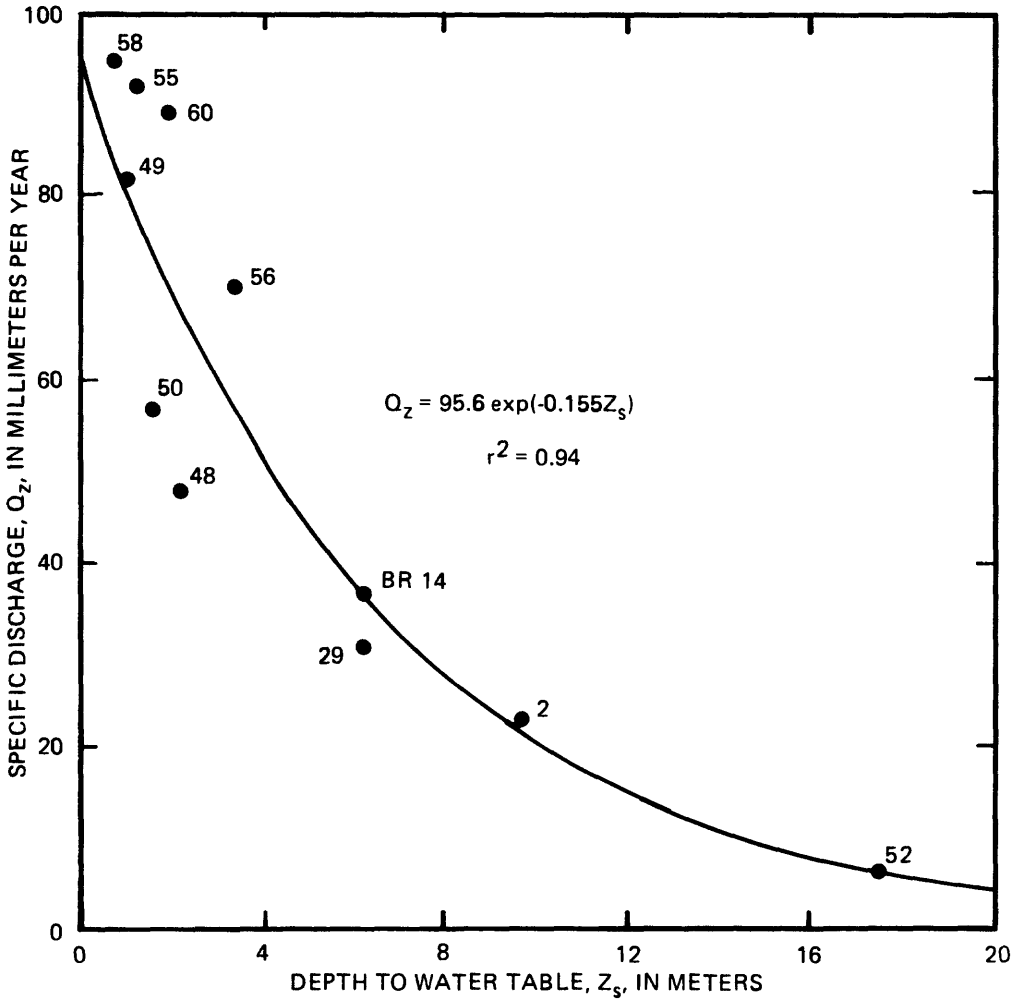

Figure 7. -- Specific discharge versus depth to water at selected test-well sites.

meet three criteria: (1) The site is within an area of ground-water discharge; (2) specific discharge is uniform throughout the depth range from the water table to a depth of 45 m (several sites were excluded at which lateral flows of cool or warm water above 45 m occur); and (3) vertical flow of water in the lower part of the annulus (immediately above the well screen) of the deeper well is negligible. The best least-squares fit to the data for 11 sites is given by the exponential function

$$Q_z = 95.6e^{-0.155\ z_s}$$

where Q_z is specific discharge, in millimeters per year (adopted value in table 8), and

z_s is depth to the water table, in meters.

The coefficient of determination (r^2) of 0.94 indicates a highly significant correlation of the logarithm of the specific discharge at a site with the depth to the water table. Scatter of the data is caused by the influence of factors other than depth to the water table, principally type of soil, vegetation, presence or absence of a salt crust, and other surface conditions and also by errors in the estimates of specific discharge. However, the correlation illustrated in figure 7 is believed sufficiently strong to be useful in deriving estimates of specific discharge as a function of depth to the water table for areas of major ground-water discharge.

As indicated by the equation above and its plot in figure 7, a water-table depth of 1 m corresponds to a specific discharge of about 82 mm/a and a water-table depth of 5 m to a specific discharge of about 44 mm/a. This relation and a map showing 1-m and 5-m lines of equal depth to water table were used to derive the areal variations in specific discharge shown in figure 8. Areas of specific recharge in figure 8 are indicated by data for test-well sites in the southern and western parts of the Soda Lakes area and at Upsal Hogback. The zero line in figure 8 represents the approximately located boundary between areas of upward and downward net vertical hydraulic gradient for the depth interval from the water table to 45 m, as measured in well pairs.

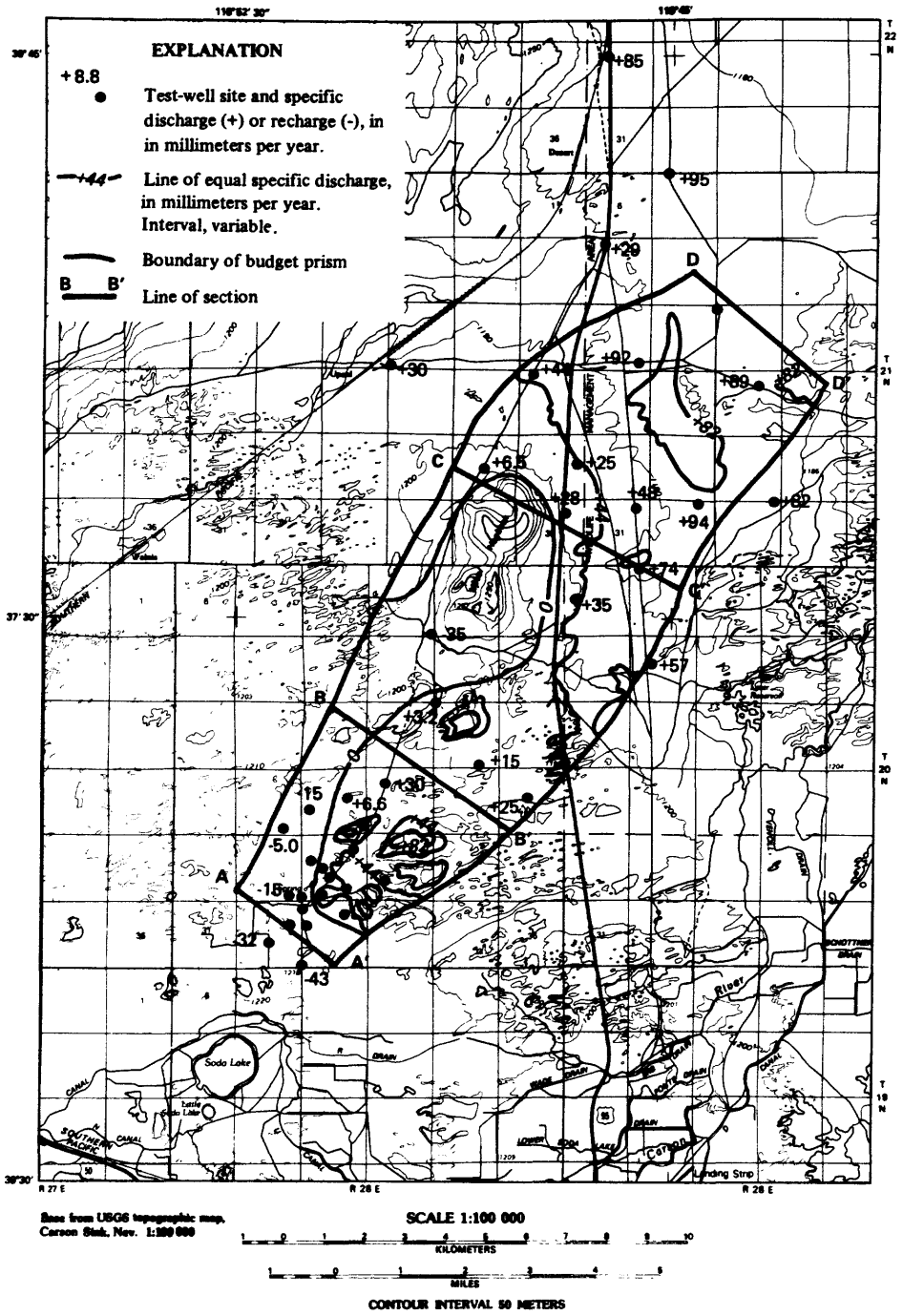

Figure 8. -- Ground-water budget prism showing estimated specific discharge or recharge between the water table and a depth of 45 m.

The values of specific discharge or recharge shown in figure 7 were integrated areally by planimeter to obtain the estimates of vertical ground-water discharge in table 8. Average specific discharge for the two upgradient subprisms is +13 mm/a, but in the down-gradient subprism (C-C' to D-D'), the specific discharge is substantially greater---+57 mm/a. Total vertical discharge for the 105.6-km^2 area of the entire budget prism was estimated to be 3.2 million m^3/a, which amounts to an average specific discharge of +30 mm/a.

As stated earlier (p. 31), the primary purpose of the ground-water budget was to estimate the discharge of thermal water from a deep source or sources. One of the items required for such an estimate is the specific discharge at the water table in response to ground-water evapotranspiration. Rates of evapotranspiration from ground water within the budget prism, based on the data in table 6 (p. 46), are shown in figure 9. Total ground-water discharge by evapotranspiration was calculated for each budget subprism from the rates shown in figure 9, as summarized in table 9. Average rates for the three budget subprisms range from 23 to 32 mm/a; for the entire budget prism, the average is 28 mm/a, which amounts to a total discharge of 2.9 million m^3/a for the 105.6-km^2 budget area. Although the estimates of total discharge for the budget prism by the vegetation and hydraulic methods differ by only about 10 percent, the estimates for the three subprisms (compare tables 8 and 9) differ more substantially. In part, the lack of agreement of the estimates for the subprisms by the two methods is only apparent and reflects the difference in depth zones considered (see discussion on p. 50), but in part, the lack of agreement is real, as discussed in the next section "Summary of the ground-water budget estimates".

Table 8. -- Estimated vertical ground-water discharge between the water table and a depth of 45 m within ground-water budget subprisms

Specific discharge (+) or recharge (-) (mm/a)		Subprism A-A' to B-B'		Subprism B-B' to C-C'		Subprism C-C' to D-D'	
Range	Average	Area (km^2)	Discharge ($x10^3 m^3/a$)	Area (km^2)	Discharge ($x10^3 m^3/a$)	Area (km^2)	Discharge ($x10^3 m^3/a$)
0 to -44	-22	8.4	-185	18.1	-398	.8	-18
0 to +44	+22	9.1	+200	16.4	+361	7.8	+172
+44 to +82	+63	3.6	+227	8.4	+529	27.2	+1,710
>+82	+90	.5	+45	.8	+72	4.5	+405
Totals (rounded)		21.6	+290	43.7	+560	40.3	+2,300
Average specific charge for subprism (mm/a)		+13		+13		+57	

Entire budget prism:

Area---------- 105.6 km^2

Vertical discharge--- --------+3,200,000 m^3/a

Average specific discharge----------+30 mm/a

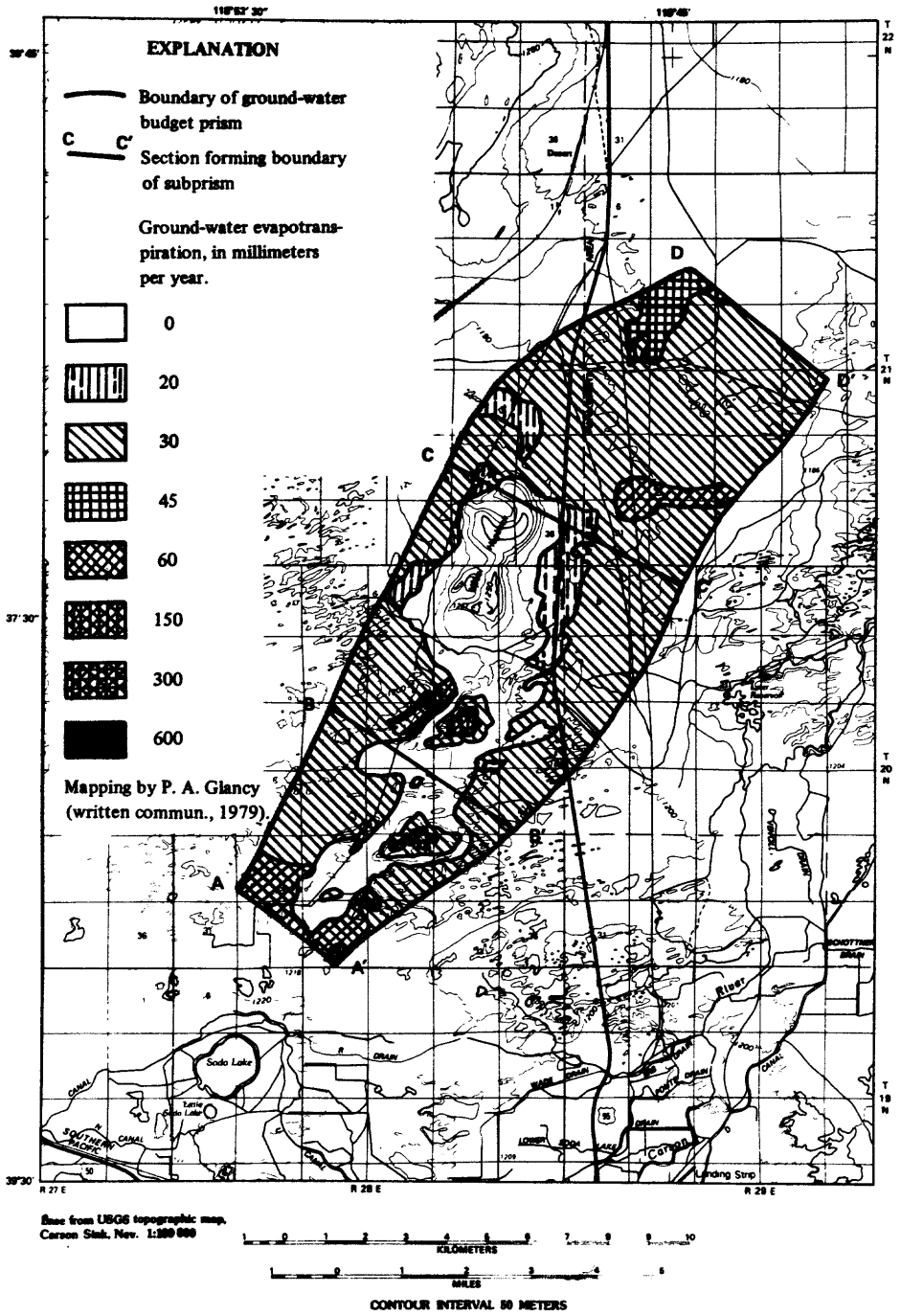

Figure 9. -- Ground-water budget prism showing ground-water evapotranspiration estimated on basis of phreatophytes and surface conditions.

Table 9. -- Estimated ground-water discharge by evapotranspiration within ground-water-budget subprisms, based on phreatophytes and surface conditions

Ground-water evapotranspiration rate	Subprism A-A' to B-B'		Subprism B-B' to C-C'		Subprism C-C' to D-D'	
(mm/a)	Area (km^2)	Discharge ($x10^3 m^3/a$)	Area (km^2)	Discharge ($x10^3 m^3/a$)	Area (km^2)	Discharge ($x10^3 m^3/a$)
0	6.53	0	16.5	0	0.79	0
20	0	0	3.47	69	1.91	38
30	11.3	339	22.6	678	33.3	999
45	0	0	0	0	2.34	105
60	3.35	201	.34	20	1.79	107
150	.14	21	.50	75	.17	26
300	.27	81	0	0	0	0
600	.02	12	.27	162	0	0
Totals (rounded)	21.6	650	43.7	1,000	40.3	1,300
Average rate for subprism (mm/a)	30		23		32	

Entire ground-water prism:
- Area---------- 105.6 km^2
- Evapotranspiration---------- 2,900,000 m^3/a
- Average discharge rate---------- 28 mm/a

Summary of Ground-Water Budget Estimates

As discussed previously, the primary purpose of the ground-water budget is to provide estimates of the discharge of thermal water from a deep source or sources into the upper part of the shallow ground-water subsystem. For this purpose, it is assumed that all the upflow of thermal water takes place in a fault-controlled conduit or conduits within subprism A-A' to B-B', which includes the hottest part of the shallow thermal anomaly. It is assumed further that estimates of lateral ground-water flow through sections A-A', B-B', C-C', and D-D', (table 3), and ground-water evapotranspiration from each subprism (table 9) are valid, and also that long-term change in ground-water storage within each subprism is zero. The unknown in the equation for each subprism is therefore ground-water inflow or outflow through the base of the subprism at a depth of 45 m. A part of this quantity in subprism A-A' to B-B' is thermal-water inflow through a conduit or conduits--the item of primary concern.

The budget is summarized in the diagrammatic longitudinal section in figure 10. The section extends along the axis of the budget prism, parallel to the ground-water flowlines, from section A-A' on the southwest to section D-D' on the northeast. Each budget item is represented by a distinctive arrow symbol indicating the direction and rate of ground-water flow, in thousands of cubic meters per year.

The estimation of thermal-water upflow into subprism A-A' to B-B' requires that all other budget items be known or estimated. Unfortunately, the upflow of nonthermal water through the base of the subprism cannot be estimated directly because vertical hydraulic gradients at a depth of 45 m are unknown. This results in having two unknown budget items for this subprism--the thermal and nonthermal upflow. Instead of a direct estimate of nonthermal upflow, therefore, an indirect estimate for subprism A-A' to B-B' was made on the basis of the assumption that the upflow rate per unit area for the entire budget prism changes linearly along the flow-paths. Using the upflow rate per unit area in the other two subprisms, an average rate and total upflow were then estimated for subprism A-A' to B-B' on the basis that the area of nonthermal upflow is 90 percent of the total area of the base of the subprism. The upflow rates for subprisms B-B' to C-C' and C-C' to D-D' could be estimated by difference because it was assumed that thermal-water upflow does not occur in those subprisms.

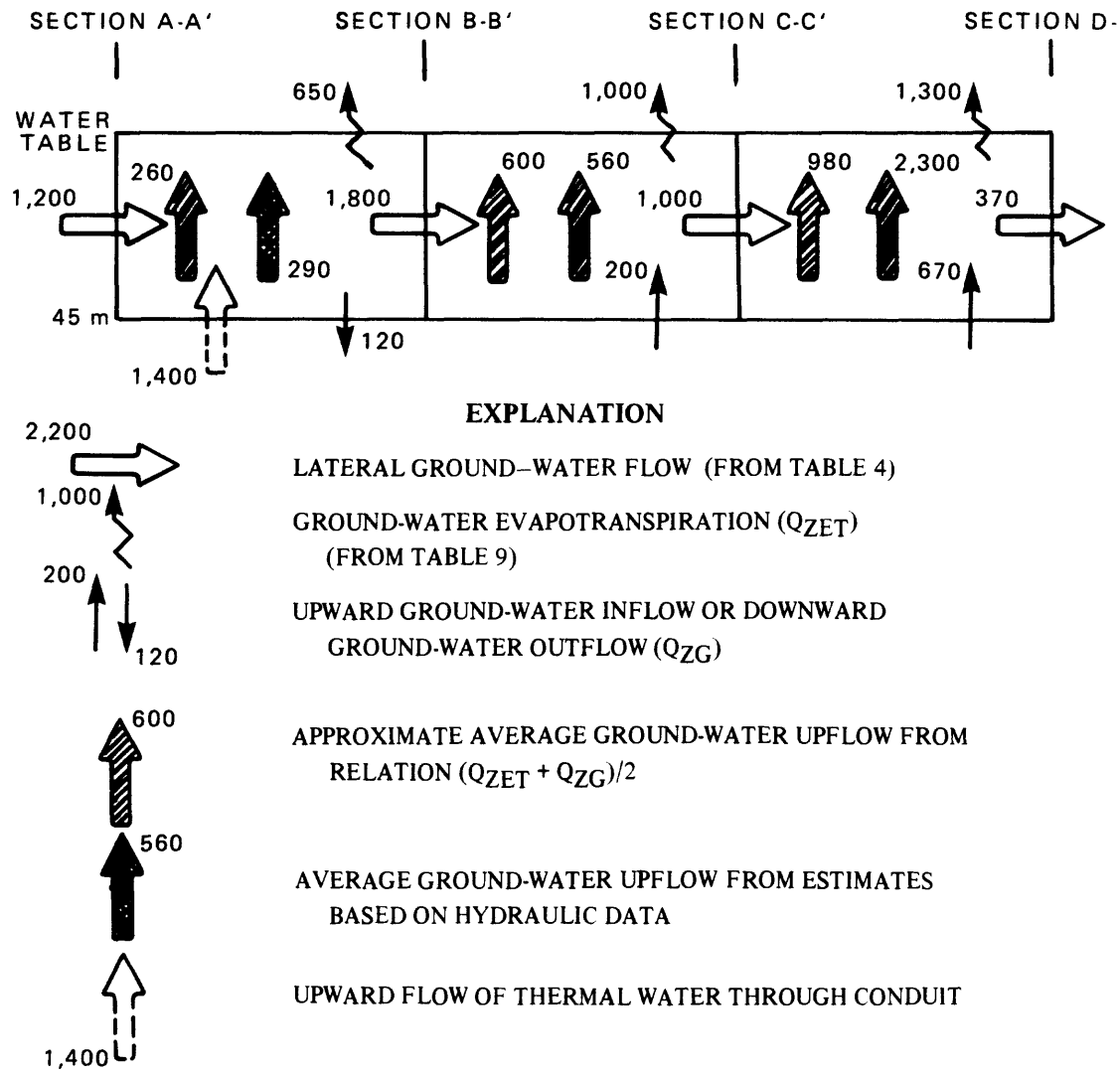

Figure 10. -- Diagrammatic longitudinal section of ground-water budget prism Showing budget items. Values are in thousands of cubic meters per year, rounded to 2 significant figures.

If the assumptions made in the ground-water budget shown in figure 10 are valid, the rate of thermal-water upflow is about 1,400,000 m^3/a (44 L/s). As shown in figure 10, if all the thermal-water upflow is by way of a conduit or conduits of very restricted lateral extent, the vertical flow of nonthermal ground water through the base of the subprism at a depth of 45 m is downward, rather than upward as in the other subprisms. The apparent downward flow may result from excess hydraulic heads in the aquifers into which the thermal water is injected laterally from the conduit or conduits, so that the water moves downward as well as upward from the overpressured aquifers.

The effect of parameter uncertainty on the estimate of thermal-water upflow was examined by applying the first law of propagation of errors (Till, 1974, p. 79). This was accomplished by assigning a standard deviation to each of the estimated items in the water budget. A more rigorous procedure would have been to evaluate the error for each of the items by estimating a standard deviation for each of the parameters used in the calculation. For example, the standard deviation of each of the estimates of lateral hydraulic gradient, lateral hydraulic conductivity, and width and thickness of the transmitting section would have been used in estimating the standard deviation of the lateral-flow estimates. This more rigorous procedure was not used because it was believed that the assignment of a standard deviation to each of the fundamental parameters would be no more accurate than the assignment to the budget items themselves. The chief problem is that many of the uncertainties, such as the sampling adequacy, cannot be accurately quantified.

Standard deviation was estimated to be 40 percent for the lateral-flow rates and 50 percent for ground-water evapotranspiration and nonthermal ground-water upflow or downflow. Using these values, a standard deviation of 860 x $10^3 m^3/a$ was obtained for the estimate of thermal-water upflow (1,400 x $10^3 m^3/a$) (fig. 10).

The rate of thermal-water upflow estimated by the water-budget method is compared with that estimated by hydrochemical and heat budgets in the final section, "Conceptual models of the hydrothermal system."

As stated on page 31, the secondary purpose of the ground-water budget was to estimate vertical ground-water flow rates above a depth of 45 m. These estimates can then be compared with estimates based primarily on measured

vertical hydraulic gradients and estimated vertical hydraulic conductivities (table 8).

Unfortunately, the budget does not provide estimates of the average vertical ground-water flow rates for the entire thickness of the budget prism. As discussed earlier (p. 50) ground-water evapotranspiration rates listed in tables 6 and 9 and shown in figures 9 and 10 represent vertical flow rates near the water table but do not necessarily represent rates at greater depths. Similarly, the rates of upward inflow or downward outflow at the bottom of the budget prism do not necessarily represent rates at shallower depths. The average of the vertical flow rates at the top and the bottom of the prism (shown by the solid-black arrows in fig. 10) furnishes a crude measure of the average vertical flow rate throughout the prism but does not necessarily correlate with the average vertical flow rate estimated from vertical hydraulic gradients and vertical hydraulic conductivities (table 5), shown by the cross-hatched arrows in figure 10. Thus, it is not possible to estimate vertical flow rates from the budget within narrow limits, nor is it possible to compare directly the estimates by the two methods.

Nevertheless, a few general conclusions may be drawn from the data. First, the rates of upflow (specific discharge) based primarily on estimated vertical permeabilities and measured vertical hydraulic gradients appear to be reasonable in spite of the large range of uncertainty in the values of vertical permeability assigned to the materials described in the lithologic logs of the test wells. That is to say, these rates do not differ from those indicated from the ground-water budget by a factor of more than 2. Second, the difference in flow rates indicated by the crude comparison described above suggests the possibility that the estimate of ground-water evapotranspiration in subprism C-C' to D-D' is low in comparison with the estimates in the other two subprisms. Thus, the assigned evapotranspiration rate of 30 mm/a appears to be too low for playa deposits lacking vegetation, especially for the areas of shallow-water table that characterize much of subprism C-C' to D-D', but it appears to be reasonable for areas of greasewood of low density and vigor where depths to the water table are large, which characterize much of the other two subprisms.

As discussed previously (p. 52) and shown in figure 7, data from wells in which vertical flows of water in the well annulus are small to moderate

indicate a fairly strong correlation of specific discharge and depth to the water table. Adequately controlled field studies are needed to define more precisely the effects of depth to water, soil type, vegetation, presence or absence of a surface crust of salt, and other factors on specific discharge at shallow depths.

Although it must be emphasized that the estimates are by no means firm, a reasonable conclusion is that average rates of ground-water upflow (specific discharge) above a depth of 45 m depend on depth to water as well as vegetation, soil type, and other surface conditions. Upflow rates probably do not exceed 100 mm/a except in small areas, principally wind-scoured depressions, and in the low-lying playa in the northeast part of the Upsal Hogback area, where the water table is at or near the land surface or a dense stand of phreatophytes is present. The average rates for the entire area of the budget subprism, as suggested by data in tables 8 and 9, may be about 30 mm/a. Vertical ground-water flow of this magnitude has a substantial effect on near-surface geothermal heat flow, as discussed in the section "Geothermal heat discharge."

AQUEOUS GEOCHEMISTRY

Major Constituents

Evapotranspiration is the major process affecting the aqueous geochemistry of ground water in the Carson Desert. The geochemical evolution of closed-basin water has been studied extensively, and some excellent overviews of the subject are available (see Eugster and Hardie, 1978; and Eugster and Jones, 1979). Brief consideration was given to the geochemical evolution of the surface water in the Carson Desert by Jones (1966). Although the details of geochemical evolution can be complex and are beyond the scope of this report, a brief discussion is presented to provide a framework for understanding the aqueous geochemistry of the study area.

The geochemical evolution of ground water is typified by a change in the dominant anion and a general increase in dissolved solids (see Freeze and Cherry, 1979, p. 237-302, for a general discussion of the subject). In the typical sequence, the initially dominant anion is bicarbonate and the final end member is chloride. This sequence has been used as an index of the "maturity" or relative age of water in a ground-water flow system. Within the chloride-dominated end member, the chloride concentration commonly is used as an additional measure of maturity or relative age because chloride is conserved in the aqueous phase over a wide range of concentration (up to saturation with halite).

The following discussion of the primarily chloride-dominated system in the western Carson Desert will use the chloride concentration as an indicator of the relative maturity of the ground water. Table 17 (end of report) lists the comprehensive analyses of water from test wells in the Soda Lakes-Upsal Hogback area. Additional water-quality data of mixed reliability are available for four wells in the Soda Lakes system that were bailed but not subsequently sampled for comprehensive chemical analysis:

Well number	Sampling depth: Below land surface (meters)	Sampling depth: Below water table (meters)	Specific conductance (micromhos)	Chloride (miligrams/liter
17A	9	7	≃6,700	≃1,900
34A	45	38	≃4,000?	---
39A	42	35	≃2,800	---
40A	41	34	≃3,300	---

Among the well waters listed in table 17 (end of report), those having *in situ* temperatures of 30°C or more are categorized arbitrarily as thermal (and represented by the letter T), and those with temperatures of less than 30°C are termed nonthermal[1/]. The nonthermal waters in table 17 are assigned to one of the following zones, on the basis of depth and salinity: A generally saline upper zone (U); a generally more dilute middle zone (M); or a saline lower zone (L).

The data in table 17 (end of report) indicate that vertical and horizontal variations in water quality are appreciable within the shallow ground-water subsystem. The variation in chloride concentration is shown in figure 11 (the line of section in figure 11 generally parallels the direction of lateral ground-water movement). The distribution of chloride indicates that the shallowest ground water is being affected by evaporation and perhaps by dissolution of chloride salts. A deeper zone, on the order of 15 to 45 m below the land surface, is relatively low in chloride,[2/] which suggests either that ground-water flow is more rapid, thereby allowing a flushing of soluble salts out of

---

[1/] The distinction made herein between thermal and nonthermal water is primarily for convenience in discussion and may not accurately reflect the origin or thermal history of the water. In principle, at least, a warm water could represent a shallow ground water heated conductively by adjacent thermal water of deep origin, whereas a cool water could represent a thermal water that has undergone extensive conductive cooling.

[2/] The lower chloride concentration at intermediate depth seems to be fairly consistent areally, even though some of the wells are as much as 5 km from the line of the section.

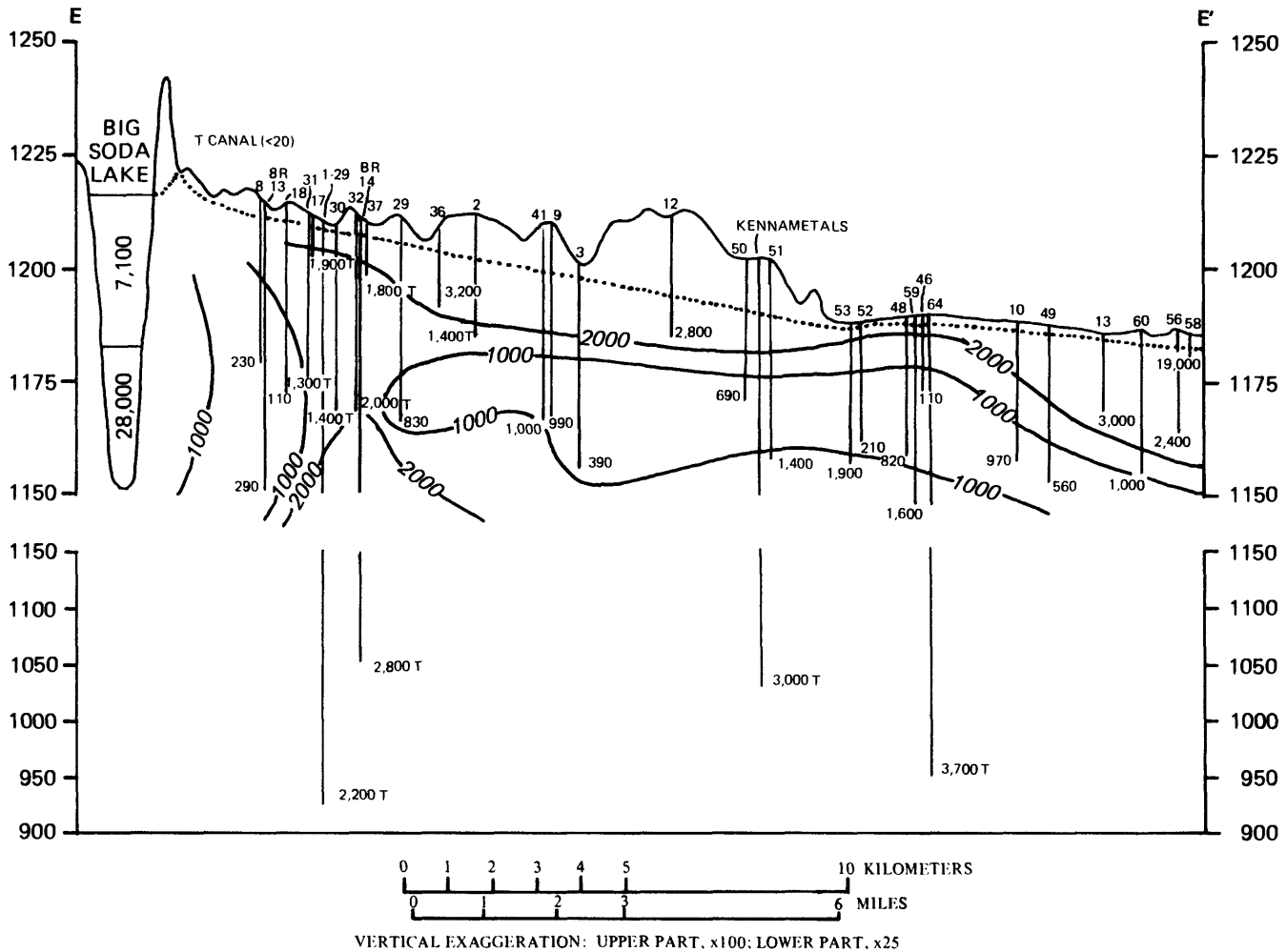

Figure 11. -- Chloride concentrations along section E-E' (pl. 2) extended. Wells situated away from line of section are projected to section along contours of confined water level for a depth of about 30 m (fig. 4). Dotted line indicates approximate position of water table at section E-E'. Chloride values for each well, in milligrams per liter, are shown at altitude of producing-interval midpoint. Thermal waters (>30°C) are indicated by "T". Lines of equal chloride concentration are approximately located. Data for Big Soda Lake are for 1980, on basis of information from Y. K. Kharaka (U.S. Geological Survey, written commun., 1983). Value for T Canal is based on U.S. Geological Survey data for Carson River.

this zone, or that concentrations of salts by evaporation has not affected the water at these depths as much as at shallower depths. Below about 45 m, chloride concentrations are greater, perhaps owing to evaporation during a period of dessication of Pleistocene Lake Lahontan. Although only chloride data are presented in figure 11, the same pattern would result in most places if either sodium or dissolved-solids data were used, because the linear correlation of chloride with sodium and dissolved solids is generally good.

Shallow to moderately deep ground water in the vicinity of the Soda Lakes has a high sulfate concentration (200-3,500 mg/L) relative to most water elsewhere in the study area (fig. 12). Because the lake basins are of volcanic origin, the sulfate may have been derived from the associated volcanic emanations. This indication is supported by the abundance of sulfate--as much as 6,990 mg/L as of 1980--in Big Soda Lake (Y. K. Kharaka, U.S. Geological Survey, written commun., 1983).

Sampled ground water from 33 to 62 m below the water table near the lakes contains 200-500 mg/L of sulfate. In contrast, shallower ground water (wells 4A, 36A, and 37A; 8 to 17 m below the water table) contains 2,200-3,500 mg/L. The high concentrations at shallow depths apparently result from at least one of the following processes: Evapotranspiration; dissolution of sulfate-rich evaporation residues; and, at well 36A and perhaps well 37A, steam loss.

Big Soda Lake and adjacent T Canal (figs. 11 and 12) may have a chemical as well as hydraulic influence on the southwesternmost part of the Soda Lakes geothermal system. The lake, which is about 4 km south-southwest of thermal wells USBR 14A and Chevron Resources 1-29, is a deep, saline water body that comprises two chemically different layers separated by a thin chemocline. The position of Big Soda Lake relative to the thermal wells, and the present-day concentrations of chloride and sulfate in the two layers, are shown in figures 11 and 12. Prior to inauguration of the Newlands Project irrigation system in the early 1900's, the lake was almost 20 m shallower and chemically homogeneous, with chloride and sulfate concentrations of about 45,000 and 13,000 mg/L, respectively (Chatard, 1890, p. 48). Chemical and bathymetric data for 1882 (Chatard, 1890, p. 48; Russell, 1885, pl. XVI) and 1980 (Y. K. Kharaka, U.S. Geological Survey, written commun., 1983), along with the bathymetric data of Rush (1972), indicate that Big Soda Lake has lost more than a third of its 1882 solute tonnage.

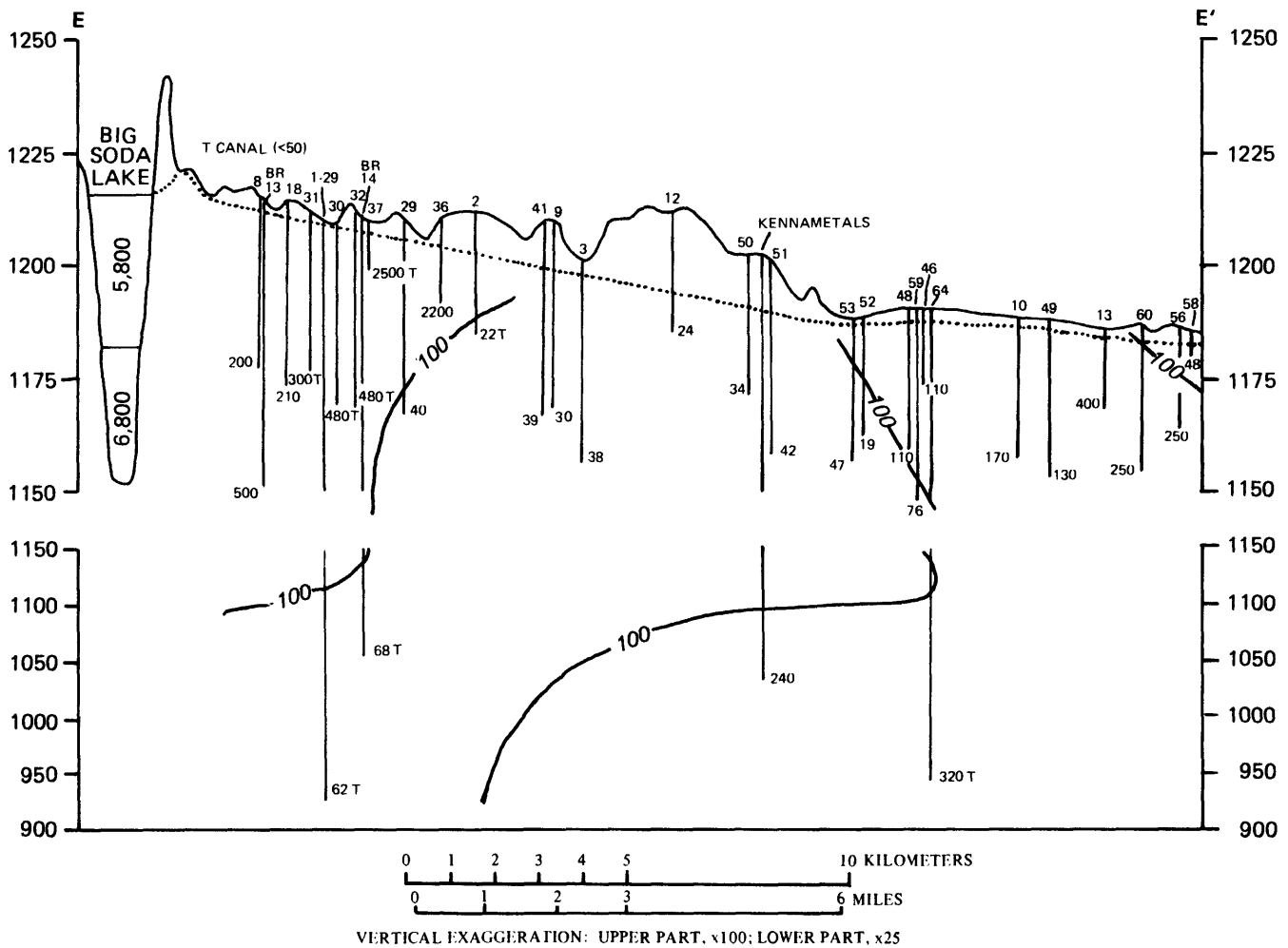

Figure 12. -- Sulfate concentrations along section E-E' (pl. 2) extended. Wells situated away from line of section are projected to section along contours of confined water level for a depth of about 30 m (fig. 4). Dotted line indicates approximate position of water table at section E-E'. Sulfate values for each well, in milligrams per liter, are shown at altitude of producing-interval midpoint. Thermal waters (>30°C) are shown by "T". Lines of equal sulfate concentrations are approximately located. Data for Big Soda Lake are for 1980, on basis of information from Y. K. Kharaka (U.S. Geological Survey, written commun., 1983). Value for T Canal is based on U.S. Geological Survey analytical data for Carson River.

[All quantities in thousands of megagrams]

1882	1980	Loss	
		Mega-grams	Percentage of 1882 tonnage
2,500	1,600	900	36

Most or all of this loss probably has taken place since the lake level began to rise in the early 1900's in response to intensive irrigation. Although the exact fate of the lost solutes is unknown, the salts presumably have been entrained as components of ground water moving hydraulically downgradient and away from the lake.

Counteracting the chemical influence of brine from Big Soda Lake is dilute leakage from the unlined T Canal (figs. 11, and 12). An average dissolved-solids concentration on the order of 150-200 mg/L for the river-fed canal seepage is suggested by data for the Carson River below Lahontan Reservoir.

Thus, ground water moving north-northeast toward the Soda Lakes geothermal system may include three components--saline lake seepage, dilute canal seepage, and native ground water of presumably intermediate salinity.

Estimated hydraulic properties of the uppermost 45 m of sedimentary deposits at section A-A' (table 4, fig. 6) suggest average mass flow rates (pore velocities) on the order of 70 m/a in a north-northeast direction, assuming an average effective porosity of 15 percent (table 2). As a result, leakage from Big Soda Lake or the T Canal could have moved as far as about 5 km (assuming displacement flow)--that is, to the vicinity of the hottest near-surface part of the Soda Lakes geothermal system--since the early 1900's.

Among the southernmost test wells in and adjacent to the Soda Lakes geothermal system, only well 8A, about 2-1/2 km north-northeast of the lake, currently (1980) yields water bearing the lake's chemical imprint. The similarity between anion proportions in the well water and in the lake is shown by figure 13--a diagram that depicts the relative abundance of major cations and anions in ground water and surface water within the adjacent to the two geothermal systems.

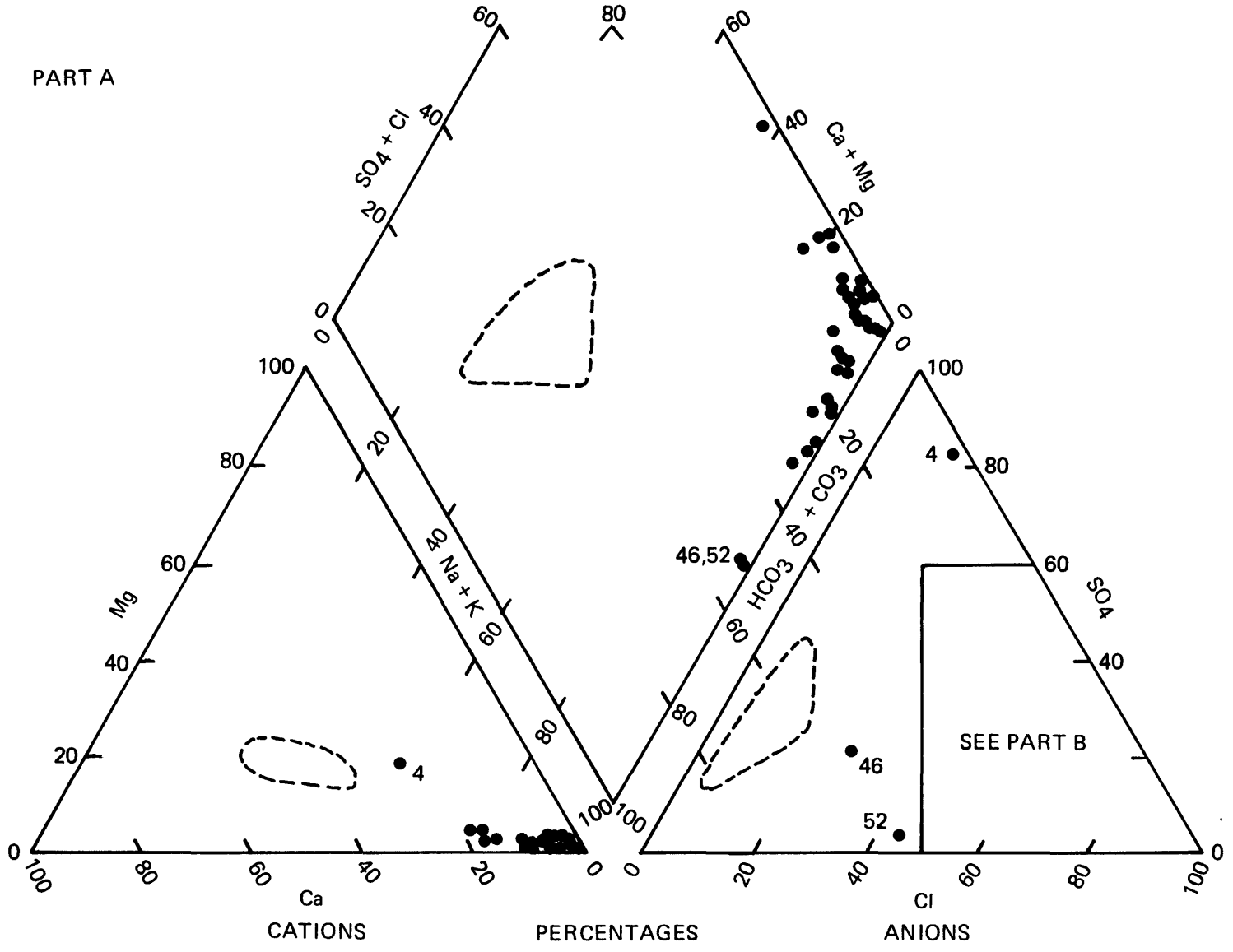
PART A
SO4 + Cl
Ca + Mg
Mg
Na + K
HCO3 + CO3
SO4
Cl
Ca
4
46,52
46
52
SEE PART B
CATIONS
PERCENTAGES
ANIONS

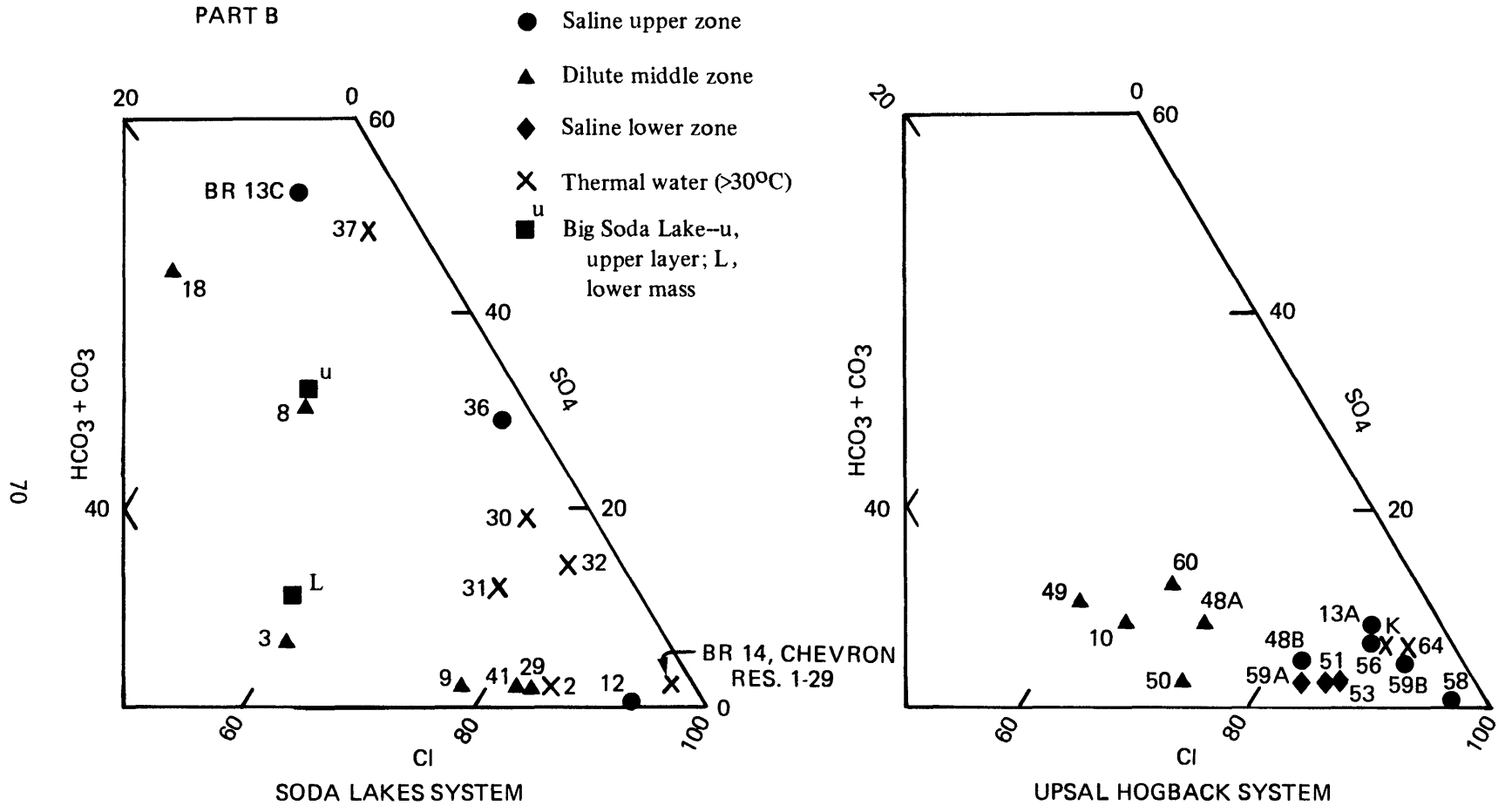

Figure 13. -- Proportions of major dissolved constituents in well water from the Soda Lakes and Upsal Hogback thermal systems, and in Big Soda Lake. Anion and cation percentages are based on milliequivalents per liter. Chemical symbols are explained in table 16. Part A shows combined data for both systems; abbreviated well designations are listed for selected sites; dashed boundary indicates limits of Geological Survey data for Carson River above and below Lahontan Reservoir. Part B shows anion proportions for each system and for Big Soda Lake; numbers indicate abbreviated well designations; K indicates Kennametals test well; data for Big Soda Lake from Y. K. Kharaka (U.S. Geological Survey, written commun., 1983).

Figure 13 also indicates that sodium is the dominant cation in both thermal and nonthermal ground water within the study area (the cation triangle in part A of the figure combines sodium and potassium, but the data in table 17 [end of report] show that sodium constitutes more than 90 percent of the combined total).

Minor Constituents

Minor constituents in geothermal water are of interest because of their potential value as an exploration tool and their possible impact on water use. Boron, fluoride, and lithium were analyzed most extensively because these constituents have proven to be good indicators of thermal water in other geothermal areas. Bromide, arsenic, and rubidium were examined for the same reason, although in lesser detail.

Above-normal concentrations of minor constituents in a water may indicate a thermal origin. However, evapotranspiration can concentrate the same minor constituents, along with conservative major constituents such as chloride, in nonthermal water. As shown in figure 14, boron and bromide correlate rather well with chloride, indicating that evapotranspiration may be the primary control for these minor constituents. Rubidium shows only a fair to poor correlation with chloride, indicating that evapotranspiration is probably not the only control for this solute. Fluoride and arsenic concentrations do not appear to be related to the chloride concentrations. Linear coefficients of determination (r^2 values) were calculated for each of the minor constituents with respect to chloride and are given in figure 14. The data for well 58B were excluded because the water from that well is much more concentrated than any of the other water sampled and inclusion of the data therefore would have biased the statistical results. The correlation with chloride was made in an attempt to evaluate more clearly the possible effect of evapotranspiration in the range of chloride concentrations (100-4,000 mg/L) found in most of the water sampled. The coefficients of determination calculated support the conclusion that the boron and bromide values are related to the chloride concentrations and that rubidium is only somewhat related to chloride.

For chloride concentrations greater than 1,000 mg/L, thermal water in the Soda Lakes system has higher lithium-to-chloride ratios than does nonthermal water (fig. 14). The thermal water has an average lithium-to-chloride ratio of

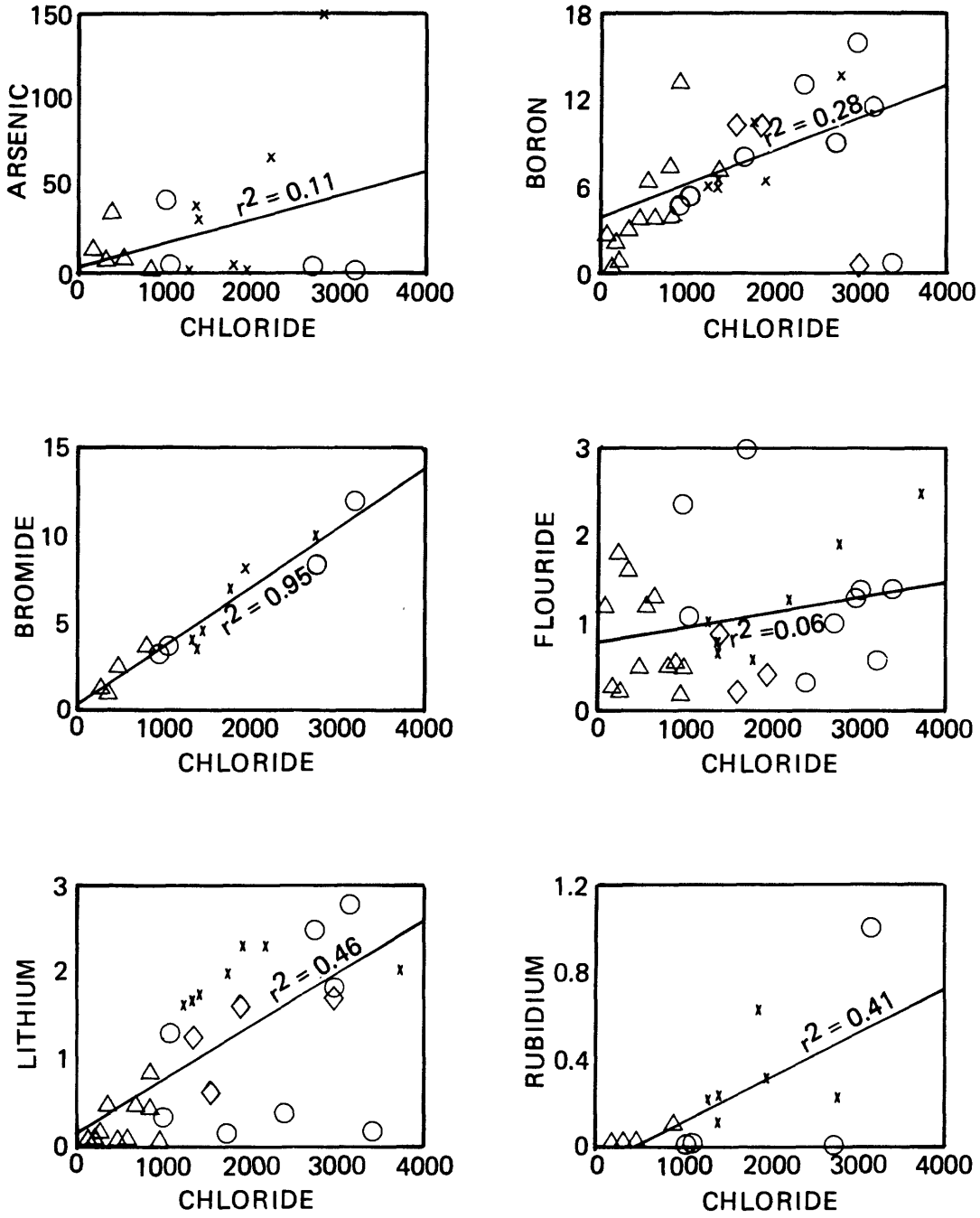

EXPLANATION

- ○ Saline upper zone
- △ Dilute middle zone
- ◇ Saline lower zone
- x Thermal water

Numbers indicate concentration in milligrams per liter

Figure 14. -- Plots of minor constituents versus chloride.

0.0012 (standard deviation, 0.0007), whereas nonthermal water having chloride concentrations greater than 1,000 mg/L has an average ratio of 0.00054 (standard deviation, 0.00046). In the Upsal Hogback system, however, the lower temperature thermal waters at well 64A and the Kennametals well have ratios within the the range found for the nonthermal water there. Thus, although the lithium-to-chloride ratio appears to be a fairly good indicator of thermal water, it should be used with caution.

Arsenic and fluoride are the minor constituents that appear to be least affected by evapotranspiration. Although arsenic is relatively high in well USBR 14A, the other thermal waters sampled do not appear to have a significantly higher concentration than the nonthermal water. Fluoride concentrations also show little relation to water temperature. Thus, neither arsenic nor fluoride seems to be a reliable indicator of a hydrothermal history in the study area.

A paucity of data limits evaluation of rubidium. The thermal-water samples all have rubidium concentrations greater than 100 μg/L, whereas the nonthermal water generally contains less than 100 μg/L. The only sample classified as nonthermal that has a distinctively high rubidium concentration is from well 36A. Although this may be a result of evapotranspiration of thermal water, the limited data prevent firm conclusions. The fair correlation between rubidium and chloride suggests that evapotranspiration may be at least partly controlling the rubidium concentrations. Additional rubidium analyses for water having chloride concentrations in the 2,000- to 4,000-mg/L range might help resolve this question.

Stable Isotopes

Studies of stable-isotope composition[1/] have demonstrated that meteoric water is the primary if not exclusive source of thermal water in most geothermal

---

1/ The stable isotopes evaluated are oxygen-18, relative to oxygen-16 ($^{18}O/^{16}O$), and deuterium (hydrogen-2), relative to hydrogen-1 ($^{2}H/^{1}H$). Each ratio is determined for a sampled water, and is then related mathematically to the comparable ratio for a standard of known isotopic composition. By convention, the computed results are expressed as "delta oxygen-18" ($\delta^{18}O$) and "delta deuterium" (δD), with the units of measure "per mil" ($^{o}/oo$). A negative delta value indicates that the sampled water is isotopically lighter than the standard (that is, the sampled water has a smaller proportion of oxygen-18 or deuterium, relative to oxygen-16 or hydrogen-1, than the standard).

systems. In general, the original isotopic composition of the water in liquid-dominated geothermal systems is modified only by a change in the proportion of oxygen isotopes. This change, commonly termed an "oxygen shift", is caused by exchange with the aquifer matrix and results in a heavier isotopic composition (less-negative delta value).

The isotopic composition of meteoric water generally falls along a regression line termed the "meteoric-water line" by Craig (1961). The general equation for the meteoric-water line is:

$$\delta D = 8\ \delta^{18}O + d.$$

Craig (1961) found a value of 10 for "d". In arid climates, the value for "d" is generally less than 10, and occasionally as low as 0. Evaporation affects both the δD and $\delta^{18}O$ values, resulting in a trend toward a heavier isotopic composition. The slope of this "evaporation trend," which depends upon isotopic fractionation between the liquid and vapor phases, is less than that of the meteoric-water line. The trend toward a heavier isotopic composition generally corresponds to an increase in chloride concentration, indicating that the main process responsible for the chloride increase is evaporation, rather than mineral dissolution. (If mineral dissolution were the dominant cause of the chloride increase, the isotopic composition would be unaffected.)

Figure 15 indicates that the isotopic composition of most thermal and nonthermal water in the study area appears to have been influenced primarily by evaporation [1/].

1/ The linear trend defined by the data in figure 15 has a slope that is typical of a system affected by evaporation, but transpiration also may have played a role. If so, figure 15 indicates that the combined effect of evaporation and transpiration on isotopic composition in the western Carson Desert is similar to the effect of evaporation alone. This in turn may indicate that (1) plant roots take up water having the same isotopic composition as the ground water being tapped, or (2) that transpiration results in an isotopic fractionation that is similar to the fractionation due to evaporation. Regardless, the term "evaporation" will be used in this section to describe the process or processes responsible for the loss of water at low (nonthermal) temperature.

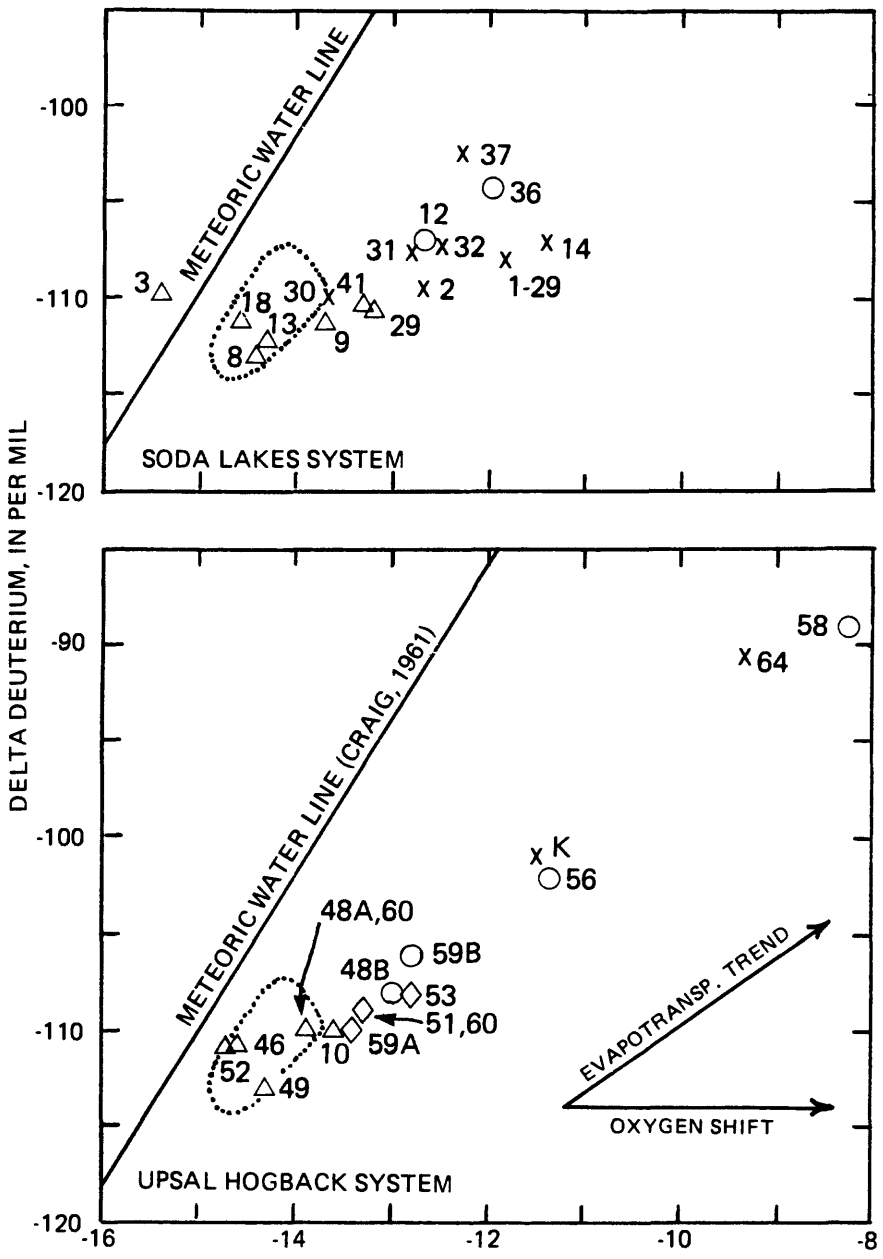

Figure 15. -- Stable isotope composition of selected well waters. Symbols: Circle, saline upper zone; triangle, dilute middle zone; diamond, saline lower zone; X, thermal water (>30°C). Numbers indicate abbreviated well designations (table 17); K indicates Kennamentals test well. Dotted boundary indicates limit of stable-isotope composition for relatively dilute ground water in the nearby Fallon area (Glancy, 1981, table 8).

The isotopic and chloride data, along with other hydrologic information, indicate that the thermal water in both the Soda Lakes and Upsal Hogback systems was modified significantly by evaporation prior to circulation downward to the deep, thermal part of the systems. In figure 15, the original isotopic composition of recharge to both the nonthermal and thermal systems would plot near the intersection of (1) a meteoric-water line applicable to the semiarid study area and (2) the evaporation trend defined by the data. The isotopically lightest middle-zone water sampled during this study and the rather dilute water (chloride concentrations generally less than 100 mg/L) sampled by Glancy (1981) in the nearby Fallon area appear to represent good approximations of the dilute, local recharge. Water having this isotopic composition would follow an evaporation trend defined by the nonthermal samples. Significant evaporation is indicated if the water sampled at Chevron Resources well 1-29 and well 64A is representative of unmixed thermal water at the two anomalies. The hydrostatic pressures present at the two sampling sites are far too great to be overcome by vapor pressure at reasonable temperatures (for boiling--vapor loss--to occur, the vapor pressure would have to exceed the existing hydrostatic pressure). Thus, a significant amount of evaporation must have occurred before the recharge water circulated to the deep, thermal part of the system, perhaps during a period of desiccation of Lake Lahontan. If the isotopic composition of the thermal water results from evaporation at shallow depths before deep circulation, then it is also evident (assuming no mixing) that the water at well 64A is not simply thermal water that has migrated northeast at depth from the Soda Lakes system.

Geothermometry

Quantitative geothermometers have been developed which allow reservoir temperatures to be estimated on the basis of the chemical composition of thermal water. The methods require that temperature-dependent equilibria exist at depth and that the composition of the water not change before sampling (Fournier and others, 1974). The most commonly used geothermometers involve (1) silica concentrations and (2) the relative proportions of principal cations. Several chemical geothermometers were applied to data from the study area; the results are presented in table 10.

One method of evaluating the results is to examine the internal consistency

Table 10.--Thermal aquifer temperature estimates

[Temperatures in degrees Celsius]

Well no.	Depth of sampling midpoint (meters)	Measured down-hole temperature (nearest 0.5°C)	Geothermometer estimates			
			Silica [1]		Na-K-Ca	
			Quartz, conductive	Chalcedony	$\beta = 1/3$ [2]	Magnesium-corrected [3]
U.S. Geological Survey wells						
2A	26	31.5	107	76	215	116
3A	44	24.5	76	45	184	125
4A	20	16.5	99	67	161	30
8A	38	18.0	98	66	160	160
			84	50	162	139
9A	40	19.0	82	49	164	91
12A	22	17.5	56	21	204	122
			77	43	201	112
29A	44	28.0	56	21	201	137
			34	-1	196	134
30A	40	102.0	152	126	158	158
			173	150	159	159
31A	38	35.0	74	40	189	76
32A	45	56.5	119	89	180	120
36A	21	27.5	117	86	200	157
			95	63	199	143
37A	13	57.5	152	126	191	115
41A	42	21.0	124	94	195	110
			116	88	197	118
46D	16	16.5	90	57	142	105

Table 10.--Thermal aquifer temperature estimates --(Continued)

[Temperatures in degrees Celsius]

Well no.	Depth of sampling midpoint (meters)	Measured down-hole temperature (nearest 0.5°C)	Geothermometer estimates			
			Silica [1]		Na-K-Ca	
			Quartz, conductive	Chalcedony	$\beta = 1/3$ [2]	Magnesium-corrected [3]
U.S. Geological Survey wells						
48A	31	26.5	101	69	158	76
48B	4.3	16.5	91	56	166	86
49A	32	18.0	95	63	136	96
50A	20	15.5	95	63	174	51
51A	44	18.5	88	56	170	48
52A	45	21.0	93	61	146	125
53A	42	24.5	103	71	162	55
56C	23	18.0	90	57	158	63
58B	2.9	16.0	56	23	194	194
59A	45	27.5	121	91	156	50
59B	4.5	13.0	75	42	99	19
60C	30	19.5	97	65	138	131
64A	244	77.5	150	124	173	120
			148	122	175	117
U.S. Bureau of Reclamation wells						
USBR 13A	15	18.0	110	79	179	56
USBR 13C	67	20.0	60	25	182	113
USBR 14A	159	144.5	169	146	141	134
Private wells						
Kennametals	174	-----	127	98	187	85
Chevron Resources 1-29	286	186	186	166	209	209

Table 10.--Thermal aquifer temperature estimates--(Continued)

1/ Calculated using the formulas as given in Fournier (1977).

2/ The Na-K-Ca geothermometer estimates using $\beta = 4/3$ were all greater than 100°C. The estimates using $\beta = 1/3$ are presented in accordance with the recommendation of Fournier (1977) that a value of 1/3 should be used for if the temperature estimate using a value of 4/3 is greater than 100°C.

3/ Calculated using the formulas given in Fournier and Potter (1979).

of the estimates. A plot of the magnesium-corrected Na-K-Ca (sodium-potassium-calcium) estimates versus the quartz-silica estimates is shown in figure 16. As discussed by Fournier and others (1974), waters that plot on the equal-temperature line are likely to be unmixed. Points below the equal-temperature line can represent waters affected by (1) mixing, (2) precipitation of calcite, (3) precipitation of silica, or (4) exchange of calcium for sodium at shallow depths. Points above the equal-temperature line can represent evaporative concentration or a high silica concentration due to equilibration with chalcedony or dissolution of volcanic glass or amorphous silica.

The thermal samples show a fair correlation between data for the quartz-silica geothermometer and the magnesium-corrected Na-K-Ca geothermometer. The quartz-silica estimate for Chevron Resources well 1-29 is less than that obtained using the magnesium-corrected Na-K-Ca method. The lower quartz-silica value could be a result of silica precipitation caused by cooling to a temperature of 186°C--the bottom-hole temperature at Chevron Resources well 1-29. The measured temperature of 199°C in Chevron Resources well 84-33 (W. R. Benoit, Phillips Petroleum Co., oral commun., 1983) suggests that the deep-aquifer temperature is closer to that indicated by the cation estimate than that by the quartz-silica estimate.

Within the Upsal Hogback thermal anomaly, only the sampled water from well 64A appears to have circulated to appreciable depth. The very good agreement between the cation and chalcedony temperature estimates implies that no mixing has occurred since equilibration at a temperature of about 120°C.

The silica and cation geothermometers yield unreasonable and inconsistent estimates when applied to the nonthermal samples. Because the proportion of major cations probably is controlled largely by exchange reactions with clay minerals, the cation geothermometers do not yield reliable results. An extreme example is the 194°C estimate for well 58B, where the water at a depth of only 2.9 m is cold and moderately saline. The unreasonably high quartz-silica estimates (such as for wells 50A, 52A, and 53A) indicate that the silica concentrations are not controlled by quartz. The most likely control is chemical kinetics (reaction rates).

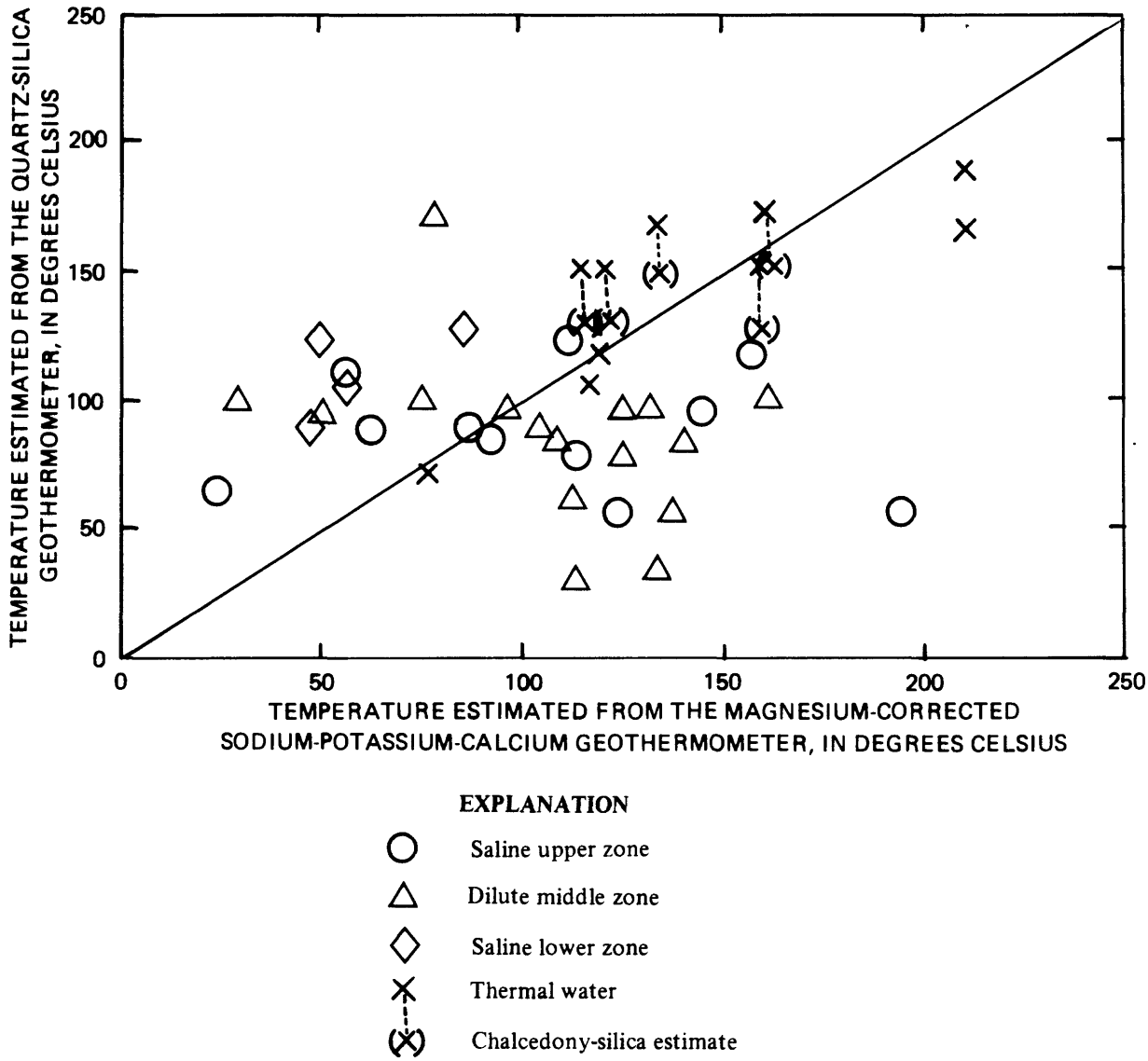

Figure 16. -- Comparison of thermal-aquifer temperature estimates by the quartz-silica and magnesium-corrected sodium-potassium-calcium geothermometers.

Geochemical History of the Thermal Water

Processes that can modify the chemical and isotopic composition of thermal water at shallow depths include (1) mixing with cooler water, (2) chemical precipitation, (3) cation exchange, and (4) loss of water vapor. For the Soda Lakes and Upsal Hogback systems, interpretation of the available data is complicated by the highly variable chemical and isotopic composition of the shallow, nonthermal water. This variability prevents the choice of a single end-member composition for cold water, making the use of mixing models tenuous at best. However,geochemical evidence (figs. 11-16) and hydrologic knowledge allow some reasonable speculations regarding the possible processes responsible for the variable composition of thermal and warm water (>30°C and 20-30°C, respectively) in the study area.

Soda Lakes System

The following discussion assumes that the water sampled at Chevron Resources well 1-29 best represents the thermal water in the Soda Lakes system.

1. Well waters 17A, 32A, USBR 14A and Chevron Resources 1-29 (temperatures, greater than 50°C; chloride, 1,900 to 2,800 mg/L) appear to be thermal waters that have not mixed with a major proportion of shallow nonthermal water.
2. In contrast, well waters 2A, 29A, 30A, 31A, and 41A (temperatures, 21-102°C; chloride, 900-1,400 mg/L) apparently are mixtures of thermal and nonthermal water.
3. Well water 3A (24.5°C and 340 mg/L of chloride) appears to have been heated conductively, although mixing with some cooled thermal water also is possible.
4. Shallow, sulfate-rich well waters 36A and 37A (27.5 and 58.0°C, and 3,200 and 1,800 mg/L of chloride, respectively) apparently have been influenced by at least one of the following processes: Steam loss, evaporation, or dissolution of sulfate-rich evaporite minerals.

The two hottest thermal waters, from USBR well 14A and Chevron Resources well 1-29, are somewhat dissimilar chemically. For example, water from USBR well 14A contains 2,800 mg/L of chloride, versus 2,200 mg/L for the deeper, hotter water from Chevron Resources well 1-29. This difference, along with

geothermometer evidence (fig. 16) suggests vapor loss at USBR well 14A. Yet, stable-isotope data (fig. 15) do not seem to support vapor loss, and the appppreciable depth of the producing interval at USBR well 14A (153 m below the water table) also argues against such a mechanism.

Upsal Hogback System

1. The highest temperature water, at a depth of 244 m in well 64A (77.5°C; about 3,800 mg/L of chloride), apparently represents conductively cooled, unmixed thermal water.
2. The shallower, warm water at wells 48A, 53A and 59A (24.5-27.5°C; 820-1,900 mg/L of chloride) reflects conductive heating, mixing of thermal and nonthermal water, or both.

Age of the Thermal Water

To help place a limit on the age of the thermal water in the Upsal Hogback system, a carbon-14 isotope analysis was made on a sample collected from well 64A. (Comparable data are not as yet available for the Soda Lakes system.) Although interpretation of the analysis is complicated by uncertainties concerning all possible sources and sinks of the aqueous inorganic carbon, several assumptions permit an estimate of maximum age for the water.

To estimate accurately the age of a water (that is, the time since recharge), the initial carbon-14 concentration must be known and all sources and sinks for carbon within the aquifer must be identified. Prior to large-scale thermonuclear testing above ground, the amount of carbon-14 in meteoric water had probably been fairly constant for several tens of thousands of years near a level that has been designated 100 pmC (percent modern carbon; Freeze and Cherry, 1979, p. 134). Assuming that concentrations less than 100 pmC arise only from radioactive decay of carbon-14, then the age of a water can be calculated using the equation:

$$t = -8{,}270 \ln R, \qquad (1)$$

where t = the age, in years, and

R = measured pmC/100 pmC (the measured percentage of modern carbon, divided by the assumed initial percentage), using a halflife of 5,730 years.[1/]

If additional sources have supplied carbon to the aqueous phase, corrections may be necessary. Possible sources of carbon other than the atmosphere (directly or through plant-root respiration) include dissolution of carbonate minerals and CO_2 from deeper (crustal or upper-mantle) sources. These sources would almost certainly provide "dead" carbon--that is, carbon with no carbon-14. If the amount of "dead" carbon supplied by these sources could be estimated, then the age could be calculated using the formula:

$$t = -8{,}270 \ln R + 8{,}270 \ln D \qquad (2)$$

where D is the fraction of dead carbon in the aqueous phase. Additional possible complicating factors include the exchange of carbon-14 for dead carbon--particularly at elevated temperatures--and mixing of waters of different ages.

An estimated age of water at well 64A can be calculated by applying several assumptions: (1) The sampling and analytical procedures provide an accurate estimate of the carbon-14 concentration; (2) no mixing has occurred; (3) the initial carbon-14 concentration was equal to 100 pmC; (4) no carbon-14 has been exchanged with "dead" carbon at depth; and (5) there are no other sources of "dead" carbon. Given these assumptions, equation (1) yields an age of 32,500 years, using the measured value of 2.0 pmC. The effect of the introduction of "dead" carbon on the age estimate can be evaluated by using equation (2). If half of the carbon were from a source of "dead" carbon (D value of 0.5), an age of 26,700 years would be indicated. Wigley (1975) has shown that values of less than 0.5 are unlikely in places where CO_2 is not generated below the water table. Therefore, if the other assumptions listed above are valid, then the water sampled at well 64A is probably more than 25,000 years

---

[1/] The halflife used in this report (5,730 years) is generally accepted as the more accurate value presently available. Published summaries generally use an earlier, less accurate value of 5,568 years to remain consistent with earlier calculations. Caution is therefore required if the ages calculated here are compared with other values.

old. Assumptions (1) and (3), above, would have to be severely violated to alter this conclusion. Thus, if mixing of thermal and nonthermal water, addition of significant amounts of CO_2 from the deep crust or upper mantle, and isotopic exchange of carbon are assumed to have been unimportant, then the age of water from well 64A is probably in the 25,000- to 35,000-year range.

SUBSURFACE TEMPERATURE, HEAT STORAGE, AND HEAT DISCHARGE

Temperature-Depth Profiles in Wells

The principal basis for the temperature and heat-flow studies consisted of measurements of temperature in relation to depth--temperature-depth profiles--in test wells. The temperature-depth profile data fall naturally into two subsets: (1) Data from deep test wells--wells 150 m or more in depth--drilled by private exploration companies, the U.S. Bureau of Reclamation, ERDA, (one well), and the U.S. Geological Survey (one well); and (2) data from shallow test wells--wells 45 m or less in depth--drilled by the U.S. Geological Survey or by the Bureau of Reclamation under the direction of the Geological Survey. Data from each of these subsets are discussed in the following paragraphs.

Deep Test Wells

Most information about the distribution of temperature with depth and the influence of convection on temperature and heat flow in the Soda Lakes geothermal system was obtained from "deep" wells ranging in depth from about 150 to 1,356 m. Much less is known about the Upsal Hogback geothermal system, where only one well--64A, 305 m in depth--was drilled deeper than 45 m. Most of the "deep" wells in the Soda Lakes area were drilled by private companies; temperature data from these wells is given in publications of the University of Utah Research Institute (1979f through j). In addition, data were obtained from two wells about 150 m deep drilled by the Bureau of Reclamation (USBR wells 13B and 14A), and from the ERDA Lahontan No.1 well, which was cased to a depth of 1,356 m (J. H. Sass and T. H. Moses, Jr., written commun., 1977).

Temperature-depth profiles in all these wells are shown in figure 17. Profiles in two of the wells in the shallower subset--DH-30A and DH-32A, both in the hottest near-surface part of the Soda Lakes geothermal area, are shown also for comparison. One group of profiles, those in which the temperature gradients in the upper part are high, exhibit features clearly related to both vertical and lateral heat transport by ground-water flow (convection or advection). The other group, the profiles in which gradients in the upper part are relatively low, appear to be dominated throughout by conductive heat transport. However, subtle effects of convection or advection may be discerned in some of these profiles, as well. Profiles of the first group characteristically have one or

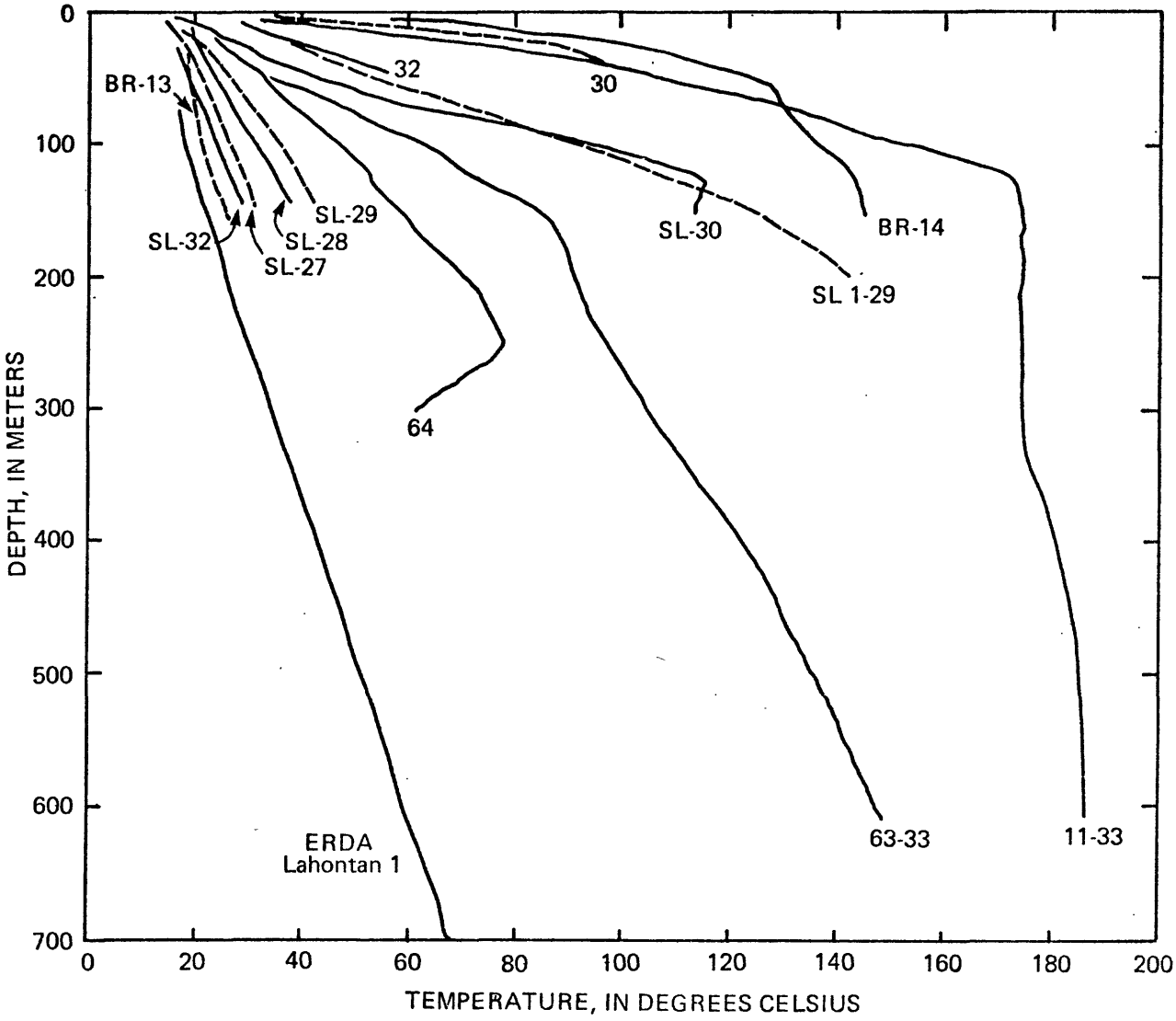

Figure 17. -- Temperature-depth profiles in deep test wells in Soda Lakes and Upsal Hogback geothermal areas.

more inflection points (abrupt changes in gradient) above which the gradient is high and below which it decreases markedly, becomes nearly zero, or even reverses (as in 64A and Chevron Resources SL-30). Depths of inflection points range from about 20 m in wells 30A and USBR 14A to 245 m in well 64A. Possible explanations for the inflection points and other features of the profiles are reviewed in the discussion of subsurface temperature distribution in a later section.

Shallow Test Wells

Temperature-depth profiles in Geological Survey test wells 45 m or less in depth are shown in figure 18 for the Soda Lakes geothermal area and in figure 19 for the Upsal Hogback geothermal area. Except for wells 11A and 17A, which are less than 10 m deep, only the parts of the profiles below depths characterized by significant or measurable seasonal temperature fluctuation--about 10-14 m in the study area--are shown. Some of the profiles in figures 18 and 19 are shown with dotted or dashed lines in order to distinguish them from other profiles where the lines are crowded or cross each other.

Most of the temperature-depth profiles in figures 18 and 19 show a roughly linear increase in temperature with depth or show small to moderate variations in gradient presumably related to differences in thermal conductivity among the materials penetrated. The temperature gradients, therefore, reflect the predominant effect of upward heat conduction at most sites and are affected only slightly to moderately by convection within the drill hole outside the well casing or in the formation beyond the drill hole. The methods used to estimate convective effects in the formation are described later (p. 106-108).

There are, however, significant departures from the foregoing generalization, especially in the Soda Lakes geothermal area (fig. 18). Temperature-depth profiles in wells 18A, 29A, 30A, 31A, 33A, 34A, and 38A all exhibit features that appear to be related to vertical or lateral transport of heat by groundwater flow. However, at least some of the irregularities could be due to upward or downward flow of water in the annulus between the well casing and the drill-hole walls: The annulus was not grouted with cement in any of the wells cited above. In the Upsal Hogback area, profiles in wells 56A (below 36 m), 58A, and 59A appear to be similarly affected, although flow in the annulus is less likely in two of these wells (56A and 58A) because they were grouted with

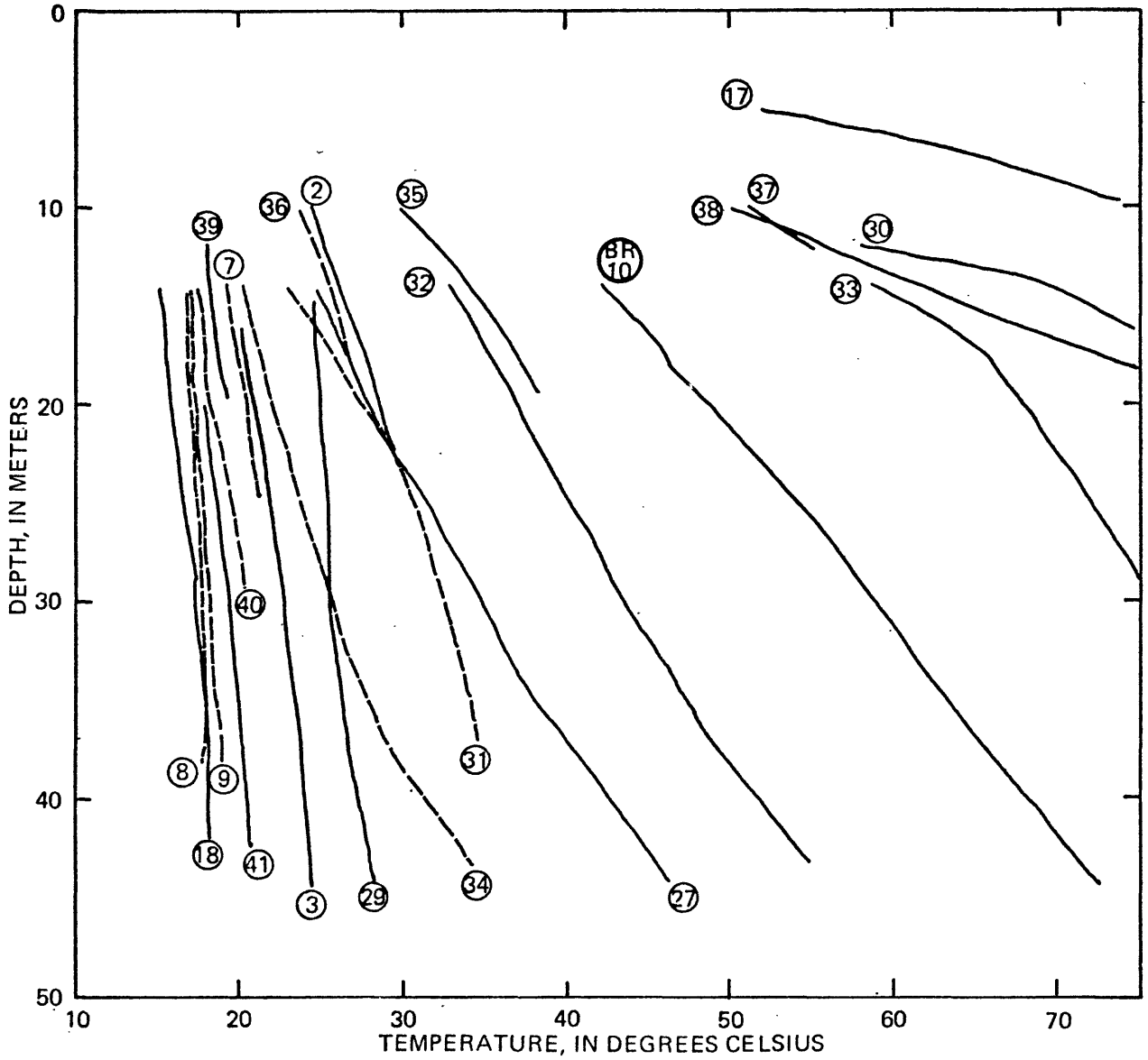

Figure 18. -- Temperature-depth profiles in shallow test wells in Soda Lakes geothermal areas.

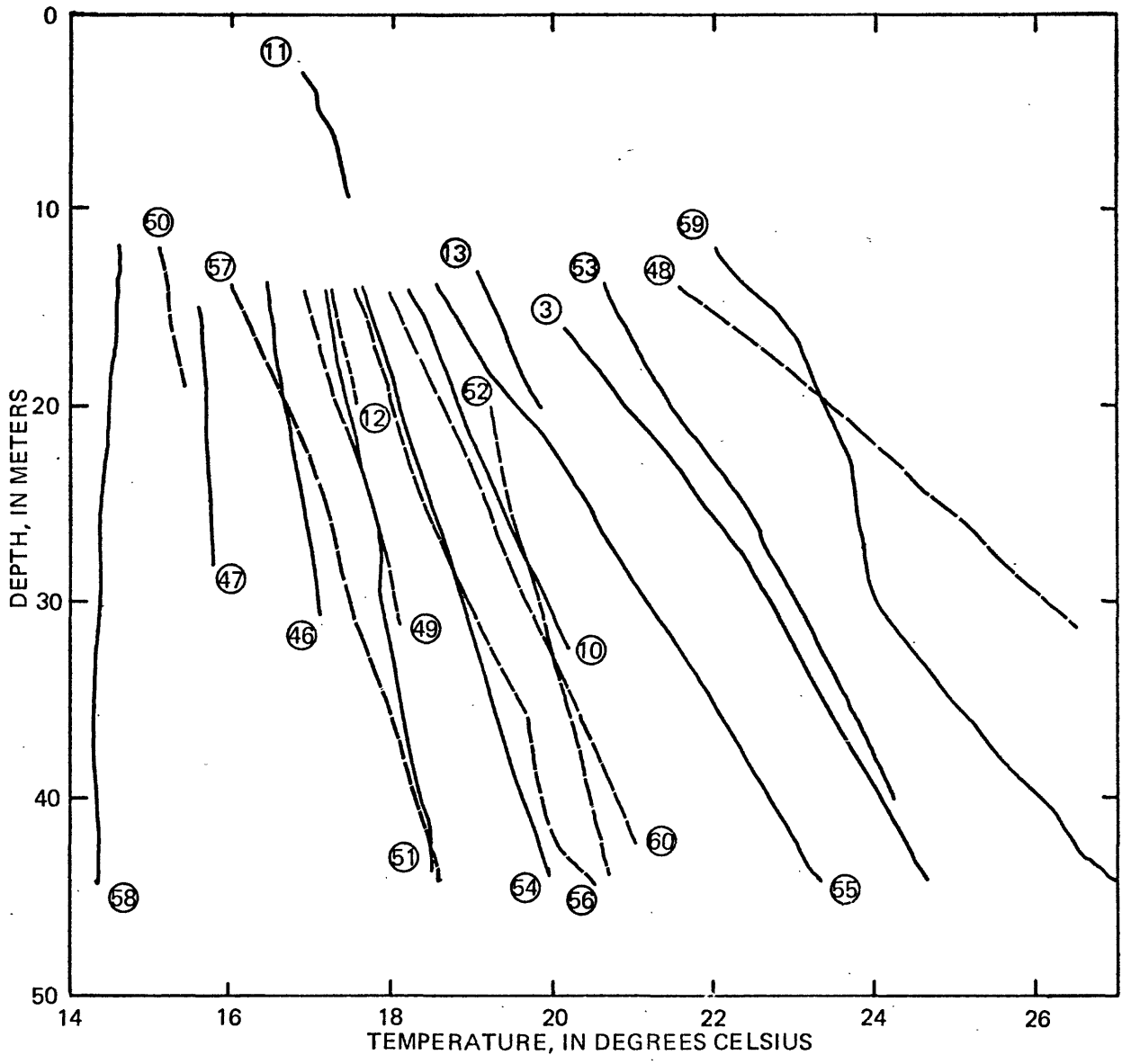

Figure 19. -- Temperature-depth profiles in shallow test wells in Upsal Hogback geothermal area.

neat cement. The profile in well 58A is unique in that it shows a decrease in temperature with depth (fig. 19).

Subsurface Temperature Distribution and Heat Storage

The subsurface temperature distribution in the study area may be characterized in a variety of ways, using the temperature-depth profiles described in the preceding section. A common procedure is to map temperatures at a particular depth datum, as was done at a depth of 30 m for the Soda Lakes geothermal area by Olmsted and others (1975, fig. 16). For present purposes, however, depth to the 150°C isotherm in the Soda Lakes area was selected in order to estimate heat stored above a depth of 3 km in that system. A temperature of 150°C was selected because that temperature was used as a lower limit for estimates of thermal energy stored in so-called "high-temperature" hydrothermal-convection systems in a National assessment by Renner, White and Williams (1975, p. 7). Present estimates of mean temperature, volume, and thermal energy in the geothermal reservoir at Soda Lakes may thus be compared with similiar estimates made in earlier resource assessments by the Geological Survey. (See Renner, White, and Wiliams, table 4, p. 16-17; Brook and others, 1979, table 5, p. 52-53.)

It was not possible to characterize the Upsal Hogback system in a manner similar to that used for the Soda Lakes system for two reasons. First, the highest temperature actually measured in the Upsal Hogback system was only 78°C at a depth of 245 m in well 64A; below that depth the temperature decreased steadily to 61°C at bottom depth of 305 m (fig. 17). The near-surface temperature and heat-flow anomaly appears to be the result of warm water from some unknown depth greater than 305 m leaking upward, thence laterally in an aquifer at a depth of about 245 m. Second, chemical geothermometry indicates a source temperature of only 120°C for the warm water at 245 m in well 64A (table 10). Thus, there is no evidence for the presence of 150°C water in the Upsal Hogback system. Any inference as to the depth and extent of such water or even of much cooler water would be unduly speculative on the basis of the meager data presently at hand.

Three data sets were used to indicate or estimate the depth to the 150°C isotherm in the Soda Lakes geothermal system: (1) Data from 3 deep wells that

actually recorded temperatures of 150°C or nearly 150°C; (2) temperature-gradient data from 10 wells from which depth to the 150°C isotherm was estimated by extrapolation; (3) near-surface heat-flow data obtained from shallow test wells in the marginal parts of the thermal anomaly from which the depth to the 150°C isotherm also was estimated by extrapolation. Depths to 150°C measured or estimated from the three data sets are shown in figure 20.

The first data set consists of the temperature profiles of Chevron Resources wells 11-33, 63-33, and SL 1-29 (UURI, 1979,f,j). Only one of these wells (11-33) actually penetrated the 150°C isotherm, but the other two encountered bottom-hole temperatures close to 150°C, and their profiles could be extrapolated with reasonable confidence to 150°C. (See fig. 17.) Temperature-depth profiles of all three wells exhibit features related to convection and (or) advection in their lower parts. For this reason, depths to the 150°C isotherm estimated on the basis of only the upper parts of the profiles would be too shallow. Clearly, the depths estimated from the second and third data sets must therefore be interpreted with caution, especially from those wells in the second set having high near-surface temperature gradients and heat flows.

Wells in the second data set include eight Chevron Resources temperature-gradient holes about 150 m deep, ERDA Lahontan No. 1, which was cased to a depth of 1,353 m, and USBR 13B, 157.5 m deep. Two assumptions were involved in extrapolating measured temperature gradients in all these wells to the depth of the 150°C isotherm: (1) Vertical heat transfer is conductive throughout the depth range of interest; and (2) the subsurface stratigraphy at each well site is represented by the section penetrated by ERDA Lahontan No. 1 (fig. 2). Temperature gradients below the bottoms of the wells were projected by adjusting the measured gradients for changes in thermal conductivity with depth.

A generalized summary of the stratigraphy and the values of thermal conductivity assigned to each major geologic unit and the corresponding depth interval is presented in table 2 (p. 25). Values of thermal conductivity assigned to the pre-Tertiary units are based on data for similar rocks reported in the heat-flow literature. (for example, see Sass and Munroe, 1974; Clark, 1966.) The value of 3.5 tcu assigned to the Quaternary deposits is approximately equal to the average estimated from logs of 42 shallow Geological Survey and Bureau of Reclamation test wells in the study area, using the values assigned to four categories of materials listed in table 3 (p. 36).

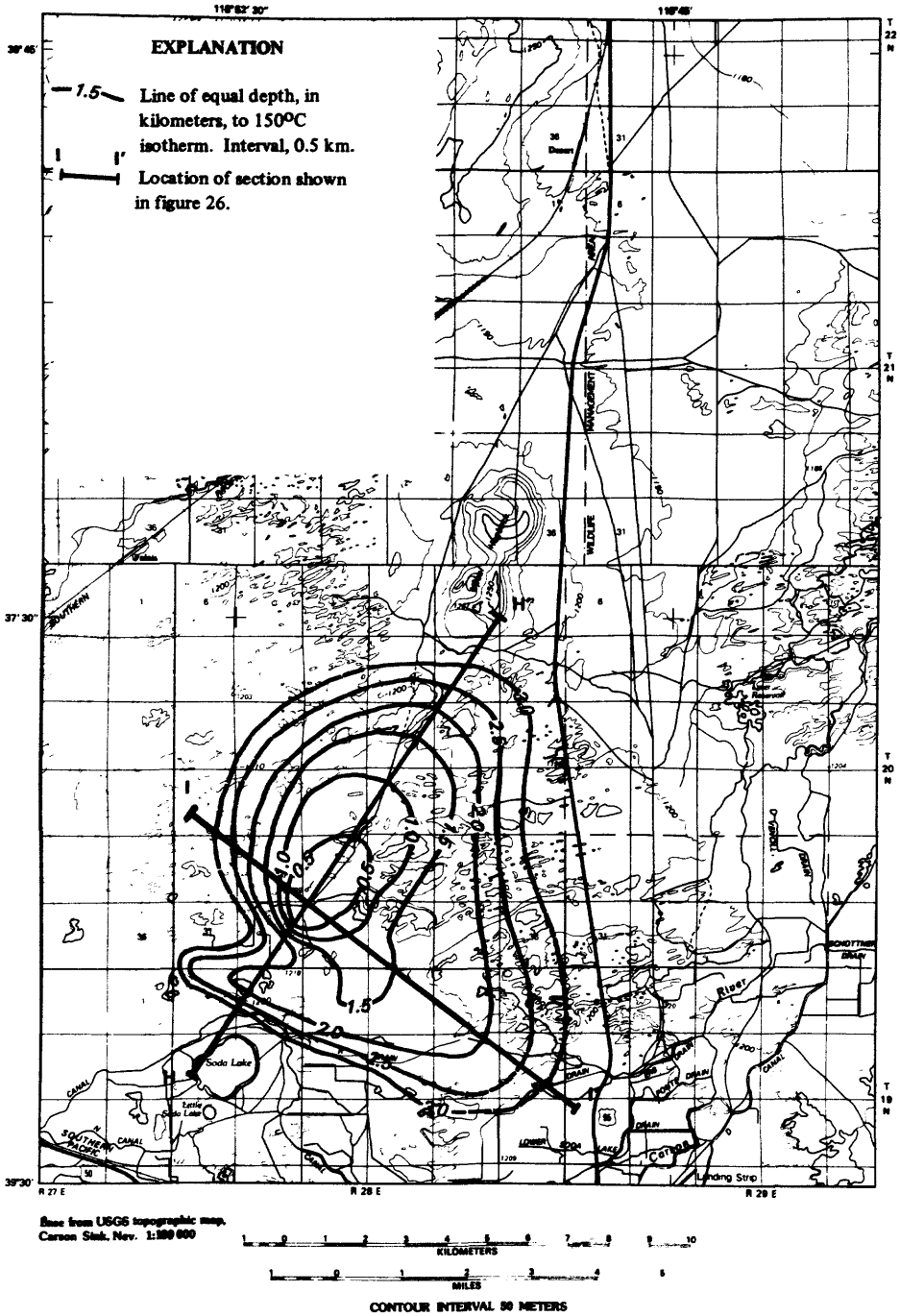

Figure 20. -- Depth to 150°C isotherm, Soda Lakes geothermal area.

The third data set consists of near-surface conductive heat flows estimated from data for shallow test wells in the marginal parts of the thermal anomaly. Derivation of these estimates is discussed in the section "Geothermal heat discharge".

Depth to the 150°C isotherm was estimated in the following manner. First, the conductive heat flow corresponding to each 0.5 km depth increment from 1.5 to 3.0 km was calculated as the product of the average temperature gradient from the land surface to the depth in question and the harmonic-mean thermal conductivity for that interval based on the values of thermal conductivity and thickness of major geologic units in table 2. The average temperature gradient was calculated as 135°C (the difference in temperature between 150°C and 15°C --the approximate mean annual temperature at land surface) divided by the depth in question. Next, heat flow used in the calculation above was adjusted to include a convective component resulting from upward ground-water flow in the near-surface deposits using a method given by Lachenbruch and Sass (1977, p. 641-643). (See equation 7 on p. 108.) In this calculation, upward flow at a rate of 30 mm/a (Darcian velocity) in the uppermost 100 m of deposits having a harmonic-mean thermal conductivity of 3.5 tcu was assumed. The pertinent data are listed below:

Depth to 150°C (km)	Average temperature gradient (°C/km)	Harmonic-mean thermal conductivity (tcu)	Heat flow at 100-m depth (assumed conductive) (hfu)	Surface heat flow (hfu)
1.5	90	4.01	3.61	4.73
2.0	67.5	4.22	2.85	3.74
2.5	54	4.36	2.35	3.08
3.0	45	4.56	2.05	2.69

Thus a surface heat flow of 2.69 hfu corresponds to a heat flow of 2.05 at a depth of 100 m, below which effects of upward ground-water flow are assumed to be absent. Finally, the location of the 1.5-, 2.0-, 2.5-, and 3.0-km lines of equal depth in figure 20 was determined by interpolation from a map showing near-surface heat flow (fig. 23), using the surface heat flows and corresponding

depths listed above.

The depth estimates from the third data set are the least certain of all the estimates because they are based primarily on data for only the uppermost 45 m. This interval is only a small fraction of the estimated depth to 150°C, and the effects of convection below 45 m could be substantial in places. All the projected depths--those from the second as well as the third data set--must be interpreted with caution, chiefly because of errors resulting from the assumption of a conductive heat-flow regime throughout the depth interval of interest, but also because of lateral variations in thermal conductivity and incorrect values of thermal conductivity assigned to the major geologic units. The net effect of all these errors is to underestimate the depth to the 150°C isotherm and thus to overestimate the volume of the system having temperatures greater than 150°C., as discussed below.

The volume of the geothermal reservoir in the Soda Lakes system was estimated using the data shown in figure 20. For present purposes, the geothermal reservoir is defined as that part of the system above a depth of 3 km having temperatures greater than 150°C. Volume of effective pore space was estimated as the product of the reservoir volume and the average effective porosity. (See table 11.) The average effective porosity was estimated using the assumed values listed in table 2. Reservoir volume was calculated as the sum of the volumes of the 0.5-km depth increments. Each incremental volume was calculated from the areas enclosed by the bounding depth contours and idealizing the irregular solid thus enclosed as the frustum of a cone. The volume of a cone frustum is

$$V = \frac{1}{3}\pi h(R^2 + Rr + r^2)$$

where h is the height, R is the radius of the base, and r is the radius of the top. In the calculations used, h is the thickness (depth increment) of the irregular solid, R is the radius of a circle having the same area as the base of the solid, and r is the radius of a circle having the same area as the top of the solid.

As indicated in table 11, the estimated reservoir volume above a depth of 3 km for the Soda Lakes system is 81 km^3. The standard error of the estimate

Table 11. -- Estimated volume of reservoir and of effective pore space more than 150°C, Soda Lakes geothermal system

Depth range (km)	Area of base (km^2)	Volume of reservoir (km^3)	Average effective porosity (percent)	Volume of effective pore space (km^3)
0.1-0.5	3.1	0.52	11.1	0.06
0.5-1.0	9.4	3.0	10.0	.30
1.0-1.5	19	7.1	7.6	.54
1.5-2.0	40	14	5.0	.70
2.0-2.5	56	24	5.0	1.20
2.5-3.0	72	32	2.0	.64
Totals or averages (rounded)	72	81	4.5	3.4

is $\pm$ 24 km^3. By comparison, Renner, White, and Williams (1975, table 4, p. 16-17) estimated a reservoir volume of 12.5 km^3 on the basis of a subsurface area of only 5 km^2 and a thickness of 2.5 km; and Brook and others (1979, table 5, p. 52-53) estimated a volume of 19.6 $\pm$ 11.3 km^3. The large difference between the present estimate and the two earlier estimates results from the much smaller areas assumed for the reservoir in the earlier estimates. The writers believe that, even allowing for the uncertainties in the present estimate, the volume of the reservoir must be several times greater than that of the earlier estimates.

The total heat content or reservoir thermal energy above a depth of 3 km is estimated to be 7.0×10^{18} cal on the basis of a mean reservoir temperature of 172°C, an ambient surface temperature of 15°C, a volumetric heat content of 0.55 cal/cm^3 C°, and a reservoir volume of 81×10^{15} cm^3. By comparison, the corresponding estimates of Renner, White and Williams (1975) and Brook and others (1979) were, respectively, 1.1×10^{18} cal and 1.8×10^{18} cal (7.5×10^{18} J).

Volume of effective pore space (which is an approximate measure of volume of recoverable fluid) was estimated to be 3.4 km^3 on the basis of the assumed effective porosities listed in table 11.

Geothermal Heat Discharge

Components of Heat Discharge

For present purposes, the discharge of geothermal heat from the Soda Lakes and Upsal Hogback thermal anomalies area may be regarded as comprising two components: (1) Anomalous or excess heat discharge--the heat discharge that results from convective heat transport by rising ground water including thermal water from great depths; and (2) regional or background heat discharge--the heat discharge that would have occurred at the land surface without the effects of ground-water upflow. The first component, of primary interest in this study, is used to estimate the rate of upflow of thermal water from the deep part of the hydrothermal system--the "geothermal reservoir". The second component presumably is equal to the heat rising through the bottom of the Soda Lakes and Upsal Hogback hydrothermal-discharge systems. It is subtracted from the total heat discharge from those systems to determine the first component. In this calculation, it is assumed that both systems are old enough to have reached steady state where total heat entering the systems is equal to total heat leaving the systems.

Modes of Heat Discharge

Heat is discharged from the Soda Lakes and Upsal Hogback geothermal systems by radiation, convection, advection, and conduction. Each of these modes is discussed briefly in the following paragraphs.

Radiation.-- Radiative heat discharge is difficult to measure. Thermal-infrared data were obtained for pre-dawn conditions in the Soda Lakes area in 1974, but no attempt was made to evaluate these data quantitatively. Theoretical considerations suggest that, although radiative discharge may be significant in a small area surrounding the old steam well in the hottest part of the Soda Lakes near-surface thermal anomaly (see Olmsted, 1977, p. B8-B9), this mode of discharge probably constitutes a very small percentage of the total heat discharge

from the Soda Lakes geothermal system. Radiative heat discharge is not included in the estimates summarized below.

Convection.-- Convective heat discharge may be regarded as the heat transported by rising ground water, including thermal water from depth. Although no liquid water presently discharges at the land surface in either of the two systems, near-surface heat flow, as estimated by two methods described farther on, includes a significant convective component as well as the predominantly conductive component, especially in the Upsal Hogback system. Estimated rates of ground-water upflow or downflow, discussed in the section, "Ground-water hydrology" (see especially the summary in table 7), were used to adjust computed conductive heat flows for convective effects, as discussed later (p. 106-108).

Advection.-- Advective heat discharge is considered to be the heat transported from the areas of anomalous near-surface heat flow by lateral ground-water flow. Because the boundaries of both heat-flow anomalies are defined so as to include only ground water significantly warmer than "normal" for the depth range considered, advective heat discharge is not estimated as a separate item.

Conduction.-- Conduction is the dominant mode of heat discharge in the study area, although, as mentioned above, the two methods used in deriving the estimates of near-surface heat discharge both include a convective component. Conductive heat flow at each test-well site was estimated as the product of the average temperature gradient in the depth interval of interest and the harmonic-mean thermal conductivity for that interval. Temperature gradients were derived in part from the measured temperature-depth profiles described earlier (p. 86-91). Derivation of the estimates of thermal conductivity is discussed in the next section.

Thermal Conductivity

As in earlier geothermal studies in the Carson Desert by the U.S. Geological Survey, (Olmsted and others, 1975; Morgan, 1982), near-surface conductive heat flow was estimated on the basis of thermal-conductivity values assigned to several lithologic categories classified from logs of the test wells. (See table 3.) However, the categories and the values of thermal

conductivity assigned to them differ from those used in the studies cited above and also in a geothermal study of southern Grass Valley, near Winnemucca, Nevada, (Welch and others, 1981), as summarized in table 12 and discussed in the following paragraphs.

The assignment of thermal-conductivity values in tables 3 and 12 is based on the principle that, in a gross sense at least, thermal conductivity of a granular deposit varies with mean grain size. The thermal conductivity of a water-saturated deposit may be considered to be affected by two major properties: (1) The lithologic or mineralogic composition of the grains constituting the solid matrix, and (2) the porosity. As shown by Sass, Lachenbruch, and Munroe (1971, p. 3392), saturated bulk thermal conductivity of such a deposit, K_b, is given by the equation

$$K_b = K_m^{1-\phi} K_w^{\phi} \qquad (1)$$

where K_m is the geometric-mean conductivity of the constituents forming the solid matrix, K_w is the thermal conductivity of water, and ϕ is porosity expressed as a volume fraction. On the average, coarse-grained deposits (sand and gravel) have higher thermal conductivity than fine-grained deposits (clay and silt) because of both their lower porosity and their higher matrix thermal conductivity as compared to the fine-grained deposits. The lower porosity results chiefly from poorer size sorting, and the higher matrix thermal conductivity results from greater abundance of quartz and other minerals of high thermal conductivity in the coarser deposits.

Laboratory data, summarized in table 13, tend to support the general relation stated above, but the results are difficult to interpret quantitatively, chiefly for two reasons. First, the assignment of the 89 core samples to three major lithologic categories in table 13 was based on visual megascopic examinations rather than on particle-size analyses and hence some of the classifications may be in error. Second, there appears to be a major discrepancy in the results obtained by the two laboratories, especially for the coarser two categories of deposits. As indicated in table 13, values of thermal conductivity reported for the core samples from the Stillwater area (W. H. Somerton, written commun., 1978) are substantially higher than those reported by Munroe (written commun., 1973-78) for presumably similar materials.

Table 12. -- Comparison of values of thermal conductivity assigned to unconsolidated deposits classified in lithologic logs of test wells in geothermal areas in northern Nevada

[Values are in thermal conductivity units, tcu.
1 tcu = 1 mcal/cm x s x °C]

Major category	Materials classified in lithologic logs	Thermal conductivity		
		Olmsted and others (1975); Morgan (1982)-Stillwater	Welch and others (1981)-southern Grass Valley	This report (table 3)
Gravel	Gravel; gravel and sand; sandy gravel	5.0	4.5	4.7
	Sand and gravel; gravelly sand	4.0		
Sand	Coarse sand; sand and scattered gravel; medium to coarse sand; sand; medium sand; fine to medium sand; coarse sand with some clay and silt	3.5	4.0	4.2
	Fine sand; silty sand; sand and silt	3.0	3.5	
	Clay and gravel; clay and coarse sand; clay, sand, and gravel	2.5	4.0	
Silt	Silt and fine sand sandy silt; silt; sandy clay; clay and sand; pebbly clay		3.5	3.2
	Clayey silt; silt and clay; silty clay and fine sand		3.0	
Clay	Silty clay; clay and silt	2.0		2.2
	Clay		2.5	

Table 13. -- Thermal conductivity of saturated unconsolidated deposits in core samples from the Carson Desert

[All measurements made perpendicular to bedding. Values are in thermal conductivity units (tcu). 1 tcu = 1 mcal/cm x s x °C]

Materials	Number of core samples	Thermal conductivity	
		Range	Average
Cores from Stillwater area (Morgan, 1982). Data from W. H. Somerton (written commun., 1978)			
Measurements made with steady-state comparator (divided-bar) apparatus			
Sand, fine to coarse	8	3.71-4.93	4.28
Silt; sandy clay	2	3.93-4.38	4.16
Clay; silty clay	4	2.27-3.05	2.60
Data from R. J. Munroe (written commun., 1973-78).			
Measurements made with needle-probe apparatus			
Sand, fine to coarse	29	2.67-4.04	3.31
Silt, sandy clay; silty sand; sandy silt	15	2.02-3.27	2.53
Clay; silty clay; clayey silt	31	1.89-2.51	2.14

Because of the problems referred to above, thermal conductivities assigned herein to major categories of deposits (tables 3 and 12) are based primarily on theoretical rather than experimental values. Values of thermal conductivity were calculated for idealized deposits having porosities and lithologic compositions believed to represent the ranges characteristic of the near-surface deposits in the study area. The calculations used equation (1) on page 99 in which the saturated bulk thermal conductivity is the geometric mean of the conductivities of the matrix and the water filling the pore space. The results of the calculations, using a range of matrix thermal conductivity of 3 to 10 thermal-conductivity units (tcu), a thermal conductivity of 1.53 tcu for water at 50°C, and a range of porosity of 0.2 to 0.8, are shown in figure 21. As stated previously, both porosity and matrix thermal conductivity tend to vary with mean grain size; the inferred limits as shown in figure 21 reflect this variation. On the basis of data from the Stillwater area (W. H. Somerton, written commun., 1978) and from other localities in northern Nevada--chiefly southern Grass Valley (Welch and others, 1981, table 4), matrix thermal conductivity was assumed to range from 3 tcu, characteristic of the clay minerals most abundant in fine-grained deposits, to 10 tcu, characteristic of a coarse-grained deposit in which the matrix consists of perhaps 70-80 percent quartz of high thermal conductivity. On the basis of the same data, porosity was assumed to range from 0.2, characteristic of ill-sorted coarse-grained deposits, to 0.8, characteristic of well-sorted, uncompacted lacustrine clays.

The value of 2.2 tcu assigned to clay and related fine-grained deposits (tables 3 and 12) is close to the average of 2.14 tcu obtained for 31 samples by Munroe (written commun., 1973-78) but is somewhat less than the average of 2.60 tcu obtained by Somerton (written commun., 1978) for only 4 samples from the Stillwater area. (See table 13).

The value of 4.2 tcu assigned to sand and related coarse-grained deposits (tables 3 and 12) is substantially greater than the average of 3.31 tcu obtained by Munroe for 29 samples but is close to the average of 4.28 tcu obtained by Somerton for 8 samples from the Stillwater area. (See table 13). In this instance, Somerton's data seem to be more consistent with theoretical values than Munroe's data unless the particular samples measured by Munroe were unusually low in quartz content, high in porosity, or both. (See fig. 21.)

The value of 3.2 tcu assigned to silt and related deposits of intermediate

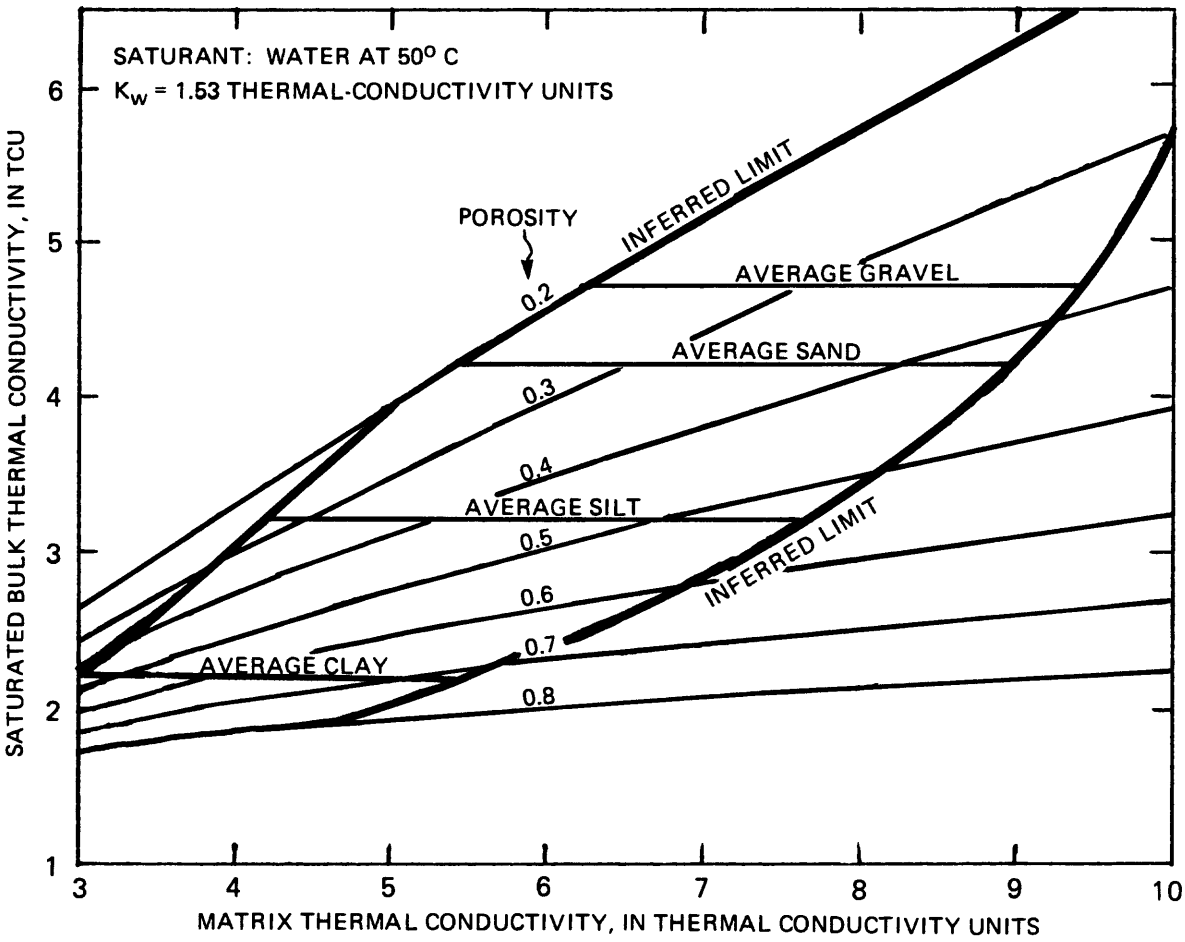

Figure 21. -- Relation of saturated bulk thermal conductivity to matrix thermal conductivity and porosity where saturant is water at 50°C.

grain size (tables 3 and 12) was selected so as to be intermediate between the values assigned to the major categories "sand" and "clay". The value seems reasonable on theoretical grounds but is not supported by experimental data from either laboratory. However, the average of 4.16 tcu for Somerton's data is based on only two samples, whereas the average of 2.53 tcu for Munroe's data, based on 15 samples seems low, like the averages for "sand". (See table 13).

A value of 4.7 tcu was assigned to the coarsest deposits, generally containing substantial quantities of gravel (tables 3 and 12) on the basis that, on the average, such deposits generally are less well sorted and therefore of somewhat lower porosity and higher thermal conductivity than sands and related deposits.

Obviously, some degree of uncertainty exists in the average values of thermal conductivity used herein. However, revision or refinement of these values must await acquisition of much more data from the area, particularly data relating thermal conductivity to porosity, lithologic or mineralogic composition, and particle size.

Estimates of Near-Surface Heat Flow

Data from test wells 45 m or less in depth provided the primary basis for estimates of heat flow in this study. In most regional heat-flow studies, data from much greater depths are used in order to minimize the effects of vertical and lateral heat transport by ground-water flow (convection and advection). One of the purposes of the present study, however, was to determine areal variations in near-surface heat flow as an aid in interpreting the shallow ground-water-flow regime and, especially, in estimating the rate of upflow of thermal water into the shallow ground-water subsystem. Ideally, for this purpose, determination of heat flow as close as possible to the land surface is desired in order to incorporate all the effects of convective and advective heat transport at greater depths on surface or near-surface heat discharge.

The problem may be illustrated conceptually by the simplified cross-section in figure 22, which is modified from a similiar diagram in Olmsted and others (1975, fig. 9). Figure 22 represents a hydrothermal discharge system in which thermal-water upflow through a steeply inclined conduit or conduit system leaks laterally into a sub-horizontal aquifer (or several aquifers) before reaching

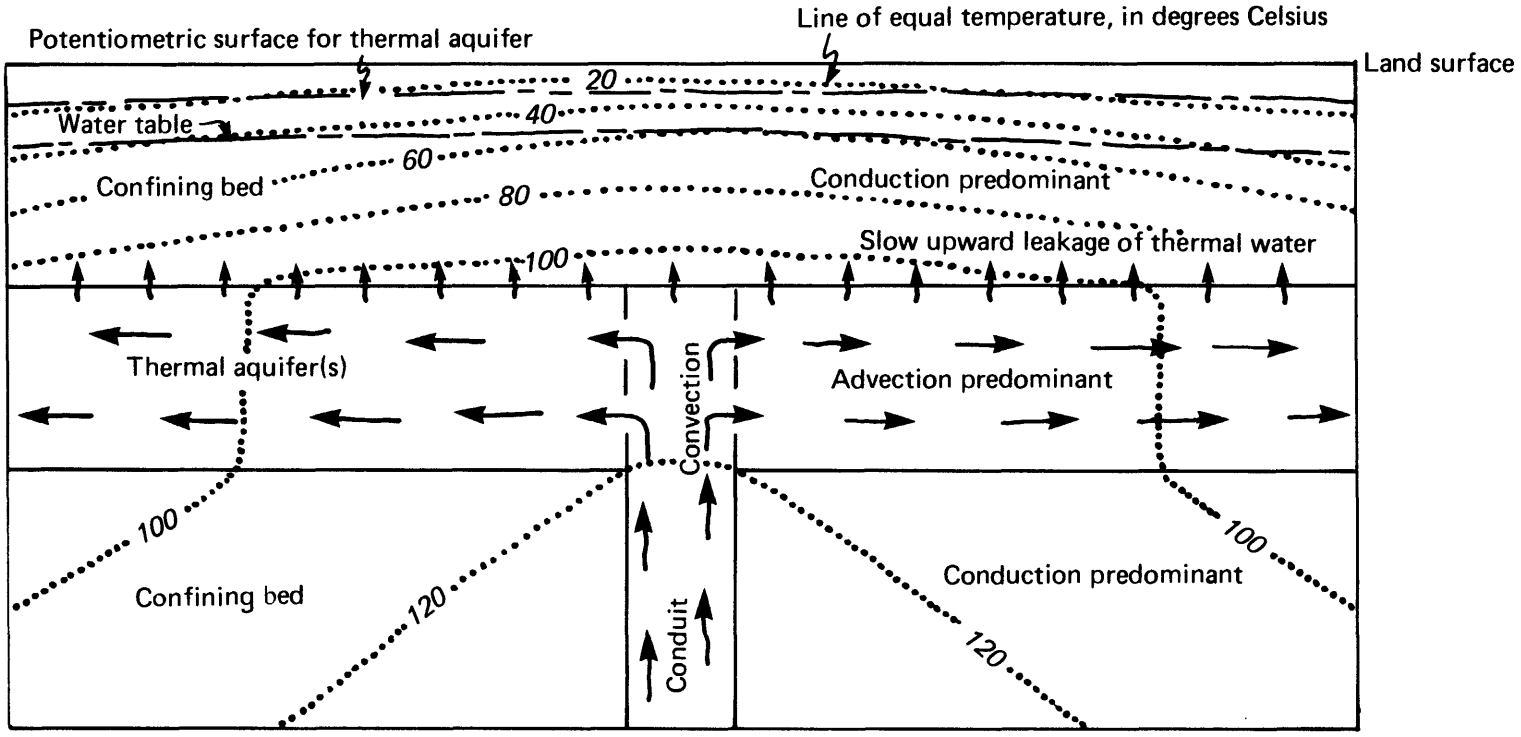

Figure 22. -- Diagrammatic cross section of discharge parts of Soda Lakes and Upsal Hogback geothermal systems.

the land surface. Both Soda Lakes and Upsal Hogback systems represent such a case.

No vertical scale is given in figure 22; it represents a wide range of depths in which lateral leakage of thermal water may occur. As discussed previously (p. 91), lateral leakage occurs at a depth of 245 m in the Upsal Hogback system but probably occurs at depths substantially less than 45 m--the depth of most of the test wells--in the hottest near-surface part of the Soda Lakes system. Thus, the upper layer--the so-called confining bed or thermal blanket in figure 22--extends to a depth much greater than that of most of the test wells in the Upsal Hogback area; the temperature-depth profiles in the wells in that area therefore reflect a predominantly conductive heat-flow regime. In the wells in the hottest near-surface part of the Soda Lakes area, however, only the uppermost parts of the temperature-depth profiles, near the water table, are predominantly conductive; this situation complicates the problem of estimating near-surface heat flow at those sites.

As indicated in figure 22, the heat flow in the top layer of the model is assumed to be chiefly conductive. However, as mentioned earlier (p. 94), this heat flow actually may include a significant convective component, depending upon the rate of vertical ground-water flow through the layer. If the layer were of uniform thermal conductivity and the flow of heat and fluid could be considered one-dimensional (vertical) and steady, the vertical flow rate could be estimated from the curvature of the temperature-depth profile according to methods described by Bredehoeft and Papadopulos (1965), Sorey (1971), and Lachenbruch and Sass (1977). If the ground-water flow were upward, the temperature-depth profile would be convex upward (temperature gradient decreasing with depth); if the flow were downward, the converse would be true.

At most sites in the study area, unfortunately, the confining beds are not sufficiently thick or uniform in thermal properties, and vertical ground-water-flow rates are not large enough to permit the determination of vertical ground-water flow directly from curvature of the temperature-depth profile. However, rates of vertical ground-water flow derived from hydraulic data (see section, "Ground-water hydrology ", especially table 9 and summary on pages 61-62) were used to adjust computed conductive heat flow at each well site for convective effects, using a method given by Lachenbruch and Sass (1977, p. 641-643), as summarized below.

Where vertical ground-water flow exists, heat flow as estimated from the vertical temperature gradient and thermal conductivity changes with depth. For the general case, the relation given by Lachenbruch and Sass (1977, p. 642, equation 10) is

$$q(z_1)/q(z_2) = e^{z/s} \qquad (2)$$

where $q(z_1)$ is heat flow at the shallower depth (z_1), in heat-flow units,
$q(z_2)$ is heat flow at the greater depth (z_2) in heat-flow units,
z is $z_2 - z_1$, in cm, and
s is a characteristic vertical distance (in cm) with the sign of v, the vertical ground-water flow (specific discharge or recharge--Darcian velocity).

The term s is calculated from the expression (Lachenbruch and Sass, 1977, p. 642, equation 11a)

$$s = k/\epsilon' c' v \qquad (3)$$

where k is thermal conductivity in thermal-conductivity units (tcu),
ϵ' is density of the moving fluid (water in this case), in g/cm^3,
c' is the heat capacity of the moving fluid, in cal/g x°C, and
v is vertical ground-water flow rate (specific discharge or recharge; Darcian velocity), in cm^3/cm^2 x s

Because both ϵ' and c', for practical purposes, are equal to unity, equation 3 simplifies to

$$s = k/v \qquad (4)$$

or, in units employed in the present report,

$$s(m) = 3{,}170k\ (tcu)/v\ (mm/a) \qquad (5)$$

Rearranging terms in equation 1 to solve for $q(z_1)$, the heat-flow at the shallower depth, the expression becomes

$$q(z_1) = q(z_2)\ e^{z/s} \qquad (6)$$

and, incorporating equation 6 with the units used in equation 5,

$$q(z_1) = q(z_2)e^{zv/3170\ k} \qquad (7)$$

Where available data permitted, two methods, designated A and B, were used to estimate near-surface heat flow [$q\ (z_1)$] at each test-well site in the study area. In both methods, a depth of 1 m was used for z_1 because of the abundant temperature data available for that depth at most well sites. Each of the two methods is described below.

Method A.-- Method A somewhat resembles a method of the same designation used by Olmsted and others (1975, p. 66-67). This method uses the interpolated temperature gradient between the depth of the well screen (or bottom of a capped well) and a depth of 1 m. Temperature at the well screen or near the bottom of a capped well was measured using the procedure described by Olmsted and others (1975, p. 37-39). Temperature at 1 m depth was used because of the abundance of data available for this depth, especially in the Upsal Hogback area, and was calculated from periodic measurements made in the ground at the well site, adjusted by least-squares linear-regression techniques to an annual average for 1977. The year 1977 was selected because the mean annual air temperature at Fallon was closest (within 0.1°C) of the long-term (1941-70) mean temperature of any of the years during the period of study. Presumably temperatures at depths greater than the limit of significant seasonal fluctuation (about 10-14 m) are in equilibrum with the long-term-average temperatures near the land surface.

Harmonic-mean thermal conductivity for the interval between the well screen or bottom and a depth of 1 m was established using the thermal-conductivity values for saturated materials listed in tables 3 and 12 and values for unsaturated materials derived from an empirical relation

$$K_u = m^a \left[\frac{b}{w^a}\right] + c \qquad (8)$$

where K_u ia unsaturated thermal conductivity, in thermal conductivity units,

m is mid-depth of bed, in meters,

a = 0.8 where saturated thermal conductivity (K_s) is 4.2 or 4.7 tcu,

= 0.7 where K_s is 3.2 tcu,

= 0.6 where K_s is 2.2 tcu,

b = 1.7 where K_s is 4.2 or 4.7 tcu,

= 1.4 where K_s is 3.2 tcu,

= 1.1 where K_s is 2.2 tcu,

w is depth to water table in meters,

c = 0.4 where K_s is 4.2 or 4.7 tcu,

= 0.7 where K_s is 3.2 tcu and,

= 1.0 where K_s is 2.2 tcu.

Values of unsaturated thermal conductivity based on equation 8 above are much less certain than those for saturated thermal conductivity, and the error of the estimated harmonic-mean thermal conductivity used in method A increases with increasing depth to the water table. However, at most sites, extrapolation of the temperature gradients measured in the saturated zone below the depth of significant seasonal temperature fluctuation to a depth of 1 m using inverse ratios of unsaturated to saturated thermal conductivity indicates temperatures very close to those measured at 1 m, which suggests that the values assigned to the unsaturated materials are reasonable.

Finally, the near-surface conductive heat flow was estimated as the product of the harmonic-mean thermal conductivity described above and the interpolated temperature gradient This heat flow at each site was adjusted to include the convective component, using the estimated vertical ground-water-flow rate (table 9) and equation 7 on page 108. The depth to which the interpolated temperature gradient was assigned in equation 6 was the mid point between 1 m and the well screen or the bottom of the well. This approximation introduces some error because the actual gradient at the mid depth is not generally the same as the interpolated gradient, but the difference usually is small.

Method B. -- Method B is essentially the same as method B of Olmsted and others (1975, p. 67-68), except that the heat flows computed as the product of the measured temperature gradients and the estimated thermal conductivities were adjusted for convective effects using the estimated vertical ground-water flow

rate (specific discharge or recharge) at each well site. Method B uses temperature gradients measured in saturated materials, usually between a depth of 14 m and the well screen or bottom. As in method A, the harmonic-mean thermal conductivity (where more than one layer is included in the interval of interest) was multiplied by the interpolated temperature gradient for the interval to give the heat flow. For most test wells, temperature gradients were calculated for different segments of the temperature profile, providing more than one calculated conductive heat-flow value for the site. The dispersion of these values at a site furnishes a useful measure of the reliability of the relative values of thermal conductivity assigned to the lithologic categories in table 3 and also to the reliability of the lithologic log of the well. As indicated in table 12, the dispersion of the heat-flow values is small at most sites.

As with method A, the heat flow at each test-well site was adjusted to include the convective component, using the estimated vertical ground-water flow rate (table 8) and equation 7 on page 108.

Summary and evaluation of estimates. -- Results of derivation of heat flow by the two methods at all the test-well sites are summarized in table 14 by letter designations "A", "B", "C", and "D". "A" values are those believed to have a standard error of less than 15 percent. The standard error for "B" values is believed to be 15-30 percent; for "C" values 30-50 percent; and for "D" values, more than 50 percent. Standard error of the heat-flow estimates for both thermal anomalies probably is about 30 percent. Application of this value to estimates of near-surface heat discharge for the two anomalies is described in a later section.

Regional Heat Flow

As discussed earlier (p. 97), the regional or background heat discharge is subtracted from the total heat discharge from the Soda Lakes and Upsal Hogback thermal anomalies in order to obtain the anomalous or excess heat discharge that results from upward ground-water flow. On the basis of available evidence it is postulated that a local crustal heat source is not present but that regional heat flow is somewhat higher than normal. Unfortunately, the regional heat flow in the Carson Desert cannot be estimated within close limits with available information. However, broad limits on this value can be assigned, as discussed

in the following paragraphs.

Recently published heat-flow maps (Sass and others, 1980, fig. 135; Muffler and others, 1979, Map 1) show an extension of the Battle Mountain heat-flow high (heat flow > 2.5 hfu) into the northwest margin of the Carson Desert, with the rest of the Carson Desert, including the present area of study, being characterized by values less than 2.5 hfu.

An uncorrected heat-flow value of 1.57 hfu was obtained from a test well 154 m deep in the Carson Sink, 43 km northeast of Fallon, drilled in 1972 by the U.S. Bureau of Reclamation (Olmsted and others, 1975, p. 83-85). (See fig. 1 for location.) The drill hole penetrated predominantly fine-grained lacustrine and playa deposits of low permeability and low thermal conductivity. Convective heat transport in the deposits can be reasonably assumed to be small on the basis of the apparent absence of significant curvature of the temperature-depth profile. However, assuming an average upward ground-water flow (specific discharge) of 10 mm/a above a depth of 154 m, the convective component of heat flow would be about 0.35 hfu. An additional correction to the conductive heat flow is estimated to be about 0.16 hfu on the basis of an assumed rate of deposition of 0.5 mm/a for the lacustrine and playa deposits at the well site. Thus the total corrected heat flow may exceed 2 hfu.

Roy and others (1968, p. 5218) reported a heat flow of 2.5 hfu (both corrected and uncorrected) from a drill hole 198 m deep in the northeastern Carson Desert, 31 km northeast of the test well described above (fig. 1).

An average temperature gradient of 81°C/km was measured in August 1977 for the depth interval 251-952 m in ERDA Lahontan No. 1 test well, 6 km west-southwest of Soda Lakes (data from J. H. Sass and T. H. Moses, Jr., written commun., 1977). Assuming the value of 4.0 tcu assigned to the sedimentary rocks of probable Tertiary age (table 2) in this interval is reasonable, the heat flow would be 3.2 hfu. The temperature gradient for the depth interval 952-1,356 m averaged 62°C/km (data from Sass and Moses, written commun., 1977). This interval also is composed chiefly of Tertiary (?) sedimentary rocks but includes andesite of probable flow origin in the top 45 m and other volcanic rocks below 1,290 m. Assuming values of 5.0 tcu for the volcanic rocks and 4.0 tcu for the sedimentary rocks (table 2), the harmonic-mean thermal conductivity for this interval would be 4.3 tcu and the heat flow, 2.7 hfu. Allowing for uncertainties in the estimates of thermal conductivity, the uncorrected heat flow at this site probably is about 3.0 ± 0.5 hfu.

Table 14. — Summary of near-surface heat flow at test-well sites in Soda Lakes and Upsal Hogback geothermal areas

[Heat-flow unit (hfu) = 1 $\mu cal/cm^2 \times s$ Quality of estimate: A, standard error < 15 percent; B, standard error 15-30 percent; C, standard error 30-50 percent; D, standard error > 50 percent]

Test well site	Depth of well (m)	Depth to water table (m)	Method A: Depth interval (m)	Method A: Heat flow (hfu)	Method B: Depth interval (m)	Method B: Heat flow (hfu)	Best estimate of heat flow (hfu)	Quality of estimate	Remarks
U.S. Geological Survey wells									
2	26.5	9.6	----	---	14-26.2	15	15	B	Slow upflow in annulus; has only small effect on temperatures.
3	44.2	2.3	1-44.4	6.9	----	---	6.9	B	Slow upflow in annulus.
7	25.0	7.8	----	---	14-25.0	5.4	5.4	B	----------
8	38.9	3.3	----	---	14-38.4	1.9	1.9	B	----------
9	39.9	9.1	----	---	12-30.0	2.4	2.4	B	Lateral flow of cool water at 30 m.
10	33.2	2.8	1-32.0	4.5	14-32.0	4.7	4.6	A	----------
11	9.46	11.5e	1-9.46	1.0	----	---	1.0	C	Entirely in unsaturated zone.
12	22.4	10.0	1-22.4	1.5	14-22.4	1.6	1.6	A	----------
13	21.1	3.1	1-20.9	7.3	----	---	7.3	B	----------
17	9.6	3.0	1-9.34	140	----	---	140	B	----------
18	41.8	4.5	1-41.7	2.5	----	---	2.5	D	Lateral flows of cool and warm water at several depths; flow in annulus.
27	44.7	4.3	----	---	14-36.0	26	26	B	Probable lateral flow of cool water at 36 m.
29	44.6	6.2	----	---	32-44.6	7.4	7.4	B	Upflow in annulus above 30 m.
30	40.5	1.6	----	---	12-18.0	70	70	B	Lateral flow of warm water at 18 m; flow in annulus above 30 m.
31	38.6	5.7	1-38.6	14	----	---	14	D	Temperature-depth profile difficult to interpret.
32	45.1	6.7	1-45.1	26	14-45.1	25	25	B	----------
33	44.6	5.3	----	---	1-20.0	70	70	C	Lateral flow of warm water at 20 m.
34	45.0	7.2	----	---	14-22.0	8.1	8.1	C	Lateral flow of cool water above 37 m; upflow below 37 m.
35	20.5	1.8	----	---	10-20.0	30	30	D	Heat flow could be 52 hfu if lateral flow of warm water occurs at 12 m.
36	21.1	8.6	----	---	10-19.0	12	12	B	Lateral flow of warm water at 19 m.
37	13.6	5.0	----	---	8-13.6	90	90	B	----------
38	21.8	6.5	----	---	10-18.0	100	100	C	Lateral flow of cool water at 18 m.
39	41.9	6.5	----	---	14-20.6	5.2	5.2	C	----------
40	41.5	7.3	----	---	14-29.0	5.1	5.1	C	----------

Table 14. -- Summary of near-surface heat flow at test-well sites in Soda Lakes and Upsal Hogback geothermal areas (Continued)

[Heat-flow unit (hfu) = 1μcal/cm^2 x s Quality of estimate: A, standard error < 15 percent; B, standard error 15-30 percent; C, standard error 30-50 percent; D, standard error > 50 percent]

Test well site	Depth of well (m)	Depth to water table (m)	Method A: Depth interval (m)	Method A: Heat flow (hfu)	Method B: Depth interval (m)	Method B: Heat flow (hfu)	Best estimate of heat flow (hfu)	Quality of estimate	Remarks
U.S. Geological Survey wells									
41	42.9	9.4	----	---	20-32.0	4.1	4.1	C	Lateral flow of cool water at 34 m; slow upflow in upper annulus.
46	31.5	1.2	----	---	14-31.45	1.7	1.7	B	----------
47	28.4	.8	1-28.4	1.1	----	---	1.1	C	Upflow in annulus.
48	31.4	2.3	1-31.4	10.8	12-31.4	11.6	11.2	B	----------
49	32.0	1.8	1-32.0	3.5	----	---	3.5	B	Upflow in annulus.
50	20.2	1.9	1-19.3	1.9	----	---	1.9	B	Upflow in annulus above 17 m.
51	44.4	12.2	1-41.8	1.7	14-41.8	1.6	1.6	B	----------
52	45.7	17.5	1-45.7	2.2	20-45.7	2.2	2.2	A	----------
53	42.4	9.8	1-42.4	5.3	14-42.4	5.4	5.3	B	Upflow in annulus above 20 m.
54	44.5	2.2	1-44.5	4.1	30-44.5	4.6	4.3	B	Upflow in annulus above 30 m.
55	44.5	1.5	1-44.5	8.1	14-44.5	8.2	8.1	A	Annulus cemented; good data.
56	44.5	3.5	1-44.5	5.0	----	---	5.0	B	Some upflow in annulus evident in spite of cement.
57	44.4	1.0	1-44.4	4.6	----	---	4.6	B	Some upflow in annulus evident in spite of cement.
58	44.1	.8	----	---	1-14.0	-1.8	-1.8	B	Annulus cemented. Only well having reversed temperture gradient.
59	45.6	4.6	1-45.2	8.4	----	---	8.4	B	Rapid upflow in annulus 16-32 m.
60	44.5	1.9	1-44.5	4.9	14-44.5	4.9	4.9	A	Annulus cemented; good data.
61	14.26	13.2	1-14.26	2.2	----	---	2.2	C	Mostly unsaturated zone; heat flow uncertain.
63	29.5	9.2	----	---	14-29.5	4.0	4.0	C	Heat flow uncertain because of absence of detailed lithologic log.
64	304.8	3e	----	---	14-22.0	12	12	C	No detailed lithologic log; thermal conductivity uncertain.
U.S. Bureau of Reclamation wells									
10	50.2	7e	----	---	14-50.2	39	39	B	----------
13	152.40	5.2	----	---	14-38.0	2.1	2.1	B	----------
14	158.96	6.3	----	---	16.5-19.5	120	120	C	----------

Table 14. -- Summary of near-surface heat flow at test-well sites in Soda Lakes and Upsal Hogback geothermal areas (Continued)

[Heat-flow unit (hfu) = 1μcal/cm^2 x s Quality of estimate: A, standard error < 15 percent; B, standard error 15-30 percent; C, standard error 30-50 percent; D, standard error > 50 percent]

Test well site	Depth of well (m)	Depth to water table (m)	Method A: Depth interval (m)	Method A: Heat flow (hfu)	Method B: Depth interval (m)	Method B: Heat flow (hfu)	Best estimate of heat flow (hfu)	Quality of estimate	Remarks
Chevron Resources Co. wells									
1-29	----	---	----	---	18.3-36.6	15	15	C	
11-33	----	---	----	---	12-24.4	91	91	C	
63-33	----	---	----	---	48.8-61.0	26	26	C	
SL-27	----	---	----	---	18.3-42.7	4.6	4.6	C	
SL-28	----	---	----	---	18.3-42.7	5.3	5.3	C	
SL-29	----	---	----	---	15.2-42.7	9.1	9.1	C	Thermal conductiviity assumed to be 3.5 tcu.
SL-30	----	---	----	---	15.2-36.6	16	16	C	
SL-31	----	---	----	---	18.3-42.7	3.9	3.9	C	
SL-32	----	---	----	---	18.3-42.7	3.4	3.4	C	
SL-33	----	---	----	---	30.5-61.0	0.5	0.5	C	
SL-34	----	---	----	---	30.5-61.0	1.7	1.7	C	
SL-35	----	---	----	---	15.2-42.7	5.6	5.6	C	

A reasonable conclusion based on the evidence cited above is that the regional or background heat flow in the study area probably is within the range 2-3 hfu.

Anomalous Heat Discharge

Anomalous heat discharge is equal to the total near-surface heat discharge from the Soda Lakes and Upsal Hogback thermal anomalies minus the regional or background heat discharge. The thermal anomalies are defined as the areas in which the near-surface heat flow exceeds the regional or background heat flow discussed in the preceding section. Total near-surface heat flow in both geothermal areas is shown in figure 23 and in the hottest part of the Soda Lakes thermal anomaly in figure 24. Both thermal anomalies are poorly defined below heat-flow values of about 5 hfu. (See fig. 23.) A crude estimate of the extent of the two anomalies at values between about 3 and 5 hfu is obtained by extrapolation of curves of heat flow versus area (shown as dashed lines in figure 25). Because of the lack of useful data in the eastern part of the Upsal Hogback area and in both eastern and western parts of the Soda Lakes area, extrapolation of areas below heat-flow values of 3 hfu is not warranted. Therefore, in the following estimates, 3 hfu is taken as the regional background value, even though the actual value could be less, as discussed previously.

Near-surface heat discharge for the Soda Lakes and Upsal Hogback thermal anomalies was estimated by integrating the heat flow-area curves in figure 25. The mean values were obtained directly from the plots in figure 25. Total discharge for the Soda Lakes anomaly is 8.6 Mcal/s; at an estimated extent of 110 km^2 and a regional background heat flow of 3 hfu, the background heat discharge is 3.3 Mcal/s. Thus, the anomalous heat discharge is 5.3 Mcal/s. For the Upsal Hogback anomaly, the total discharge is 3.5 Mcal/s; the estimated extent, 60 km^2, the background discharge, 1.8 Mcal/s; and the anomalous discharge, 1.7 Mcal/s. All these estimates are highly uncertain, owing to (1) the poor definition of the extent of the thermal anomalies below heat-flow values of 5 hfu, (2) systematic errors in the heat-flow estimates, and (3) uncertainty as to the regional background heat flow. Because standard error of the heat-flow estimates for both thermal anomalies is believed to be about 30 percent (p. 110), the anomalous heat discharge at Soda Lakes probably is within the range of 3.7-6.9 Mcal/s, and at Upsal Hogback 1.2-2.2 Mcal/s. However, because regional

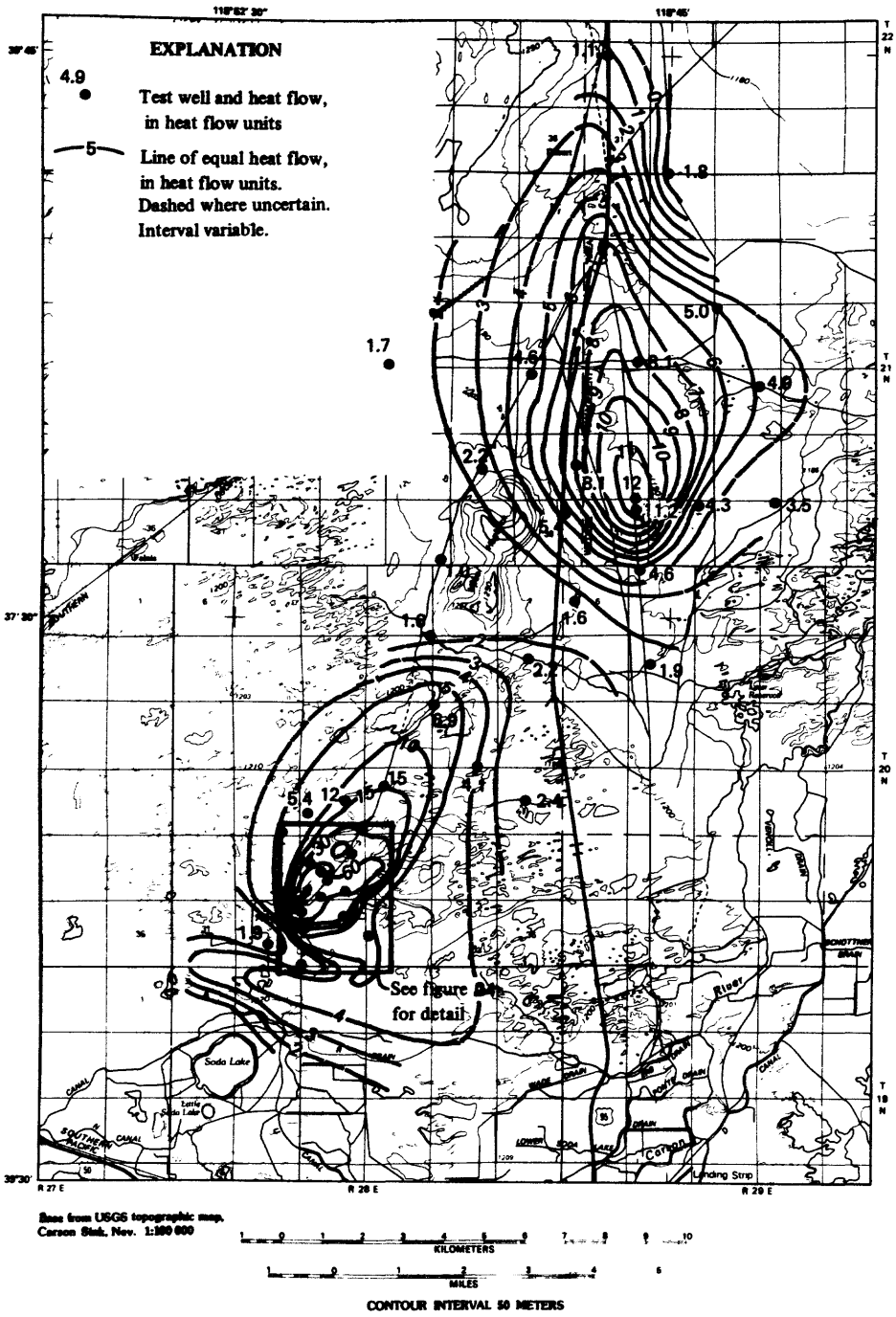

Figure 23. -- Near-surface heat flow, Soda Lakes and Upsal Hogback geothermal areas.

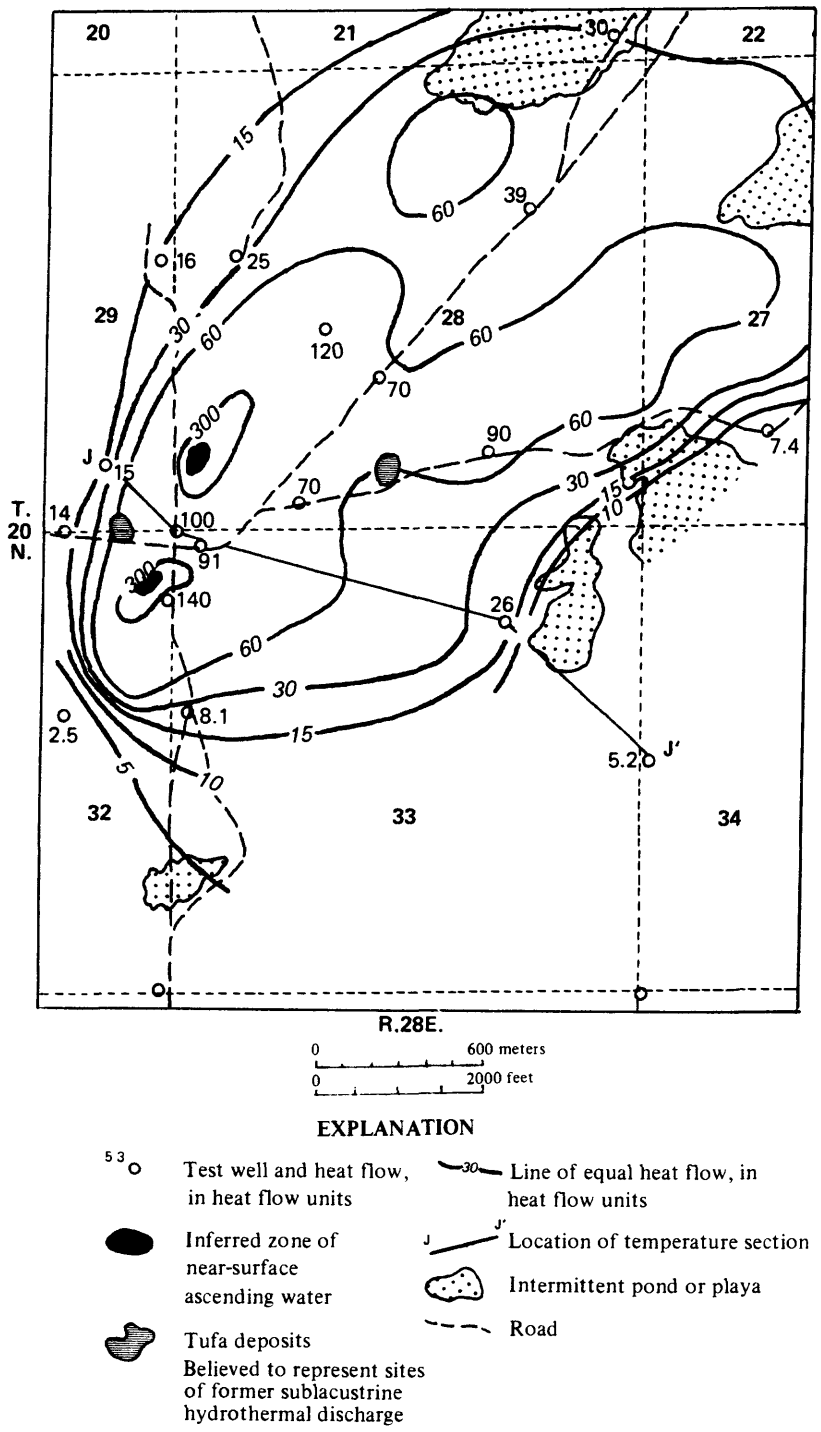

Figure 24. -- Near-surface heat flow, hottest part of Soda Lakes anomaly.

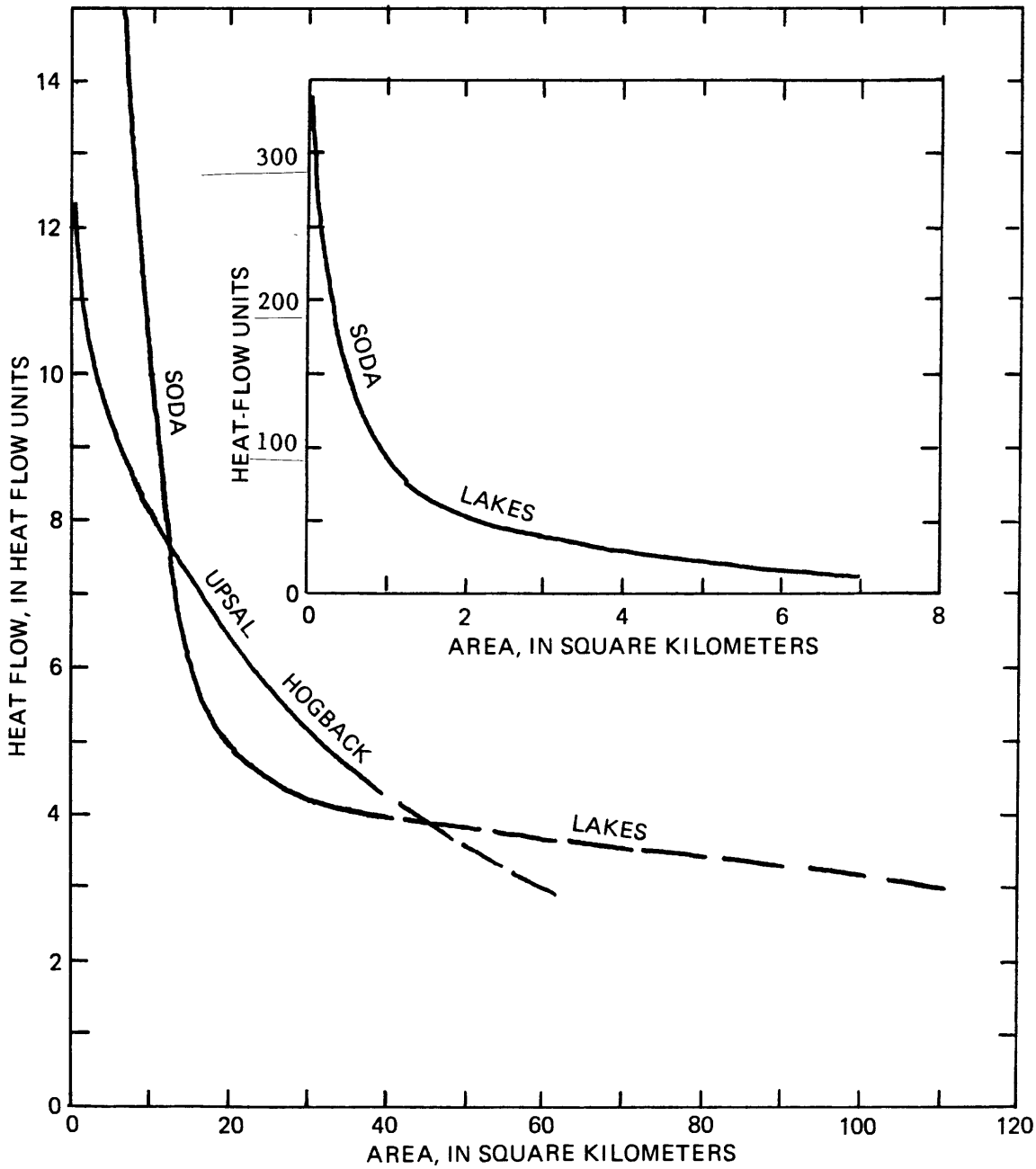

Figure 25. -- Relation of near-surface heat flow to area, Soda Lakes and Upsal Hogback thermal anomalies.

background heat flow probably is less than 3 hfu, the estimates of the extent of the anomalies and both the total and the net (anomalous) heat discharge are believed to be conservatively low. Hence, the most likely values of anomalous heat discharge probably are in the upper part of the range just given, but more precise estimates are not possible with available data. The values for anomalous heat discharge of 5.3 Mcal/s for Soda Lakes and 1.7 Mcal/s for Upsal Hogback are used in the next section to derive crude estimates of the thermal-water upflow in both systems.

CONCEPTUAL MODELS OF THE GEOTHERMAL SYSTEMS

Information obtained during the present and earlier studies permits reasonable speculation as to the nature of the Soda Lakes and Upsal Hogback geothermal systems. Several alternative conceptual models of the systems are possible within the constraints of existing data. As more data are obtained from deep drilling and testing, the most realistic among these alternative models can be selected. Numerical modeling can then be used to interpret the dynamics of the systems, both before and after development. The discussion in the following pages summarizes the results of the present analytical studies and interprets these results in terms of the extent and configuration of the systems, the physiochemical nature of the thermal and nonthermal fluids, the present sources and fluxes of heat and thermal fluid, the movement of thermal fluid, and the origin and age of the two systems.

Because of deep test drilling by private companies and other government agencies in the Soda Lakes area, much more is known about that system than about the Upsal Hogback geothermal system. For this reason, the inferences as to the nature of the latter system are necessarily more sketchy and tentative than of the former system.

Soda Lakes System

Configuration and Extent

The boundaries of the Soda Lakes geothermal system are largely unknown. Delineation of these boundaries would require detailed information about the hydraulic-head distribution throughout the system and the flow paths of the deeply circulating thermal water. This kind of information generally is available only for highly developed geothermal systems in which many deep wells have been drilled. Nevertheless, information obtained during the present study permits reasonable inference as to the approximate configuration and extent of that part of the system characterized by upflow of ground water, which probably includes deeply circulating thermal water as the major component. In addition, less firm inference is possible as to the total extent of the system on the basis of several simplified assumptions discussed later.

In a general way, the upflow part of the Soda Lakes geothermal system is

outlined by the near-surface thermal anomaly--the area characterized by near-surface heat flow that exceeds the regional or background value, estimated to be 2-3 hfu (p. 115). Although its outer part is poorly defined at heat flows less than about 4 hfu, the anomaly appears to be markedly asymmetrical and elongated toward the northeast, with the hottest part near the southwest edge (fig. 23). Temperature surveys at 1-m depth, snowmelt patterns, temperatures and heat flow determined from shallow test drilling, and distribution of Russian Thistle all indicated two en echelon temperature and heat-flow maxima, with the hotter one to the north, centered at the old steam well (Olmsted and others, 1975, p. 111; Olmsted, 1977, p. B8-B9). (See fig. 24.)

The asymmetrical pattern having the northeast-southwest long axis was interpreted by Olmsted and others (1975, p. 117-118) as resulting from lateral flow of water toward the northeast in sands between confining beds of clay and silt after the water rises along steeply inclined or vertical fault-controlled conduits beneath the hottest parts of the anomaly. Later data from temperature measurements at a depth of 1 m suggested a possible linear hydrothermal conduit or conduit system extending almost 700 m northeast of the old steam well (Olmsted, 1977, p. B8-B9).

More recent data obtained during the present study suggest that the inferred fault zone having a N. 55°W. strike may be more important in providing a path or paths for the ascent of thermal fluid than the northeast-trending faults interpreted from patterns of near-surface temperature and heat flow, at least at depths below about 200-300 m. The asymmetrical subsurface-temperature pattern shown in sections I-I' and J-J' and data from Chevron Resources well 63-33 (figs. 26 and 27) suggest that the hottest water at depth may lie southeast of the hottest part of the near-surface heat-flow anomaly and that the deep thermal water rises toward the northwest. The most recent deep exploratory wells drilled by private companies are, in fact, southeast of the hottest near-surface anomaly.

Crude estimates of the areal extent of the Soda Lakes system are made on the basis of the following highly simplified or generalized assumptions: (1) Regional heat flow--the heat flow at the base of the hydrothermal-convection system--is 3 hfu; (2) the hydrothermal-convection system is hydraulically continuous and consists of an upflow or discharge part characterized by near-surface heat flow exceeding 3 hfu (the thermal anomaly) and an adjacent or

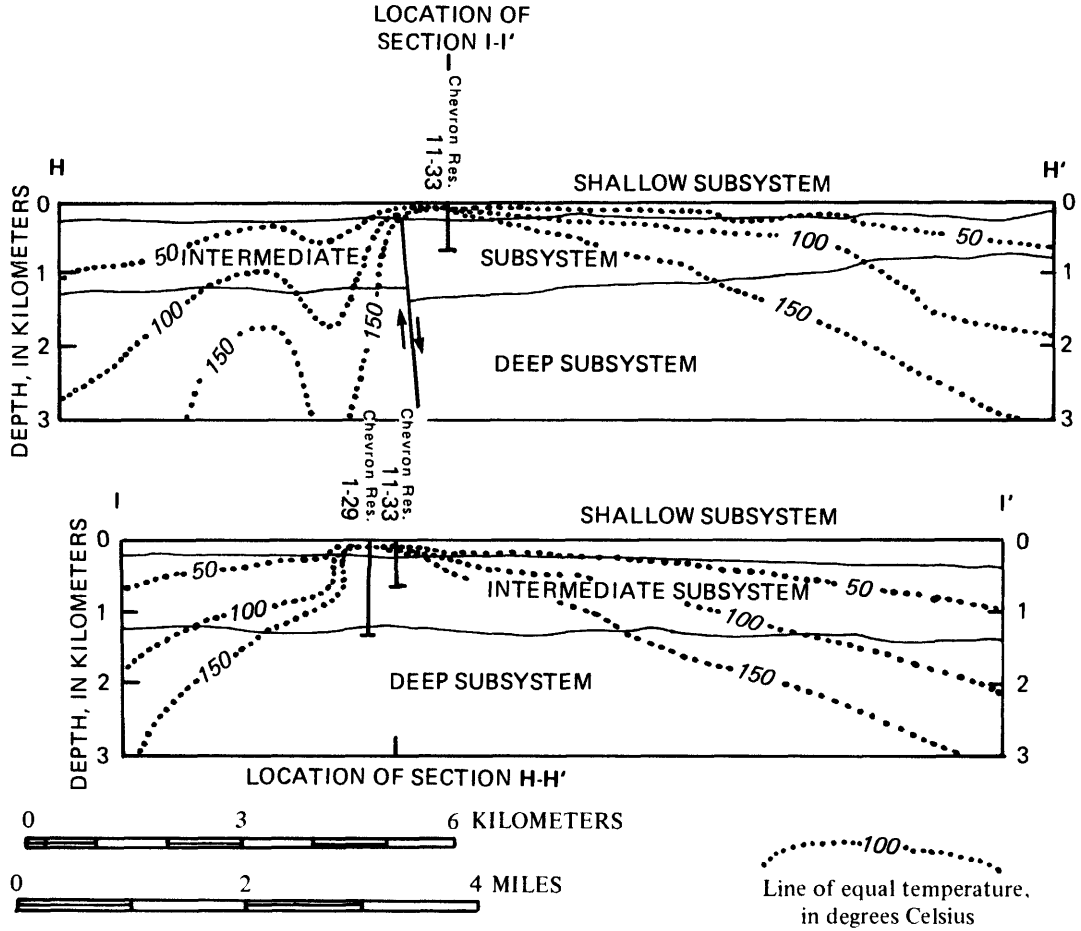

Figure 26. -- Sections H-H' and I-I' across Soda Lakes' thermal anomaly. Locations of sections shown in figure 20.

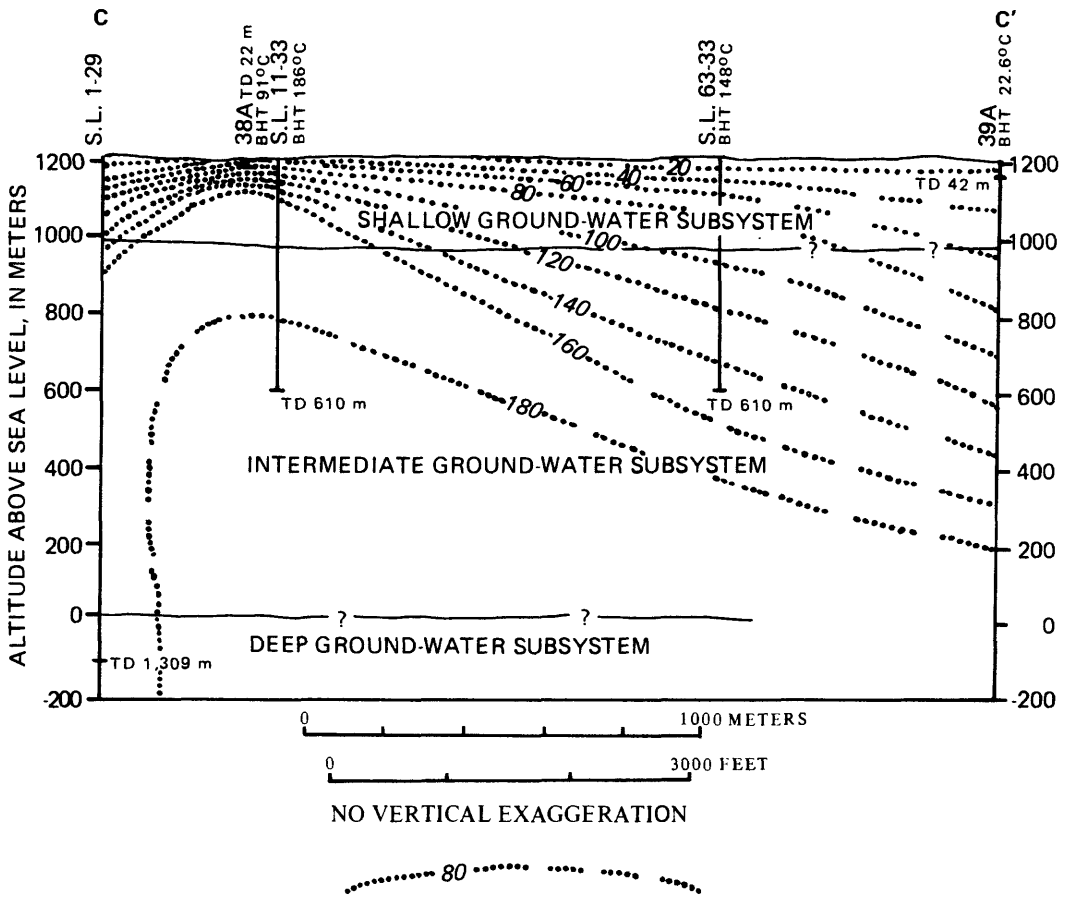

Figure 27. -- Sections J-J' across hottest part of Soda Lakes' thermal anomaly. Locations of sections shown in figure 24.

surrounding downflow or recharge part characterized by near-surface heat flow less than 3 hfu; (3) the average near-surface heat flow in the downflow or recharge part of the system is within the range of 1-2 hfu; and (4) the system has attained a steady-state condition both thermally and hydrologically--rates of inflow of heat and fluid equal rates of outflow. Under the above assumptions, for the entire area occupied by the system, excess near-surface heat discharge resulting from thermal-water upflow must equal deficient near-surface heat discharge resulting from downflow or recharge. As stated in the previous section (p. 115), the excess (net) heat discharge amounts to 5.3 Mcal/s over an area of 110 km^2. Because the deficient heat discharge also must be 5.3 Mcal/s, the area of the downflow or recharge part of the system is

$$\frac{5.3 \times 10^6 \text{ cal/s}}{(3.0 - 1.0) \times 10^{-6} \text{ cal/cm}^2 \text{ s}} = 2.6 \times 10^{12} \text{ cm}^2$$

or 260 km^2 at an average heat flow of 1 hfu,

or $$\frac{5.3 \times 10^6 \text{ cal/s}}{(3.0 - 2.0) \times 10^{-6} \text{ cal/cm}^2 \text{ s}} = 5.3 \times 10^{12} \text{ cm}^2$$

or 530 km^2 at an average heat flow of 2 hfu. Total area occupied by the system, therefore, is within the range of 110 + 260 to 110 + 530 km^2, or 370-640 km^2 under the assumption stated above. If the area were circular, its diameter would be 22 to 29 km. By comparison, the entire Carson Desert has an area of 5,677 km^2 (Glancy and Katzer, 1975, table 2), which, if the area were circular, would have a diameter of 85 km.

The highly uncertain nature of the estimate above deserves emphasis. The simplified or generalized model implied in the assumptions probably diverges widely from reality, especially with regard to the assumptions of hydraulic continuity and steady-state conditions. The extent of the Soda Lakes system would be greater than the values cited above if (1) regional heat flow were less than 3 hfu (believed likely), (2) average heat flow within the area of downflow or recharge were greater than 2 hfu, or (3) recharge to the deep, thermal part

of the system exceeded discharge of thermal fluid, or (4) the system were cooling. Opposite assumptions would result in a smaller estimated extent. Evidence bearing on whether the Soda Lakes geothermal system is in thermal or hydrologic equilibrium is discussed later.

The depth and total volume of the Soda Lakes geothermal system must be largely conjectural on the basis of present information. Maximum depths of fluid circulation are governed by rock-mechanical characteristics--the depths to which interconnected open fractures exist in the rocks. Numerical-modeling studies would be required to estimate circulation depths required under various assumptions as to maximum temperature attained by the thermal fluid, configuration and length of flow paths, regional heat flow, age of the system (as related to whether steady-state conditions have been reached), and other factors. Minimum depths of 2.9-5.2 km are estimated on the basis of conduction-only, steady-state conditions, regional heat flow of 2-3 hfu, the stratigraphy and thermal-conductivity values given in table 2, and a maximum fluid temperature of 209°C. The depths required for steady-state convection, with fluid-flow paths of finite length, would be substantially greater, the depths being dependent chiefly on the length and configuration of the flow paths and the flow rate. If the system were losing heat (cooling), the circulation depths would be correspondingly less, and vice versa.

Evidence from magnetotelluric data, interpreted by Stanley and others (1976, p. 33), suggests the presence of a layer having an electrical resistivity of less than 1 Ω-m at depth of 4-7 km beneath the western Carson Desert. This layer could be a geothermal reservoir of considerable lateral extent and could represent the maximum depths to which thermal fluids circulate in the system.

In summary, thermal fluids in the system almost certainly circulate to depths greater than 3 km, the depth used to estimate the volume of the geothermal reservoir (p. 95), and they may reach depths approaching 6-7 km.

As shown in table 11, the part of the Soda Lakes geothermal system above a depth of 3 km where temperatures exceed 150°C is estimated to occupy an area of about 72 km^2 and have a volume of 81 km^3. At an estimated average effective porosity of 4.2 percent, the volume of effective pore space above 3-km depth is 3.4 km^3. Most of this volume represents the hottest part of the system, where near-surface heat flow exceeds the regional or background value of 2-3 hfu.

The entire system, including the recharge parts and the parts containing nonthermal water, may have a volume of 1,100-3,800 km^3 on the basis of an estimated areal extent of 370-640 km^2 and an estimated depth of 3-6 km.

Physicochemical Nature of Fluids

Present data yield a fairly coherent picture of the physicochemical nature of the fluids in the Soda Lakes geothermal system. All evidence indicates a hot-water rather than a vapor-dominated (steam) system, although a steam cap of small thickness and extent may be present in the hottest part of the near-surface thermal anomaly, in the vicinity of the old steam well (fig. 24). The hottest water actually sampled had a temperature of 186°C at the bottom-hole depth of 610 m in Chevron Resources well 11-33, 330 m south of the steam well (UURI, 1979f). A temperature of (199°C) has been measured in Chevron Resources well 84-33. (See fig. 17.) As shown in table 10, geothermometry indicates thermal-aquifer temperatures of 186°C (quartz-silica) and 209°C (Na-K-Ca) for a sample of water from this well. A sample from a depth of 159 m in USBR well 14A, 650 m northeast of the old steam well, gave a quartz-silica temperature of 169°C, a chalcedony-silica temperature of 146°C, and a magnesium-corrected Na-K-Ca temperature of 141°C. The latter two geothermometer temperatures are close to the measured temperature of 144.7°C, suggesting that thermal water, which was originally hotter, had re-equilibrated with shallow-aquifer material after rising from much greater depth in the vicinity of the steam well and then flowing about 650 m northeastward. The most reasonable conclusion from these data is that the deep thermal water attains temperatures at least as high as 199°C and possibly more than 200°C in the deepest parts of the system.

In addition to the water at Chevron Resources well 1-29, water from several other wells appears to have had a thermal history. On the basis of the stable-isotopic composition and chloride concentration, water from wells 17A, 32A, and USBR 14A appears to be thermal water that has not mixed with a major proportion of shallow nonthermal water. In contrast, water from wells 2A, 29A, 30A, and 41A apparently is a mixture of thermal and nonthermal components. Shallow, sulfate-rich water from wells 36A and 37A apparently has been influenced by at least one of the following processes: Steam loss, evaporation, or dissolution of sulfate-rich evaporite minerals.

A comparison of the isotopic composition and chloride concentration of the

thermal and nonthermal water indicates that the source of recharge to the thermal system is ground water that was subjected to considerable evaporation prior to downward movement into the deep system. A possible source is water in which dissolved constituents were concentrated during desiccation of Lake Lahontan.

Differentiation of thermal from nonthermal water is made difficult by the fact that most indices such as concentrations of dissolved solids and chloride have a large range in the nonthermal water and overlap values characteristic of the thermal water. The minor-constituent data collected during the study also yield only tenuous evidence of the existence of thermal water. The high chloride concentrations in the nonthermal water mimic those in the thermal water, making estimates of the mixing ratios of the two types of water risky at best.

Source and Flux of Heat

Although the most recent eruptions that formed the present cone at Soda Lakes probably took place within the last 6,900 years (p. 21), no clear evidence indicates a localized shallow-crustal heat source beneath the Soda Lakes geothermal system. The eruptions that formed the cone enclosing the lakes may have been fed by narrow, vertical or nearly vertical basaltic dikes which originated deep within the crust or within the upper mantle. Such dikes probably would have lost most of their heat, even within the brief span of 6,000-7,000 years.

Alternatively, the eruptions at Soda Lakes may have resulted from the explosive release of carbon dioxide and other gases through a fault-controlled conduit system from a magma body at great depth. No significant heat anomaly may ever have been present, even during the eruptions.

In any event, the most likely source of heat for the Soda Lakes geothermal system is the above-normal regional heat flow in this part of the Basin and Range province.

Anomalous heat discharge from the Soda Lakes geothermal system is estimated to be 5.3 Mcal/s on the basis of a regional heat flow of 3 hfu. This value represents the approximate excess near-surface heat discharge that results from convective upflow of thermal water within the system. Because virtually none of the thermal water discharges at the land surface as liquid, and other forms of heat discharge probably are negligible, the excess or anomalous near-surface discharge takes place chiefly by conduction with some convection at rates above

regional conductive heat flow.

Source and Flux of Thermal Fluid

Like most other geothermal systems, a meteoric origin for the thermal fluid in the Soda Lakes system is indicated by the stable-isotopic composition of the water (p. 73-74). Hydrologic and hydrochemical evidence indicates that the thermal fluid was affected by evapotranspiration prior to downward percolation to the deep part of the system (p. 76). Possible sources of recharge were water present in Lake Lahontan during a recent period of desiccation or from Carson River water that was affected by evapotranspiration.

The apparent age of the water in the Upsal Hogback system of 25,000-35,000 years (p. 85) raises the possibility that the source of recharge to the system may have changed, owing to changing climatic conditions during the past few tens of thousands of years. Precipitation and accompanying runoff from mountains along the margins of the Carson Desert probably contribute only minor additional recharge, owing to the general aridity of the region. Even during wetter periods during the last few tens of thousands of years, this source probably contributed only a small fraction of the total recharge.

It is not possible to estimate with in reasonable limits the present rate of recharge to the deep subsystem that contains the thermal fluid. However, the rate of upflow of thermal fluid may be estimated using three approaches: (1) A heat budget; (2) a hydrochemical budget (chloride balance) for the upper part of the shallow ground-water subsystem; and (3) a water budget, also for the upper part of the shallow ground-water subsystem. Each of these approaches is reviewed briefly below.

Heat Budget. -- The rate of upflow of thermal water may be estimated on the basis of the anomalous near-surface heat discharge and the net enthalpy of the thermal water at depth, where it starts to rise. As stated earlier, anomalous near-surface heat discharge is estimated to be about 5.3 Mcal/s. For present purposes, the net enthalpy of the deep thermal water is assumed to be (188 to 198) x 10^3cal/kg on the basis of a source temperature of 199-209°C (enthalpy (203-213) x 10^3cal/kg) and an ambient surface temperature of 15°C (enthalpy 15 x 10^3cal/kg). Thermal upflow, therefore, is

$$\frac{(5.3) \times 10^6 \text{ cal/s}}{(1.88 \text{ to } 1.98) \times 10^5 \text{ cal/kg}} = 28 \text{ to } 31 \text{ kg/s}$$

This is the estimated upflow rate where the thermal water starts to rise. If cooler water mixes with this upflow, the upflow rate increases correspondingly at shallower depths. Converting the mass flow rate above to a volume flow rate, the discharge of thermal water leaving the deep source at a temperature of 199 to 209°C is

$$\frac{28 \text{ to } 31 \text{ kg/s} \times 3.17 \times 10^7 \text{ s/a}}{853 \text{ to } 881 \text{ kg/m}^3} = 10.1 \text{ to } 11.5 \times 10^5 \text{ m}^3/\text{a}$$

Thus, the upflow of thermal water from a deep reservoir estimated on the basis of a heat budget is 1,010,000 to 1,150,000 m^3/a.

Hydrochemical budget (chloride balance). -- Upflow of thermal water also may be estimated on the basis of a hydrochemical budget, using chloride as a conservative dissolved constituent in thermal, nonthermal, and mixed ground waters. The estimate is based on a mass-balance calculation for inflow and outflow of both water and dissolved chloride for ground-water budget subprism A-A' to B-B' (figs. 5 and 10) using equations 1 and 2 below:

$$W + X = Y + Z, \qquad (1)$$

$$AW + BX = CZ, \qquad (2)$$

where W = is inflow of nonthermal water,
X = is inflow of thermal water (assumed equal to upflow of thermal water),
Y = is vapor discharge of nonthermal and mixed water (evapotranspiration),
Z = is liquid outflow of mixed water,
A = is chloride concentration of nonthermal inflow,
B = is chloride concentration of thermal inflow, and
C = is chloride concentration of liquid outflow.

In the equations above, small differences in water density between thermal and

nonthermal water are neglected; mass-flow rates in kilograms per second are assumed equal to volume flow rates in liters per second, and chloride concentrations in milligrams per kilogram equal to concentrations in milligrams per liter. Because chloride concentration of vapor discharge (evapotranspiration) is assumed to be zero, this term is omitted from equation 2; all chloride is therefore assumed to leave subprism A-A' to B-B' in the liquid outflow.

The terms X (thermal inflow) and Z (mixed outflow) are the unknowns in equations 1 and 2 above. The other quantities are assumed to be as follows:

W = 1,200,000 m^3/a (see fig. 10),

Y = 650,000 m^3/a (see fig. 10),

A = 200 mg/L (the approximate concentration of chloride in waters from wells 8A, 18A, and USBR 13C),

B = 2,200 mg/L (the concentration of chloride in thermal water from Chevron Resources well 1-29), and

C = 1,000 mg/L (as suggested by data shown in fig. 11).

Substituting these values in equations (1) and (2) and combining the equations yields

X (thermal upflow) = 260,000 m^3/a, and

Z (mixed outflow) = 810,000 m^3/a.

Thus, upflow of thermal water into ground-water budget subprism A-A' to B-B' (saturated materials above a depth of 45 m) estimated on the basis of a hydrochemical budget (chloride balance) is about 260,000 m^3/a.

Water Budget. -- The third method of estimating upflow of thermal water in the Soda Lakes geothermal system uses the water budget described in the section "Ground-water hydrology" (p. 60; fig. 10). This method is only semi-independent of the hydrochemical budget just described because the hydrochemical budget uses values calculated from the water budget for lateral ground-water flow through section A-A' and ground-water evapotranspiration in sub-prism A-A' to B-B'.

The water-budget estimate of upward inflow of thermal water into subprism A-A' to B-B' through conduits of small lateral extent is 1,400,000 m^3/a (fig. 10). The standard deviation of this estimate is 860,000 m^3/a (p. 60).

Discussion of Estimates. -- In summary, the estimates of thermal upflow from a deep reservoir at Soda Lakes are 1,010,000-1,150,000 m^3/a by the heat-budget method, 260,000 m^3/a by the hydrochemical (chloride-balance) method, and 1,400,000 $\pm$ 860,000 m^3/a by the water-budget method.

Unfortunately, these estimates are not directly comparable. Both the hydrochemical-budget and the water-budget estimates indicate only the thermal water that rises to a depth of 45 m or less, whereas the heat-budget estimate includes thermal water that may flow laterally at greater depths. Moreover, the water-budget estimate of thermal upflow may include a significant fraction of water substantially cooler than 199-209°C which has mixed with the hotter water during upflow.

The range of uncertainty almost certainly is larger for the hydrochemical- and water-budget estimates than for the heat-budget estimate. In fact, at the 95-percent confidence level, the water-budget estimate does not establish that any thermal upflow occurs at all. The hydrochemical-budget estimate is subject to sizable error if the chloride concentrations of the thermal, nonthermal, and mixed waters differ appreciably from the values of 2,200, 200, and 1,000 mg/L, respectively, used in the chloride-balance calculation.

Considering all the uncertainties described above, the best guess is that upflow of 199-209°C water from a deep thermal reservoir is on the order of 1,000,000 m^3/a, or 27 kg/s.

Movement of Thermal Fluid

Although details of the movement of thermal fluid through the Soda Lakes geothermal system are poorly understood, the general pattern may be inferred with some degree of confidence. Like several other hydrothermal convection systems in the northern Basin and Range province, the thermal fluid appears to ascend from depth along a fault-controlled conduit system. Recharge most likely occurs by slow downward movement over a much broader area, although the possibility of zones of localized recharge, also fault-controlled, cannot be ruled out on the basis of present information. Lateral movement in the deep groundwater subsystem probably takes place also, but its details are virtually unknown.

As described earlier, the main avenue of thermal upflow seems to be a concealed fault or fault system that has a N.55°W. strike. Close to the surface, a northeast-trending fault or faults appear to provide conduits that allow

at least some of the thermal fluid to ascend to within a few tens of meters of the land surface.

Unlike some northern Basin and Range systems, such as the Leach Hot Springs system in southern Grass Valley (Welch, Sorey, and Olmsted, 1981), in which little subsurface lateral leakage occurs, virtually all the thermal fluid leaks laterally from the Soda Lakes conduit system before reaching the surface. The leakage is swept northeastward, in the general direction of flow paths in the shallow ground-water subsystem. This accounts in large part for the strongly asymmetric pattern of the near-surface heat-flow anomaly (fig. 23).

If the thermal fluid rises with sufficient velocity, it may start to boil at the hydrostatic depth where boiling occurs. The boiling point versus hydrostatic depth curve for pure water at an altitude of 1,220 m (characteristic of the hottest part of the Soda Lakes thermal anomaly) is shown in figure 28. Also shown in figure 28 are temperature-depth profiles for test wells in the hottest part of the thermal anomaly. As indicated, none of the profiles actually intersects the depth-boiling point curve, although the profile for Chevron Resources well 11-33 is close at a hydrostatic depth of about 115 m. Assuming rapid upflow in the conduits, none of the wells appears to intersect a conduit, with the possible exception of well 11-33. The noncondensable-gas content of the fluid penetrated by well 11-33 may be sufficiently high so that the partial pressure of the gas lowers the boiling temperature of the fluid, and boiling does, in fact, occur at a depth of 115 m. It seems equally likely, however, that well 11-33, which is about midway between the two near-surface heat-flow maxima (fig. 24), does not actually intersect an upflow conduit.

If the dimensions of the flow system carrying the thermal fluid from where it enters the system as cold recharge to where it is discharged ultimately by evapotranspiration were known, it would be possible to estimate the residence time or time of travel of a parcel of thermal water on the basis of the flow rate discussed earlier and an assumption of piston (displacement) flow. Radiocarbon dating of thermal water in the discharge part of the system would help place an upper limit on such an estimate. Unfortunately, the requisite dimensions are very poorly known, and radiocarbon dates of the thermal water are not yet available. Highly speculative limits for the residence time or travel time can be assigned, however. Such limits are useful for the purpose of inferring whether the system is in hydrologic or thermal equilibruim and also for future

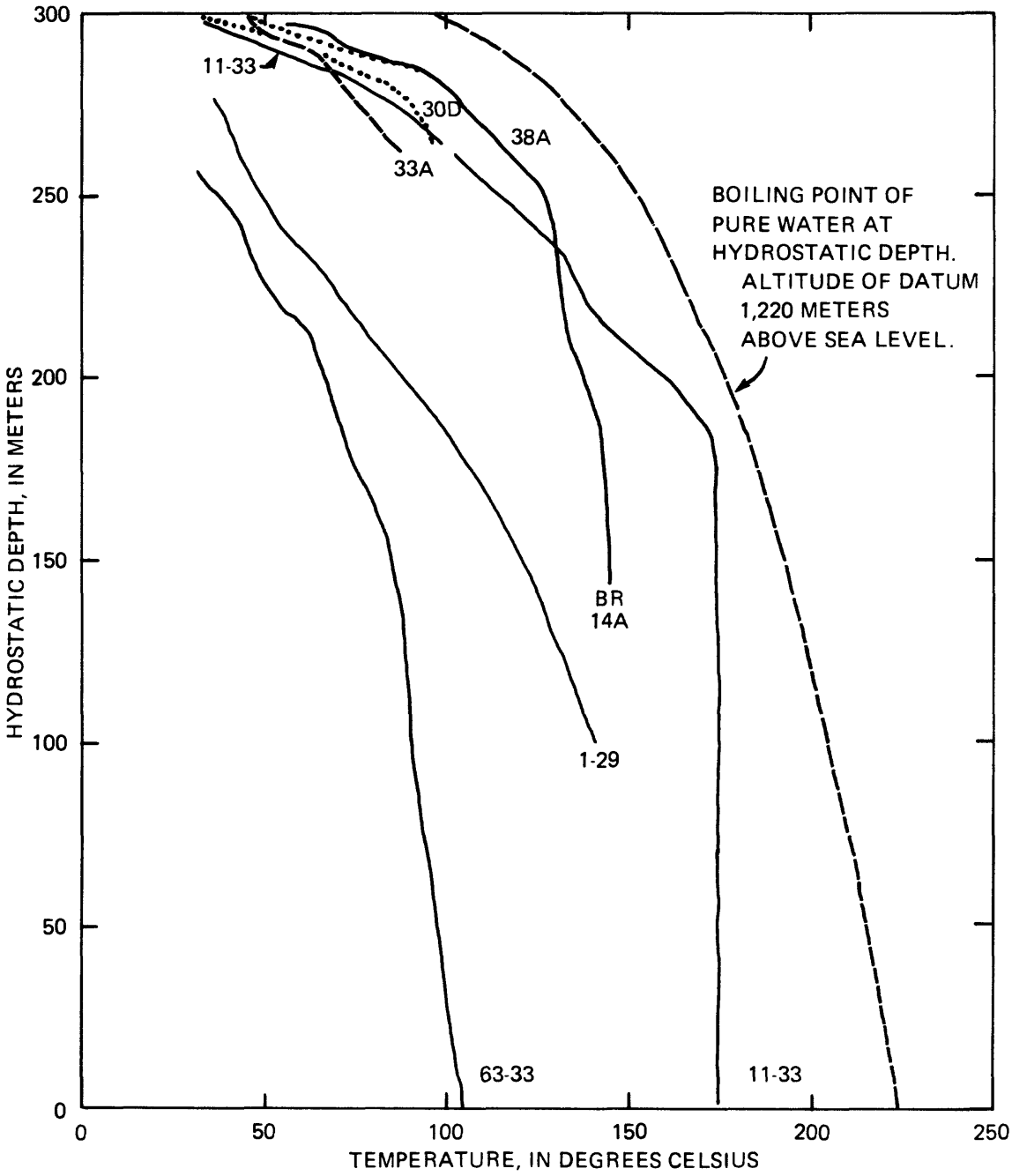

Figure 28. -- Boiling point of pure water at hydrostatic depth and temperature profiles in test wells in hottest part of Soda Lakes geothermal areas. Hyphenated numbers indicate wells of the U.S. Geological Survey or U.S. Bureau of Reclamation (prefix BR).

modeling studies to determine the effects of development on the thermal and hydrologic regimes.

In order to estimate upper and lower limits for travel time of thermal fluid through the system, two configurations for the flow system are postulated, as shown in the diagramatic section in figure 29. In both configurations, piston or displacement flow throughout the system and an estimated flux of thermal fluid of 1,000,000 m^3/a (p. 131) are assumed.

The first configuration (diagram A in fig. 29) gives a maximum travel time for the thermal fluid. The following characteristics are postulated: (1) The entire geothermal system has an areal extent of 640 km^2 (the upper limit of the estimated range, p. 126), a depth of 6 km, and the distribution of effective porosity with depth summarized in table 2; (2) all the water in the system above a depth of 3 km that has a temperature of 150°C or more has circulated through the deep part of the system--this represents the water in the upflow part of the system; (3) recharge of the thermal water occurs by slow downward movement over an area of 72 km^2-- the same as the area occupied by water of 150°C or higher temperature above a depth of 3 km in the upflow part of the system (table 11); and (4) the recharge (downflow) and discharge (upflow) parts of the system are connected by a zone of lateral flow of thermal water between depths of 4 and 6 km in which the average effective porosity is 1 percent (table 2). The derivation of the estimated volume of effective pore space through which piston flow of thermal fluid occurs is given in table 15.

As shown in table 15, the effective pore space through which piston flow of thermal fluid takes place occupies a volume of 34 km^3. At the estimated flux of thermal fluid of 1,000,000 m^3/a (p. 131), the time of travel is about 34,000 years.

The second configuration (diagram B in fig. 29) gives a minimum estimated volume of the flow system and therefore a minimum travel time for the thermal fluid. The following characteristics are postulated: (1) The entire geothermal system has an areal extent of 370 km^2 (the lower limit of the estimated range--p. 126); (2) recharge of thermal water occurs only within a fault zone or zones of limited areal extent and volume; (3) thermal water circulates within a localized conduit system that extends to depths of 8 km or more (deeper circulation than the 6-km depth postulated in configuration A would be required in order to attain an equivalent maximum temperature of 199-209°C); (4) thermal

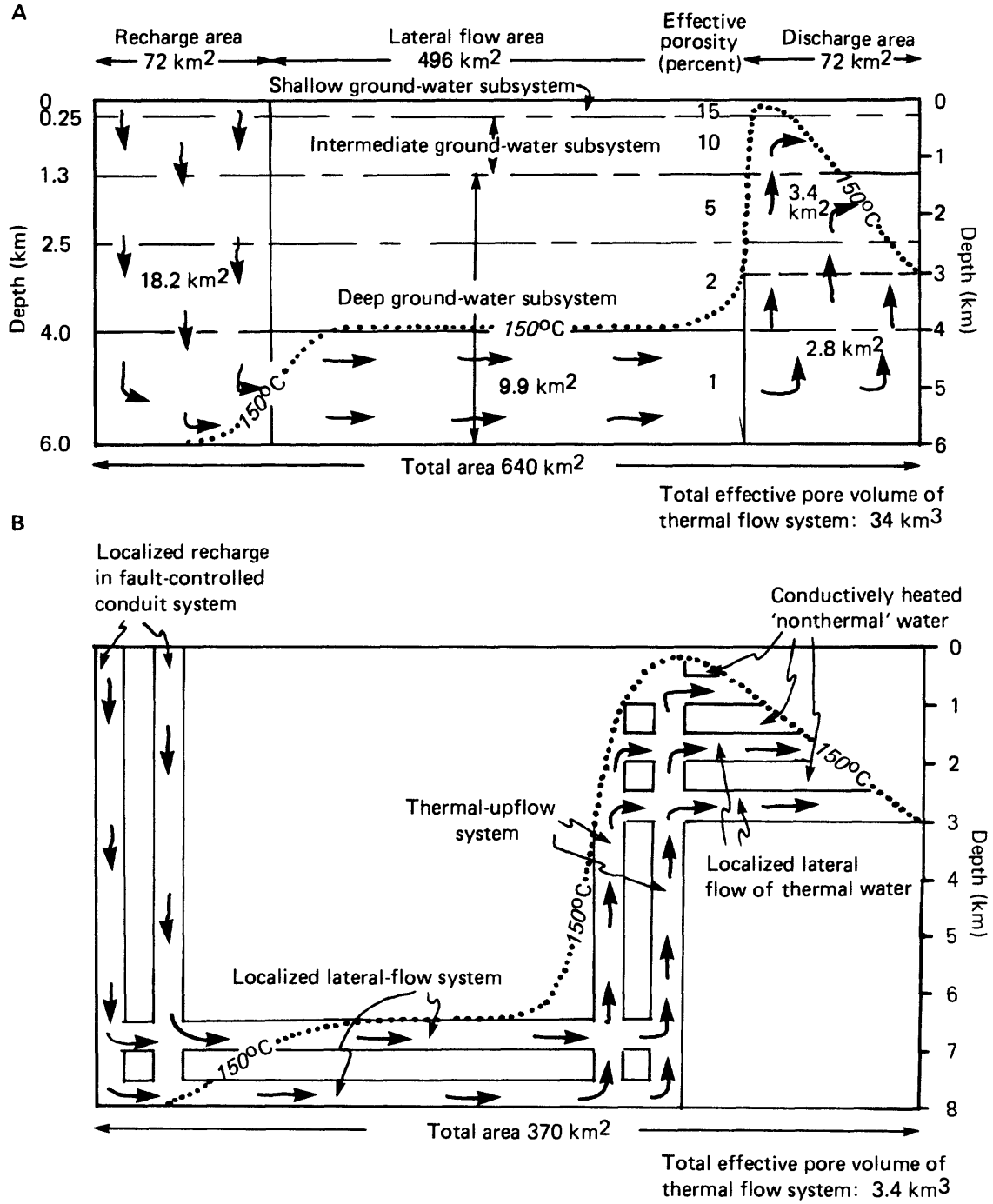

Figure 29. -- Two hypothetical configurations of Soda Lakes thermal flow system.

Table 15. — Maximum estimated volume of effective pore space through which piston flow of geothermal fluid occurs in Soda Lakes geothermal system (configuration A of fig. 29)

Depth (km)	Thickness (km)	Area (km^2)	Total volume (km^3)	Effective porosity (percent)	Volume of effective pore space (km^3)
Recharge area:					
0-0.25	0.25	72	18	15	2.7
0.25-1.3	1.05	72	76	10	7.6
1.3 -2.5	1.2	72	86	5	4.3
2.5 -4.0	1.5	72	108	2	2.2
4.0 -6.0	2.0	72	144	1	1.4
0-6.0	6.0	72	432	4.2	18.2
Lateral flow area:					
4.0-6.0	2.0	496	992	1	9.9
Discharge area:					
0-3.0	3.0	72	81[1/]	4.2[1/]	3.4[1/]
3.0-4.0	1.0	72	72	2	1.4
4.0-6.0	2.0	72	144	1	1.4
0-60	6.0	72	297	2.1	6.2
Totals (rounded)					
0-6.0	6.0	640	1,700	2.0	34

[1/] From table 13.

upflow occurs only within a restricted fault-controlled system and lateral flow from this conduit system also is restricted to a discrete aquifer or aquifers. Much of the water of 150°C or higher temperature in this part of the system therefore is not truly deep "thermal" water but instead is shallower water that has been heated conductively by the rising thermal water. The total volume of effective pore space in this configuration (diagram B in fig. 29), is even more speculative than that in the first configuration (diagram A in fig. 29). Arbitrarily, the volume is assumed to be one tenth that of the first configuration--that is, about 3.4 km^3. Hence, the estimated time of travel is of the order of 3,400 years at the estimated flux of 1,000,000 m^3/a.

Thus, the estimated limits for the age of a parcel of thermal fluid that has moved through the entire Soda Lakes geothermal system are about 3,400 to 34,000 years. These figures, although crude, have important implications as to the age and origin of the system and as to whether the system is in hydrologic or thermal equilibrum, as discussed in the next section.

Origin and Age of the System

As discussed earlier in the section, "Source and flux of heat" (p. 127), the most likely source of heat for the Soda Lakes geothermal system is above-normal heat flow in this part of the Basin and Range province rather than a localized shallow-crustal heat source associated with the eruptions that formed the craters surrounding the lakes. This interpretation tends to be substantiated by the failure to encounter high temperatures in Chevron Resources well 44-5, which is 1,488 m deep and about 1 km north of Big Soda Lake (Hill and others, 1979, p. 307), and also by the fact that the present Soda Lakes thermal anomaly is several kilometers northeast of the lakes.

If the eruptions that produced the Soda Lakes craters were not the apparent cause of the Soda Lakes geothermal system, another origin must be sought. High regional heat flow does not, of itself, produce hydrothermal-convection systems like that at Soda Lakes. The requisite ingredient is a system of faults that provide channelways for hot fluids at depth to rise with sufficient velocity to retain most of their heat. The inception of such faulting is difficult to date, but the faults at Soda Lakes certainly are related to Basin and Range faulting. Basin and Range faulting probably began at different times in different parts of the province; in the region including the Carson Desert, this style of faulting

has been predominant during the last 17 m.y. (Stewart, 1971, p. 1036). Thus, some form of hydrothermal activity could have been initiated as long ago as the middle Tertiary. However, there is no clear evidence that the Soda Lakes system is that old; the age of its inception remains enigmatic on the basis of available evidence.

As discussed in the previous section, the time required for a parcel of fluid to move through the deep part of the geothermal system from its recharge source to its discharge ultimately by evapotranspiration probably is at least several thousand and may be several tens of thousands of years. During such a period of time, climatic and perhaps subsurface-thermal conditions have not remained uniform (see Morrison, 1964, p. 97-114). In other words, the system probably cannot be assumed to be in hydrologic and thermal equilibrium. The most recent eruptions at Soda Lakes (within the last 7,000 years or so) and perhaps at Upsal Hogback (within the last 25,000 years ?) may post-date the recharge of a parcel of water presently being discharged as evapotranspiration. During this time, Lake Lahontan has occupied the area more than once, only to subsequently desiccate to present conditions (Morrison 1964). Present evidence does not, however, permit reliable inference as to whether the Soda Lakes geothermal system is presently cooling or heating or whether present recharge to and discharge from the deep part of the system are more or less than the long-term-average rates.

Upsal Hogback System

Extent and Configuration

The boundaries of the Upsal Hogback geothermal system, like those of the Soda Lakes system, are unknown. However, the areal extent of the Upsal Hogback system may be estimated in a manner similiar to that used to estimate the extent of the Soda Lakes system.

First, assume hydrologic and thermal equilibrium (steady-state conditions). Then, for the area occupied by the entire system, deficient near-surface heat discharge within the area of below-background heat flow must equal excess near-surface heat discharge within the area of above-background heat flow.

At a background heat flow of 3 hfu, excess heat discharge is 1.7 Mcal/s

within an area of 60 km^2 (p. 115). Assume that average near-surface heat flow outside the thermal anomaly is within the range of 1-2 hfu. Then, at an average heat flow of 1 hfu, the area of deficient near-surface heat discharge is

$$\frac{1.7 \times 10^6 \text{cal/s}}{(3.0-1.0) \times 10^{-6} \text{cal/cm}^2 \times \text{s}} = 8.5 \times 10^{11} \text{ cm}^2,$$

or 85 km^2. At an average heat flow of 2 hfu, the area of deficient near-surface heat discharge is

$$\frac{1.7 \times 10^6 \text{ cal/s}}{(3.0-2.0) \times 10^{-6} \text{ cal/cm}^2 \times \text{s}} = 1.7 \times 10^{12} \text{ cm}^2,$$

or 170 km^2. Total area occupied by the Upsal Hogback system therefore is 85 to 170 + 60 = 140 to 230 km^2.

If the area were circular, the corresponding diameter would be 13 to 17 km. By comparison, the Soda Lakes system is estimated to have an extent of 370 to 640 km^2, corresponding to a circular area 22 to 29 km in diameter. The Upsal Hogback geothermal system therefore is both smaller--about one-third to one-half as extensive--and has a less intense heat-flow anomaly--maximum near-surface heat flow of about 12 hfu as compared to more than 300 hfu--than the Soda Lakes system. The entire Upsal Hogback system, including the recharge parts and the parts containing nonthermal water, may have a volume of 420-1,400 km^3 on the basis of the estimated areal extent of 140-230 km^2 and an estimated depth of 3-6 km.

The Upsal Hogback thermal anomaly is somewhat asymmetrical, but less so than the Soda Lakes anomaly. The anomaly is somewhat elongated in a northerly direction, and the near-surface heat-flow maximum is in the southern part (fig. 23). Apparently, the Upsal Hogback anomaly is less affected than the Soda Lakes anomaly by heat transported laterally by shallow ground water. As shown in figure 17, thermal water flows laterally at a depth of 245 m at the site of well 64A, definitely within the intermediate ground-water subsystem at this location. The reversal in temperature gradient at 245 m in well 64A suggests

the possibility that thermal water rises somewhere else and flows laterally at this location. Although well 64A has the highest known shallow heat flow in the Upsal Hogback area, the actual heat-flow maximum within the anomaly (and presumably the site of thermal upflow) is elsewhere. The most likely place is less than 1 km north or northwest of well 64A. Temperature data at a depth of 1 m do not clearly indicate the location of the maximum, but the amplitude of the heat-flow and temperature anomaly is sufficiently small that the 1-m temperature data are not definitive (Olmsted, 1977).

Perhaps the most striking feature of the heat-flow pattern is the high lateral heat-flow gradient on the southeast side of the anomaly (fig. 23). This feature may be related to a northeast-trending high-angle fault on the southeast side of the buried structural high indicated by ground-magnetic and gravity data. The inferred buried fault or fault zone may contain the conduit or conduit system that transmits thermal fluid upward from depth to where it flows laterally in the zone at a depth of about 245 m.

The depth and temperature of the Upsal Hogback system below the maximum drilled depth of about 300 m at well 64A are unknown. The measured bottom temperature at that well was 61°C and the temperature was still decreasing with depth (reversed temperature gradient) above that depth. Geothermometric data, reviewed in the next section, suggest an equilibrium temperature of about 120°C for the thermal fluid in well 64A (actual temperature 78°C), but the depth and origin of this fluid remain conjectural. Deeper test drilling would be required to resolve this question.

Physicochemical Nature of Fluids

The physicochemical nature of the Upsal Hogback geothermal system is not well known; only one well penetrates a zone of deeply circulating thermal water. The highest-temperature water in well 64A appears to have undergone considerable conductive cooling. The cooling is suggested by the distinct temperature reversal (decreasing temperature with increasing depth) and a significantly lower source temperature (78°C) than that estimated using selected cation and silica geothermometers (117-120°C).

The source of recharge to the geothermal system appears to be somewhat saline water that had been subjected to evaporation. The water at well 64A (the

hottest and deepest water sampled in the Upsal Hogback anomaly) has a stable-isotope composition that indicates the following: (1) The primary process responsible for the elevated chloride concentration is evaporation; (2) the original isotopic composition of the water (prior to being affected by evaporation) was similiar to that found for the thermal water in the Soda Lakes anomaly; and (3) Soda Lakes and Upsal Hogback are separate systems (assuming that samples from Chevron Resources well 29-1 and well 64A are representative of the unmixed thermal water at the two anomalies). The good agreement between the selected silica and cation geothermometer estimates for the water at well 64A implies that mixing has not occurred since equilibration at a temperature of about 120°C.

There is no geochemical evidence for the existence of thermal water other than at well 64A within the Upsal Hogback system. Thermal water may exist in the shallow ground-water subsystem north of well 64A, but it has not been detected as yet.

Origin and Age of the System

Much of the discussion concerning the origin and age of the Soda Lakes system applies to the Upsal Hogback anomaly. The most likely source of heat for the Upsal Hogback system appears to be the above-normal heat flow in this part of the Basin and Range province. The apparent association with a buried bedrock high rather than the volcanically formed Upsal Hogback makes the volcanism a less likely source for the heat.

The age of the system is somewhat enigmatic. As discussed in the section on the Soda Lakes anomaly, the system could have been formed as early as the early Tertiary. Faulting due to loading and unloading caused by filling and desiccation of Lake Lahontan may be in part responsible for keeping the fracture system open.

The question of hydrologic and thermal equilibrium is as difficult to assess for the Upsal Hogback system as it is for the Soda Lakes system. The changing climatic conditions during the past few tens of thousands of years prevents determination of whether the system is in hydrologic equilibrium. The thermal water presently rising in the vicinity of well DH-64A may be older (>30,000 years) than the volcanically formed Upsal Hogback (25,000 years ?) raising the possibility that the area may not be in thermal equilibrium.

SUMMARY AND CONCLUSIONS

The Soda Lakes and Upsal Hogback geothermal systems are in the west-central Carson Desert, about 110 km east of Reno, Nev. Big and Little Soda Lakes lie about 15 km northwest of the town of Fallon. The lakes occupy craters formed by repeated explosive eruptions which ceased within the last 6,900 years. Upsal Hogback, 10-15 km north-northeast of Soda Lakes, is a group of low, overlapping cones formed of basaltic tuff by repeated eruptions which may have ended about 25,000-30,000 years ago. Apart from these features, the only surface manifestation of hydrothermal activity within the last 30,000 years in the Carson Desert consists of a small tract of hydrothermally altered sand and clay and a few intermittently active fumaroles surrounding a former well 4 km north-northeast of Big Soda Lake. The well reportedly encountered steam and boiling water at a depth of about 18 m.

Shallow ($\leq$ 45 m) test drilling established that the Soda Lakes geothermal area lies chiefly northeast of the old "steam" well and southwest of Upsal Hogback and is characterized by anomalously high temperatures and heat flows at shallow depths. Later drilling delineated the Upsal Hogback geothermal area, which lies east and north of the Hogback.

Geologic materials exposed in the Carson Desert area range from clastic sedimentary rocks and minor carbonate and igneous rocks of Triassic and Jurassic age to unconsolidated fluvial, lacustrine, and eolian deposits of Quaternary age. The older rocks, including volcanic and sedimentary rocks of Tertiary age, have been penetrated by test drilling but are not exposed within most of the study area.

Geologic structure in the Carson Desert is dominated by basin-and-range normal faults associated with regional east-west crustal extension. Gravity, seismic, magneto-telluric, and resistivity surveys indicate the presence of concealed faults within the Tertiary and older rocks, although only a few northeast- to north-trending faults transect the exposed nearly flat-lying Quaternary deposits within the study area. The hottest part of the Soda Lakes thermal anomaly may coincide with the intersection of faults that trend north-northeast and northwest. The hottest known part of the Upsal Hogback thermal anomaly appears to overlie a north-trending buried bedrock ridge.

The ground-water system beneath the study area is subdivided into shallow, intermediate, and deep subsystems on the basis of differences in hydrologic

properties of the rocks and deposits and inferred differences in the ground-water-flow regime. The shallow subsystem is composed of unconsolidated deposits of Quaternary age; its average thickness may be about 250 m. Because of the abundance of hydrologic data obtained from shallow test wells, the ground-water flow regime in the upper 45 m of the subsystem is fairly well known. The intermediate subsystem consists predominantly of slightly to moderately consolidated sediments of Tertiary and Quaternary (?) age, with minor intercalations of basalt flows, sills, or dikes, and it averages slightly more than 1,000 m in thickness in the Soda Lakes geothermal area. As in the shallow subsystem, ground water presumably moves chiefly through intergranular pores, but average permeability of the intermediate subsystem probably is substantially less than that of the shallow subsystem. Direction of ground-water flow in the intermediate subsystem is poorly known. The deep subsystem, which is composed predominantly of volcanic rocks of presumed Tertiary age and pre-Tertiary igneous, metamorphic, and sedimentary rocks, contains water chiefly in fractures and other secondary openings. The deep flow system is probably complex and largely not understood at this point.

The dissolved-solids concentrations of undiluted thermal water in the Soda Lakes and Upsal Hogback systems are thought to be about 4,000 and 6,500 mg/L, respectively, dominated by sodium and chloride. These characteristics, along with stable-isotope data, suggest that the source of recharge to each thermal system is ground water that (1) was subjected to considerable evaporation prior to deep percolation and (2) underwent only minor chemical modification--principally cation exchange and an increase in silica concentration, with limited net transfer of mass to the aqueous phase--in the thermal aquifer.

Throughout the study area, most shallow ground water (less than 50 m below the water table) having a temperature in excess of 20°C exhibits the geochemical imprint of one or more of the following processes, all of which post-date thermal upflow: Mixing of thermal and nonthermal water, conductive heating, steam loss, evaporation, and, near the Soda Lakes, acquisition of sulfate of apparently volcanic origin.

Evaporation is the dominant control on the concentration of the minor constituents boron and bromide, as shown by the strong correlation of these constituents with chloride. However, rubidium and lithium show only fair correlation, and fluoride and arsenic, no correlation with chloride. Thermal

water in the Soda Lakes geothermal system has higher lithium-to-chloride ratios than those found in the nonthermal water, indicating that this ratio may be a useful indicator of thermal activity. Unlike the situation in many geothermal areas, fluoride and arsenic do not appear to be good indicators of thermal water.

Temperature information about the deeper parts of the Soda Lakes and Upsal Hogback geothermal systems was obtained from wells ranging in depth from 150 to 1,356 m, most of which were drilled by private companies. Temperature-depth profiles in these wells form two groups: (1) Those characterized by high gradients in the upper part and having one or more inflection points, below which the gradient decreases abruptly or even reverses; and (2) those characterized by low gradients in the upper part, in which the gradients persist throughout the depth range penetrated by the well. The first group exhibits features clearly related to convection or advection caused by vertical or lateral ground-water flow. The temperature-depth profiles of the second group appear to be dominated by conduction, although subtle effects of convection or advection are present in some of these profiles too.

Information about the shallower parts of the system was obtained from Geological Survey test wells 45 m or less in depth. Most of the temperature-depth profiles in these shallow wells are dominated by conduction, but some show features related to convection or advection.

Temperature-depth data, supplemented by projected temperature-depth profiles based on assumed values for thickness and average thermal conductivity of materials below depths penetrated by wells, were used to estimate the depth to the 150°C isotherm in the Soda Lakes geothermal system. The 150°C isotherm could not be defined in the Upsal Hogback system because the maximum temperature observed in that system was only 78°C and because chemical geothermometry indicates a source temperature of only 120°C for that water.

Using the 150°C isotherm as the minimum-temperature boundary, the estimated volume of the geothermal reservoir above a depth of 3 km for the Soda Lakes system is 81 ± 24 km^3. The volume of effective pore space is estimated to be 3.4 ± 1.2 km^3. The total heat content or reservoir thermal energy is estimated to be 7.0×10^{18} cal. These values are several times greater than previous estimates by the Geological Survey.

Geothermal heat discharge from the Soda Lakes and Upsal Hogback thermal

anomalies--the areas of above-normal near-surface heat flow--comprises two components: (1) anomalous or excess discharge that results from convective heat transport by rising ground water, including thermal water from great depths; and (2) regional or background discharge--the heat that would have discharged at the land surface without the effects of ground-water upflow. Most of the total near-surface heat discharge is by conduction, although convection is locally significant.

Conductive heat flow at each test-well site was estimated as the product of the average temperature gradient within the depth interval of interest and the harmonic-mean thermal conductivity of that interval. Harmonic-mean thermal conductivity was estimated using values assigned to several categories of materials reported in lithologic logs of the test wells. The assigned thermal conductivities were based primarily on theoretical values rather than the experimental values obtained for 89 core samples obtained from the Carson Desert. Estimated values of conductive heat flow were adjusted to include convective effects caused by vertical ground-water flow in the materials penetrated by the drill hole, using vertical ground-water flow velocities calculated from measured vertical hydraulic gradients and estimated values of vertical hydraulic conductivity. Two methods of estimating near-surface heat flow were used, using different depth intervals and different ways of measuring or estimating the temperature gradients. Overall accuracy of the estimates is judged to be $\pm$ 30 percent.

Regional heat flow in the Carson Desert probably is within the range of 2-3 hfu. The most likely source of heat for both the Soda Lakes and the Upsal Hogback systems is above-normal heat flow in this part of the Basin and Range province.

Both the Soda Lakes and the Upsal Hogback thermal anomalies are poorly defined below heat-flow values of about 5 hfu. At a background heat flow of 3 hfu, the estimated extent of the Soda Lakes and Upsal Hogback anomalies is, respectively, 110 and 60 km^2; the anomalous heat discharge is, respectively, 5.3 $\pm$ 1.6 Mcal/s and 1.7 $\pm$ 0.5 Mcal/s.

The Soda Lakes anomaly, which outlines the upflow part of the system, is strongly asymmetrical and elongated toward the northeast. The hottest part of the anomaly is near the southwest margin. The anomaly also is asymmetrical in a northwest-southeast direction, with lateral temperature and heat-flow gradients

being greater toward the northwest than toward the southeast. The hottest near-surface part of the anomaly probably coincides with the intersection of the faults that trend north-northeast and northwest (N.55°W.) The faults provide steeply inclined conduits for thermal fluids that may rise from depths of 3 to 7 km within fractured Tertiary and (or) pre-Tertiary rocks to as shallow as about 20 m below land surface, where near-surface heat flows exceed 300 hfu. The hottest water at depth may be southeast of the hottest part of the near-surface anomaly.

The Upsal Hogback anomaly also is asymmetrical, but less so than the Soda Lakes anomaly. The Upsal Hogback anomaly is elongated in a northerly direction, and the near-surface heat-flow maximum, where heat flow is about 12 hfu, is in the southern part. Apparently that anomaly is less affected than the Soda Lakes anomaly by heat transported laterally by shallow ground-water flow. Location of the conduit or conduits for upflow into a thermal aquifer at a depth of 245 m is unknown, but it may be a short distance north or northwest of the test well (64A) having the highest known shallow heat flow in the area.

All evidence indicates that the Soda Lakes system is a hot-water system rather than a steam system, although a small steam cap may be present in the hottest part of the near-surface anomaly. The hottest water sampled had a temperature of 186°C at a depth of 610 m in a private-company well 330 m south of the old steam well. The quartz-silica and cation geothermometers indicate, repectively, 186°C and 209°C for a sample from this well. Close agreement between chemical-geothermometer and measured temperatures for some samples indicates that some thermal water at Soda Lakes has re-equilibrated at lower temperatures. Water at some sites appears to be either conductively heated or a mixture of thermal and nonthermal water.

The depth and temperature of the Upsal Hogback system below the maximum drilled depth of about 300 m are unknown. The highest temperature observed (78°C at 245 m) is significantly lower than that estimated from chemical geothermometry (about 120°C). Assuming no mixing of thermal and nonthermal waters, the thermal water in the Upsal Hogback system is not a result of deep flow from the Soda Lakes system. Age of the thermal water in the Upsal Hogback system is indicated by radiocarbon dating to be about 25,000-35,000 years.

The entire Soda Lakes geothermal system, including the recharge part and the part containing nonthermal water, may have a volume of 1,100-3,800 km^3 on

the basis of an estimated areal extent of 370-640 km^2 and an estimated depth of 3-7 km. Upflow of thermal water from the deep part of the Soda Lakes system is estimated to be 1,010,000-1,150,000 m^3/a by the heat budget method, 260,000 m^3/a by the hydrochemical budget (chloride-balance) method, and 1,400,000-1,430,000 $\pm$ 860,000 m^3/a by the water-budget method. Considering the many uncertainties in these estimates, the most reasonable guess is that the upflow amounts to about 1,000,000 m^3/a (27 kg/s) of 199-209°C water. The upflow appears to take place in a fault-controlled conduit system, but recharge to the thermal system most likely occurs by slow downward movement over a much broader area. Recharge along fault-controlled zones of restricted lateral extent cannot be ruled out on the basis of available evidence, however.

Lower and upper limits of travel time or residence time of thermal water in the Soda Lakes system are estimated to be respectively 3,400 and 34,000 years on the basis of a flux of 1,000,000 m^3/a, an effective pore-space volume of 3.4 to 34 km^3, and assumed piston or displacement flow.

Assuming that the water of Chevron Resources well 1-29 is representative of undiluted thermal fluid in the Soda Lakes system, the upflow (an estimated 1,000,000 m^3/a) contributes approximately 4,000 metric tons/a of dissolved solids, of which a little more than half is chloride.

REFERENCES CITED

Bedinger, M. S., 1961, Relation between median grain size and permeability in the Arkansas River valley, in U.S. Geological Survey Professional Paper 424-C: p. C31-C32.

Bredehoeft, J. D., and Papadopulos, I. S., 1965, Rates of vertical groundwater movement estimated from Earth's thermal profile: Water Resources Research, v.1, no. 2, p. 325-328.

Brook, C. A., Mariner, R. H., Mabey, D. R., Swanson, J. R., Guffanti, Marianne, and Muffler, L. J. P., 1978, Hydrothermal convection systems with reservoir temperature $\geq$ 90°C, in Muffler, L. J. P., ed., Assessment of geothermal resources of the United States--1978: U.S. Geological Survey Circular 790, p. 18-85.

Craig, Harmon, 1961, Isotopic variations in meteoric waters: Science, v. 133, no. 3465, p. 1702-1703.

Eakin, T. E., and Maxey, G. B., 1951, Ground water in Ruby Valley, Elko and White Pine Counties, Nevada, in Contributions to the hydrology of eastern Nevada (1951): Nevada State Engineer, Water Resources Bulletin 12, p. 65-93.

Eugster, H. P., and Hardie, L. A., 1978, Saline Lakes, Chapter 8, in Lakes: chemistry, geology, physics, (Abraham Lerman, ed.): New York, Springer-Vertag, p. 237-249.

Eugster, H. P., and Jones, B. F., 1979, Behavior of major solutes during closed-basin brine evolution: American Journal of Science, v. 279, p. 609-631.

Evans, S. H., Jr., 1980, Summary of potassium/argon dating--1979: Department of Geology and Geophysics, University of Utah, Salt Lake City, Utah, Topical Report, 23 p.

Fournier, R. O., 1977, Chemical geothermometers and mixing models for geothermal systems: Geothermics, v. 5, p. 41-50.

Fournier, R. O., White, D. E., and Truesdell, A. H., 1974, Geochemical indicators of subsurface temperature, Part I, Basic Assumptions: U.S. Geological Survey Journal of Research, v. 2, no. 3, p. 259-262.

Fournier, R. O., and Potter, R. W., II, 1979, A magnesium correction for the Na-K-Ca chemical geothermometer: U.S. Geological Survey Open-File Report 78-796, 24 p.

Freeze., R. A., and Cherry, J. A., 1979, Groundwater: Englewood Cliffs, N.J., Prentice-Hall, Inc., 604 p.

Garside, L. J., and Schilling, J. H., 1979, Thermal waters of Nevada, Bulletin 91: Nevada Bureau of Mines and Geology, MacKay School of Mines, University of Nevada, Reno, 163 p.

Glancy, P. A., 1981, Geohydrology of the basalt and unconsolidated sedimentary aquifers in the Fallon Area, Churchill County, Nevada: U. S. Geological Survey Open-File Report 80-2042, 94 p.

Glancy, P. A., and Katzer, T. L., 1975, Water-resources appraisal of the Carson River basin, western Nevada: Nevada Division of Water Resources Reconnaissance Series Report 59, 126 p.

Hardman, George, 1936, Nevada precipitation and acreages of land by rainfall zones: University of Nevada Agriculture Experimental Station mimeo. rept. and map, 10 p.

Hardman, George, 1965, Nevada precipitation map, adapted from map prepared by George Hardman and others, 1936: University of Nevada Agriculture Experimental Station Bulletin 183, 57 p.

Hardman, George, and Mason, H. G., 1949, Irrigated lands of Nevada: University of Nevada Agriculture Experimental Station Bulletin 183, 57 p.

Hill, D. G., Layman, E. B., Swift, C. M., and Yungul, S. H., 1979, Soda Lakes, Nevada, thermal anomaly: Geothermal Resources Council, Transactions, v. 3, p. 305-308.

Horton, R. C., 1978, Lithologic log and interpretation of instrument logs, NURE project Carson Sink, Nevada, borehole: U.S. Department of Energy, 1978, 36 p.

Johnson, A. I., Moston, R. P., and Morris, D. A., 1968, Physical and hydrologic properties of water-bearing deposits in subsiding areas in central California: U.S. Geological Survey Professional Paper 497-A, 71 p.

Jones, B. F., 1966, Geochemical evolution of closed-basin water in the western Great Basin: Second symposium on salt, Northern Ohio Geological Survey, (Rau, J. L., ed.), v. 1, p. 181-200.

Kharaka, Y. K., and Barnes, Ivan, 1973, SOLMNEQ-solution mineral equilibrium computations: Menlo Park, California, U.S. Geological Survey, Computer contribution, 81 p.; available only from U.S. Department of Commerce, National Technical Information Service, Springfield, VA 22151, as Report PB-215 899.

Krumbein, W. C., and Monk, G. D., 1942, Permeability as a function of the size parameters of unconsolidated sand: Transactions of the American Institute of Mining Engineers, v. 151, p. 153-163.

Lachenbruch, A. H., and Sass, J. H., 1977, Heat flow in the United States and the thermal regime of the crust, in The Earth's crust, J. G. Heacock, ed.: American Geophysical Union, Monograph 20, p. 626-675.

Mariner, R. H., Presser, T. S., Rapp, J. B., and Willey, L. M., 1975, The minor and trace elements, gas, and isotope compositions of the principal hot springs of Nevada and Oregon: U.S. Geological Survey Open-File Report, 27 p.

Morgan, D. S., 1982, Hydrogeology of the Stillwater area, Churchill County, Nevada: U.S. Geological Survey Open-File Report 82-345, 95 p.

Morris, D. A., and Johnson, A. I., 1967, Summary of hydrologic properties of rock and soil materials, as analyzed by the Hydrologic Laboratory of the U.S. Geological Survey, 1948-60: U.S. Geologic Survey Water-Supply Paper 1839-D, 42 p.

Morrison, R. B., 1964, Lake Lahontan: Geology of the southern Carson Desert, Nevada: U.S. Geological Survey Professional Paper 401, 156 p.

Muffler, L. J. P., Guffanti, Marianne, Sass, J. H., Lachenbruch, A. H., Smith R. L., Shaw, H. R., Brook, C. A., Mariner, R. H., Maybey, D. R., Swanson, J. R., Sammel, E. A., Wallace, R. H., Kraemer, T. F., Taylor, R. E., Wesselman, J. B., 1979, Assessment of geothermal resources of the United States--1978: (Muffler, L. J. P. ed.) U.S. Geological Survey Circular 790, 163 p.

National Oceanic and Atmospheric Administration, 1975, Climatological Data, Nevada, Annual Summary 1975: U.S. Department of Commerce, National Oceanigraphic and Atmospheric Administration (formerly U.S. Weather Bureau) v. 90, no. 13.

Nevada Department of Conservation and Natural Resources, 1960-74, Reconnaissance Series Reports 1-60.

Nevada State Engineer Water Planning Report, 1971, Water for Nevada #3, Nevada's water resources: Nevada State Engineers' Office, 87 p.

Olmsted. F. H., 1977, Use of temperature surveys at a depth of 1 meter in geothermal exploration in Nevada: U.S. Geological Survey Professional Paper 1044-B, 25 p.

Olmsted, F. H., Glancy, P. A., Harrill, J. R., Rush, F. E., and VanDenburgh, A. S., 1973, Sources of data for evaluation of selected geothermal areas in northern and central Nevada: U.S. Geological Survey Water-Resources Investigations 44-74, 78 p.

---1975, Preliminary hydrogeologic appraisal of selected hydrothermal systems in northern and central Nevada: U.S. Geological Survey Open-File Report 75-56, 267 p.

Renner, J. L., White, D. E., and Williams, D. L., 1975, Hydrothermal convection systems, in Assessment of geothermal resources of the United States--1975 (White, D. E., and Williams D. L, eds.) U.S. Geological Survey Circular 726, p. 51-57

Roy, R. F., Decker, E. R., Blackwell D. D., and Birch, Francis, 1968, Heat flow in the United States: Journal of Geophysical Research, v. 73, p. 5207-5221.

Rush, F. E., 1972, Hydrologic reconnaissance of Big and Little Soda Lakes, Churchill County, Nevada: Nevada Department of Conservation and Water Resources Water Resources-Information Service Report 11.

Sass, J. H., Blackwell, D. D., Chapman, D. S., Costain, J. K., Decker, E. R., Lawver, L. A., Swanberg, C. A., and others, 1980, Heat flow from the crust of the United States, Chapter 13 in Touloukian, Y. S., Judd, W. R., and Roy, R. F., editors, Physical properties of rocks and minerals: New York, McGraw-Hill Book Co.

Schaefer, D. H., 1980, Water resources of the Walker River Indian Reservation, west-central Nevada: U.S. Geological Survey Open-File Report 80-427, 59 p.

Sibbett, B. S., 1979, Geology of the Soda Lakes geothermal area: Earth Science Laboratory, University of Utah Research Institute, Publication DOE/ET 283293-34 78-1701.b.1.2.3 ESL-24, 14 p., 4 well logs, 1 plate.

Sibbett, B. S., and Blackett, R. E., 1982, Lithologic interpretation of the DeBraga #2 and Richard Weishaupt # 1 geothermal wells, Stillwater project, Churchill County, Nevada: Earth Science Laboratory, University of Utah Research Institute, Publication DOE/ID/12079-57, ESL-70, 10 p., appendix.

Sorey, M. L., 1971, Measurement of vertical ground water velocity from temperature profiles in wells: Water Resources Research, v. 7, no. 4, p. 963-970.

Stanley, W. D., Wahl, R. R., and Rosenbaum, J. G., 1976, A magnetotelluric study of the Stillwater-Soda Lakes, Nevada, geothermal area: U.S. Geological Survey Open-File Report 76-80, 38 p.

Stark, Mitchel, Wilt, Michael, Haught, J. R., and Goldstein, Norman, 1980, Controlled-source electromagnetic survey at Soda Lakes geothermal area, Nevada: Laurence Berkeley Laboratory Report LBL-11221, 93 p.

Stewart, J. H., 1971, Basin and Range structure: A system of horsts and grabens produced by deep-seated extension: Geological Society of America Bulletin, v. 82, p. 1019-1044.

Till, Rodger, 1974, Statistical methods for the earth scientist: New York, John Wiley and Sons, 154 p.

University of Utah Research Institute, 1979a, Dipole-dipole resistivity survey, Soda Lake, Nevada: Salt Lake City, University of Utah Open-File item Soda Lake (CRC)-1, 13 p.

---1979b, Magnetotelluric survey, Soda Lake, Nevada: Salt Lake City, University of Utah Open-File item Soda Lake (CRC)-2, 104 p.

---1979c, Magnetotelluric survey, Soda Lake, Nevada: Salt Lake City, University of Utah Open-File item Soda Lake (CRC)-3, 88 p.

---1979d, Reflection seismic survey, Soda Lake, Nevada: Salt Lake City, University of Utah Open-File item Soda Lake (CRC)-4, 31 p.

---1979e, Reflection seismic survey, Soda Lake, Nevada: Salt Lake City, University of Utah Open-file item Soda Lake (CRC)-5.

---1979f, Test hole data, Soda Lake, Nevada: Salt Lake City, University of Utah Open-file item Soda Lake (CRC)-6, 16 p.

---1979g, Test hole data, Soda Lake Nevada: Salt Lake City, University of Utah Open-file item (CRC)-7, 6 p.

---1979h, Test hole data, Soda Lake, Nevada: Salt Lake City, University of Utah Open-file item (CRC)-8, 21 p.

---1979i, Test hole data, Soda Lake, Nevada: Salt Lake City, University of Utah Open-file item (CRC)-9, 22 p.

---1979j, Test hole data, Soda Lake, Nevada: Salt Lake City, University of Utah Open-file item Soda Lake (CRC)-10.

---1979k, Ground magnetics and gravity maps, Desert Peak, Nevada: Salt Lake City, University of Utah Open-file item Desert Peak (PPC)-2.

Voegtly, N. E., 1981, Reconnaissance of the Hot Springs Mountains and adjacent areas, Churchill County, Nevada: U.S. Geological Survey Open-File Report 81-134, 10 p.

Wentworth, C. E., 1922, A scale of grade and class terms for clastic sediments: Journal of Geology, v. 30, p. 377-392.

Wigley, T. M. L., 1975, Carbon 14 dating of groundwater from closed and open systems: Water Resources Research, v. 11, p. 324-328.

Willden, Robert, and Speed, R. C., 1974, Geology and mineral deposits of Churchill County, Nevada: Nevada Bureau of Mines and Geology, Bulletin 83, 95 p.

Wood, W. W., 1976, Guidelines for collection and field analysis of ground-water samples for selected unstable constituents: U.S. Geological Survey Techniques of Water-Resources Investigations, Book 1, Chapter D2, 24 p.

Table 16. -- Records of test wells

Test well number	Location number	Latitude north ° ' "	Longitude west ° ' "	Altitude of land surface above sea level (m)	Height of measuring point above land surface (m)	Depth of screen or cap at bottom (m)	Nominal inside diameter of casing (mm)	Type of completion [1]	Geophysical logs available [2]	Other data available [3]
U.S. Geological Survey test wells										
AH-1A	19/28-9dda	39 31 20	118 50 13	1,217.069	0.549	6.16-6.77	38	St,Sc	----	L,W
AH-2A	20/28-22bca1	39 35 16	118 49 56	1,211.400	.213	25.91-26.52	38	St,Sc	G,G^2,N	L,W,Tp,C
AH-2B	-22bca2	39 35 16	118 49 56	1,211.400	.158	9.78-10.39	38	St,Sc	----	W
AH-3A	-14bbb1	39 36 21	118 49 04	1,200.232	.518	43.56-44.17	38	St,Sc	G,G^2,N	L,W,Tp,C
AH-3B	-14bbb2	39 36 21	118 49 04	1,200.232	-0.015	6.89-7.19	38	St,Sc	----	W
AH-4A	19/27-1aad	39 32 43	118 53 37	1,219.770	.671	20.12-20.73	38	St,Sc	G,G^2,N	L,W,Tp,C
AH-7A	20/28-21ccb1	39 34 54	118 51 18	1,213.247	1.006	44.50	38	St,Sc	G,G^2,N	L,Tp
AH-7B	-21ccb2	39 34 54	118 51 18	1,213.247	.372	7.71-8.32	38	St,Sc	----	W
AH-8A	-32cad1	39 33 09	118 51 55	1,216.280	.457	37.95-38.86	38	St,Sc	G,G^2,N	L,W,Tp,C
AH-8B	-32cad2	39 33 09	118 51 54	1,216.280	.475	3.02-3.63	38	St,Sc	----	W
AH-9A	-24bdd1	39 35 06	118 47 30	1,207.810	1.341	39.32-39.93	38	St,Sc	G,G^2,N,T, Co	L,W,Tp,C
AH9B	-24bdd2	39 35 06	118 47 30	1,207.810	.195	9.57-10.18	38	St,Sc	----	W
AH-10A	21/28-24bba1	39 40 46	118 47 26	1,189.759	.244	32.31-33.22	38	St,Sc	G,G^2,N	L,W,Tp,C
AH-10B	-24bba2	39 40 46	118 47 26	1,189.759	.768	2.28-2.89	51	P,Sl	----	----
AH-10C	-24bba3	39 40 46	118 47 26	1,189.759	.732	3.25-3.86	51	P,Sl	----	W

Table 16. -- Records of test wells (Continued)

Test well number	Location number	Latitude north ° ' "	Longitude west ° ' "	Altitude of land surface above sea level (m)	Height of measuring point above land surface (m)	Depth of screen or cap at bottom (m)	Nominal inside diameter of casing (mm)	Type of completion [1]	Geophysical logs available [2]	Other data available [3]
U.S. Geological Survey test wells										
AH-11A	-34ddc	39 38 15	118 48 57	1,205	.305	9.45	38	St,C	G	L,Tp,T
AH-12A	20/28-10aaa1	39 37 04	118 49 06.2	1,206.874	.853	21.46-22.37	38	St,Sc	G,G^2,N	L,W,Tp,C
AH-12B	-10aaa2	39 37 14.5	118 49 06	1,206.874	.725	14.14-14.60	39	St,Sc	----	W
AH-13A	21/29-7bac1	39 42 26	118 46 09	1,189.092	1.158	21.18	38	St	G,G^2,N,T, Co	L,W,Tp
AH-13B	-7bac2	39 42 25	118 46 09	1,189.092	.600	2.48-3.09	51	P,Sl	----	----
AH-13C	-7bac3	39 42 26	118 46 09	1,189.092	.634	4.22-4.83	51	P,Sl	----	W
AH-17A	20/28-32aad1	39 33 35	118 51 20.9	1,212.217	.579	8.99-9.60	38	St,Sc	G,G^2,T, Co	L,W,Tp
AH-17B	-32aad2	39 33 35.4	118 51 21	1,212.217	.546	6.10-6.56	38	St,Sc	----	W,Tp
AH-18A	-32adc1	39 33 22	118 51 36	1,214.680	.396	41.15-41.76	38	St,Sc	G,G^2,N,T	L,W,Tp,C
AH-18B	-32adc2	39 33 22.1	118 51 36	1,214.680	.396	4.72-5.33	38	St,Sc	----	W
DH-27A	-33aca1	39 33 30.7	118 50 37.5	1,211.674	.366	44.07-44.68	51	P,Sc	G,G^2,N,T	L,W,Tp
AH-27B	-33aca2	39 33 30.7	118 50 37.6	1,211.674	.503	4.77-4.97	51	P,Sl	----	W
DH-29A	20/28-27cca1	39 33 56.0	118 49 55.3	1,211.071	1.158	43.95-44.56	38	St,Sc	G,G^2,N,T	L,W,Tp
AH-29B	-27cca2	39 33 56.0	118 49 55.3	1,211.071	.448	6.22-6.68	38	St,Sc	----	W
DH-30A	-28cdc1	39 33 46.8	118 33 46.8	1,209.611	.579	39.93-40.54	38	St,Sc	G	L,W,Tp,C
JH-30B	-28cdc2	39 33 46.7	118 51 03.0	1,209.611	1.131	1.55-2.01	51	P,Sl	----	W

Table 16. -- Records of test wells (Continued)

Test well number	Location number	Latitude north ° ' "	Longitude west ° ' "	Altitude of land surface above sea level (m)	Height of measuring point above land surface (m)	Depth of screen or cap at bottom (m)	Nominal inside diameter of casing (mm)	Type of completion [1]	Geophysical logs available [2]	Other data available [3]
U.S. Geological Survey test wells										
AH-30C	-28cdc3	39 33 46.7	118 51 03.2	1,209.611	.463	2.56-3.17	51	P,Sl	----	W
DH-30D	-28cdc9	39 33 46.8	118 51 01.9	1,209.611	.341	37.03-38.25	51	St,C	T	Tp
DH-31A	-32aab	39 33 43.4	118 51 36.2	1,214.601	.610	38.01-38.62	38	St,Sc	G,G^2,N	L,W,Tp
DH-32A	-28bcd1	39 34 14.8	118 51 12.2	1,213.723	.610	44.53-45.14	38	St,Sc,	G,G^2,N,R, Co	L,W,Tp,C
AH-32B	-28bcd2	39 34 14.8	118 51 12.0	1,213.723	.341	6.58-7.19	51	P,Sl	----	W
DH-33A	-28cad1	39 34 01.0	118 50 51.3	1,212.272	.853	43.95-44.56	38	St,Sc	G,G^2,R	L,W,Tp
AH-33B	-28cad2	39 34 00.9	118 50 51.3	1,212.272	.305	6.16-6.77	51	P,Sl	----	W
DH-34A	-33bcb1	39 33 22.9	118 51 17.7	1,215.997	.671	44.44-45.05	38	St,Sc	G,G^2,N,R, Co	L,W,Tp
AH-34B	-33bcb2	39 33 22.9	118 51 17.8	1,215.997	.411	6.89-7.50	38	St,Sc	----	W
AH-35A	-21ddd1	39 34 42.4	118 50 18.1	1,206.011	.853	20.06-20.51	38	St,Sc	G,G^2,N	L,W,Tp
AH-35B	-21ddd2	39 34 42.3	118 50 18.1	1,206.011	.384	1.98-2.59	51	P,Sl	----	W
AH-36A	-21acd	39 35 03	118 50 36	1,212.376	.427	20.67-21.12	38	St,Sc	G,G^2,N	L,W,Tp
AH-37A	-28dca	39 33 52.8	118 50 35.6	1,211.830	.488	13.14-13.59	38	St,Sc	G,G^2,N	L,W,Tp
AH-38A	-33bbb1	39 33 43.4	118 51 20.6	1,215.506	.671	21.37-21.82	38	St,Sc	G	L,W,Tp
DH-39A	-34cbb1	39 33 17	118 50 11	1,214.238	.610	41.27-41.88	51	P,Sl,	G,G^2,N	L,Tp

Table 16. — Records of test wells (Continued)

Test well number	Location number	Latitude north ° ' "	Longitude west ° ' "	Altitude of land surface above sea level (m)	Height of measuring point above land surface (m)	Depth of screen or cap at bottom (m)	Nominal inside diameter of casing (mm)	Type of completion [1]	Geophysical logs available [2]	Other data available [3]
U.S. Geological Survey test wells										
DH-39B	-34cbb2	39 33 17	118 33 17	1,214.238	.332	6.17-6.78	51	P,Sl	----	W
DH-40A	-20dcd1	39 34 38	118 51 41	1,214.543	.884	41.09-41.54	51	P,Sl	G,G^2,N	L,Tp
DH-40B	-20dcd2	39 34 38	118 51 41	1,214.543	.424	11.41-11.87	51	P,Sl	----	W
DH-41A	-14dcc1	39 35 31	118 48 24	1,208.242	.213	41.85-42.86	51	P,Sl	G,G^2, N, T	L,W,Tp
DH-41B	-14dcc2	39 35 31	118 48 24	1,208.242	.646	11.35-11.81	51	P,Sl	----	W
DH-46A	21/28-16ddd1	39 40 51.0	118 50 00.6	1,189.238	.549	25.66-26.58 31.47	38	St,C,P_F	G,G^2,N	L,Tp
DH-46B	-16ddd2	39 40 51.0	118 50 00.6	1,189.238	.329	3.93-4.54	51	P,Sl	----	W
AH-46C	-16ddd3	39 40 51.0	118 50 00.7	1,189.238	.585	.94-1.55	51	P,Sl	----	W
AH-46D	-16ddd4	39 40 51.1	118 50 00.7	1,189.238	.695	16.08-16.54	38	St,Sc	----	W,Cs,Tp
DH-47A	22/29-30bac	39 45 06	118 46 09	1,184	.457	28.35	51	P,C	G,G^2,N	L,Tp,W
DH-48A	21/29-31aab1	39 38 58.0	118 45 36.6	1,189.762	0.518	30.94-31.39	38	St,Sc	G,G^2,N	L,W,Tp
DH-48B	-31aab2	39 58 57.9	118 45 36.6	1,189.762	.177	4.11-4.57	51	P,Sl	----	W
DH-49A	-33aaa1	39 39 03	118 43 13	1,184.599	.610	31.55-32.00	38	St,Sc	G,G^2,N	L,Tp,W
DH-49B	-33aaa2	39 39 03	118 43 13	1,184.599	.460	4.38-4.84	51	P,Sl	----	W
AH-49C	-33aaa3	39 39 03	118 43 13	1,184.599	.530	1.54-1.85	51	P,Sl	----	W

Table 16. -- Records of test wells (Continued)

Test well number	Location number	Latitude north ° ' "	Longitude west ° ' "	Altitude of land surface above sea level (m)	Height of measuring point above land surface (m)	Depth of screen or cap at bottom (m)	Nominal inside diameter of casing (mm)	Type of completion [1]	Geophysical logs available [2]	Other data available [3]
U.S. Geological Survey test wells										
DH-50A	20/29-8bdc1	39 36 50.1	118 45 25.3	1,190.921	0.457	19.29-20.21	51	P,Sl	G,G^2,N	L,W,Tp
AH-50B	-8bdc2	39 36 50.1	118 45 25.5	1,190.921	.232	2.22-2.53	51	P,Sl	----	W
DH-51A	-6bca1	39 37 43	118 46 41	1 202.930	.518	43.91-44.37	38	St,Sc	G,G^2,N	L,W,Tp
AH-51B	-6bca2	39 37 43	118 46 41	1,201.930	1.073	11.95-12.41	38	St,Sc	----	W
DH-52A	21/28-26bdd1	39 39 28	118 48 18	1,206.959	.335	44.81-45.72	51	P,Sc	G,G^2,N	L,W,Tp
DH-52B	-26bdd	39 39 28	118 48 18	1,206.959	.500	19.86-20.32	38	St,Sc	----	W
DH-53A	-36abd1	39 38 53.5	118 46 51.6	1,199.272	.457	41.92-42.38	51	P,Sc	G,G^2,N	L,W,Tp
AH-53B	-36abd2	39 38 53.5	118 46 51.6	1,199.272	.308	10.51-10.97	38	St,Sc	----	W
DH-54A	21/29-32aab1	39 38 59	118 44 29	1,186.873	.610	44.48	38	St,Sc,c	G,G^2,N	L,Tp
DH-54B	-32aab2	39 38 59	118 44 29	1,186.873	.198	2.97-3.43	51	P,Sl	----	W
DH-55A	-18ddb1	39 40 55	118 45 36	1,186.577	.610	42.22-43.43 44.50	38	St,C,c,P_F	G,G^2,N	L,Tp
DH-55B	-18ddb2	39 40 55	118 45 36	1,186.577	.457	2.09-2.55	51	P,Sl	----	W
AH-55C	-18ddb3	39 40 55	118 45 36	1,186.577	.658	.88-1.49	51	P,Sl	----	W
DH-56A	-16bbb1	39 41 40	118 44 14	1,185.855	.610	42.46-43.68 44.50	38	St,C,c,P_F,	G,G^2,N	L,Tp

Table 16. -- Records of test wells (Continued)

Test well number	Location number	Latitude north ° ' "	Longitude west ° ' "	Altitude of land surface above sea level (m)	Height of measuring point above land surface (m)	Depth of screen or cap at bottom (m)	Nominal inside diameter of casing (mm)	Type of completion [1]	Geophysical logs available [2]	Other data available [3]
U.S. Geological Survey test wells										
DH-56B	-16bbb2	39 41 40	118 44 14	1,185.855	0.381	5.27-5.73	51	P,Sl	-----	W
AH-56C	-16bbb3	39 41 40	118 44 14	1,185.855	.933	22.81-23.27	38	St,Sc	-----	W,Tp
DH-57A	20/29-5bbb1	39 38 08	118 45 34	1,188.129	.655	41.35-42.56 44.43	38	St,C,c,P_F	G,G^2,N	L,Tp
DH-57B	-5bbb2	39 38 08	118 45 34	1,188.129	.427	5.71-6.16	51	P,Sl	-----	W
AH-57C	-5bbb3	39 38 08	118 45 34	1,188.129	.277	1.57-1.88	38	St,Sc	-----	W,Tp
DH-58A	22/29-32ccd1	39 43 26	118 45 05	1,183.048	.506	42.08-43.29 44.11	38	St,C,c,P_F,	G,G^2,N	L,Tp
DH58B	-32ccd2	39 43 26	118 45 05	1,183.048	.488	2.63-3.08	51	P,Sl	-----	W
AH-58C	-32ccd3	39 43 27	118 45 05	1,183.048	.015	1.00	51	P	-----	T,W
DH-59A	21/28-25add1	39 39 33	118 46 38	1,192.993	.579	45.10-45.56	38	St,Sc	G,G^2,N	L,W,Tp
AH-59B	-25add2	39 39 33	118 46 38	1,192.993	.311	4.11-4.87	51	P,Sl	-----	-----
AH-59C	-25add3	39 39 33	118 46 38	1,192.993	.229	6.19-6.65	38	St,Sc	-----	W
DH-60A	21/19-21abd1	39 40 36	118 43 31	1,184.684	.552	41.51-42.73 44.49	38	St,C,c,P_F,	G,G^2,N,	L,Tp
DH-60B	-21abd2	39 40 36	118 43 31	1,184.684	.396	2.65-3.11	51	P,Sl	-----	W
AH-60C	-21abd3	39 40 36	118 43 31	1,184.684	.552	30.22-30.68	38	St,Sc	-----	W,Tp

Table 16. — Records of test wells (Continued)

Test well number	Location number	Latitude north ° ' "	Longitude west ° ' "	Altitude of land surface above sea level (m)	Height of measuring point above land surface (m)	Depth of screen or cap at bottom (m)	Nominal inside diameter of casing (mm)	Type of completion [1]	Geophysical logs available [2]	Other data available [3]
U.S. Geological Survey test wells										
AH-61A	20/28-12bda	39 36 58	118 47 28	1,209	.732	14.26	38	St,C	----	W,Tp
AH-63A	19/28-11abb1	39 31 55	118 48 30	1,213.762	.351	29.09-29.55	38	St,Sc	----	W,Tp
AH-63B	-11abb2	39 31 55	118 48 30	1,213.762	.878	9.35-9.81	38	St,Sc	----	W,Tp
DH-64A	21/29-30ddc1	39 39 07.6	118 45 37.1	----	.000	242.16-244.91 304.8	51	St,C,c,P_F	G(3),G^2, N,R,T(2)	Tp
U.S. Bureau of Reclamation test wells										
DH-10A	20/28-28aca	39 34 21	118 50 31	1,212	1.097	50.26	32	St,C	----	L,Tp
-13A	-32ddd1	39 32 51	118 51 21	1,216.847	.213	14.40-1500	51	P,Sl,c	R,Sp,G,G^2	L,W,Tp
-13B	-32ddd2	39 32 51	118 51 21	1,216.847	.488	152.40-153.31	51	St,Sc,c	----	L,W,Tp
-13C	-32ddd3	39 32 51	118 51 21	1,216.847	.427	66.14-67.06	51	St,Sc,c	----	L,W,Tp,C
-14A	-28cab1	39 34 07	118 51 00	1,213.195	.628	158.50-159.41	51	St,Sc,c	----	L,W,Tp,Cs,C
-14B	-28cab2	39 34 07	118 51 00	1,213.195	.732	12.19-13.11	51	St,Sc	----	W,Tp
Private wells Chevron Resources Co.										
1-29	20/28-29ddb	39 33 51.1	118 51 30.5	1,213	-----	1,309	--	---	----	L,Tp
44-5	19/28-5bdd	39 32 24.9	118 52 01.0	1,215.5	-----	1,538	--	---	----	L
36-78	20/28-33bdb	39 33 26.6	118 50 59.3	1,210	-----	610	--	---	----	L

Table 16. -- Records of test wells (Continued)

Test well number	Location number	Latitude north ° ' "	Longitude west ° ' "	Altitude of land surface above sea level (m)	Height of measuring point above land surface (m)	Depth of screen or cap at bottom (m)	Nominal inside diameter of casing (mm)	Type of completion [1]	Geophysical logs available [2]	Other data available [3]
Private wells										
Chevron Resources Co.										
11-33	-33bbb2	39 33 41.5	118 51 16.3	1,214.5	-----	610	--	---	---	L,Tp
63-33	-33abd	39 33 32.3	118 50 31.2	1,211.9	-----	610	--	---	---	L,Tp
SL-27	19/28-5adb	39 32 38.0	118 51 34.0	1,219	-----	147.5	--	---	---	Tp
-28	-3bbb	39 32 46.8	118 50 08.8	1,213	-----	141.7	--	---	---	Tp
-29	20/28-27ccc	39 33 46.5	118 50 10.2	1,206	-----	143.9	--	---	---	Tp
-30	-29add	39 34 09.2	118 51 24.1	1,213	-----	147.5	--	---	---	Tp
-31	-29bcd	39 34 10.2	118 52 22.5	1,216	-----	152.4	--	---	---	Tp
-32	-31cdd	39 32 51.8	118 53 04.5	1,219	-----	147.5	--	---	---	Tp
-33	19/28-6dad	39 32 13.5	118 52 29.7	1,225	-----	147.5	--	---	---	Tp
-34	-9bcc	39 31 33.7	118 51 17.3	1,218	-----	147.5	--	---	---	Tp
-35	20/28-21bcb	39 35 07.3	118 51 20.6	1,213	-----	147.5	--	---	---	Tp
Kennametals Test Well										
	20/28	39 38 06	18 47 29	1,215	-----	184-191	219	St,O	---	---

[1] St, galvanized-steel pipe; P, polyvinyl chloride (PVC) pipe; Sc, screen or well point at bottom; c, cement seal in annulus (all other holes sealed with drill cuttings and/or surface materials), C, cap at bottom; P_F, gun-perforated; O, open hole.

[2] G, natural gamma log; G^2, gamma-gamma (density) logs; N, neutron log; T, temperature log; R, resistivity log; Co, conductivity.

[3] L, lithologic log; W, water-level measurements; Tp, temperature profile.

Table 17. -- Water-quality data

[Analyses were performed at U.S. Geological Survey Central Laboratories, except as noted]

Well number	Well designation (see text)	Sampling depth below land surface (m)[1]	Sampling depth below water table (m)[1]	Altitude of sampling point (m)[1]	Water temperature (°C)[2]	Date of sample	pH	Specific conductance (micromhos)[3]	Dissolved solids (mg/L)	Silica, dissolved (mg/L as SiO_2)	Calcium, dissolved (mg/L as Ca)	Magnesium, dissolved (mg/L as Mg)	Sodium, dissolved (mg/L as Na)	Potassium, dissolved (mg/L as K)	Bicarbonate (mg/L as HCO_3)[3]	Carbonate (mg/L as CO_3)[3]	Sulfate, dissolved (mg/L as SO_4)	Chloride, dissolved (mg/L as Cl)
U.S. Geological Survey test wells																		
AH-2A	T	26.2	16	1,185.2	31.5	76-05-06	--	4,980	2,740	56	26	9.0	940	100	350	2	22	1,400
-3A	M	43.9	41	1,156.3	24.5	76-05-20	--	1,630	928	29	5.9	1.5	330	23	310	3	38	340
-4A	U	20.4	17	1,199.4	16.5	73-06-27	--	6,950	5,890	47	420	190	1,100	67	150	0	3,500	490
						76-05-04	--	7,170	--	--	--	--	--	--	--	--	--	--
-8A	M	38.4	35	1,177.9	18.0	73-06-27	--	1,030	612	46	1.7	.1	210	8.8	130	2	120	160
						76-04-22	--	1,180	--	--	--	--	--	11	--	--	--	--
						80-03-26	9.03	1,350	809	33	3.2	.5	270	12	110	6	200	230
-9A	M	39.6	30	1,168.2	19.0	73-06-27	--	3,780	2,120	32	5.2	2.7	810	28	390	20	30	990
						76-05-20	--	3,860	--	--	--	--	--	33	--	--	--	--
-10A	M	32.8	30	1,157.0	20.5	78-11-09	8.72	4,200	2,470	35	2.3	1.2	920	20	530	77	170	970
-12A	U	21.9	-12	1,185.0	17.5	76-05-20	--	8,460	4,770	16	33	10	1,700	130	260	4	24	2,700
						78-11-21	8.09	8,800	4,870	28	46	13	1,700	130	280	2	6.3	2,800
-13A	U	21.2	18	1,167.9	20.0	74-08-01	7.84	10,200	5,870	59	89	37	2,000	110	310	0	400	3,000
-18A[8]	M	41.5	-36	1,173.2	18.5	74-08-01	--	--	--	--	--	--	180	8.2	--	--	210	110
DH-29A	M	44.3	38	1,166.8	28.0	76-04-02	--	3,160	1,650	16	23	4.0	560	55	180	0	30	860
						80-04-02	9.18	3,100	1,720	8.8	21	3.9	620	54	230	27	40	830
-30A	T	40.2	39	1,169.4	102.0	76-05-05	--	5,630	3,370	130	100	2.4	1,100	50	180	0	480	1,400
						80-03-28	7.58	5,370	3,320	180	110	2.5	1,000	49	200	0	470	1,400
-31A	T	38.3	33	1,176.3	35.0	76-05-05	--	5,130	2,920	26	53	17	960	74	350	3	300	1,300
-32A	T	44.8	38	1,168.9	56.5	76-05-06	--	7,110	4,090	71	140	17	1,300	90	200	0	450	1,900
						80-03-31	--	--	--	--	--	--	1,300	90	--	--	480	2,000
AH-36A	U	20.9	12	1,191.5	27.5	76-05-06	--	12,800	8,760	68	480	33	2,400	240	210	0	2,200	3,200
						80-04-01	7.56	11,500	7,790	43	370	33	2,200	210	240	0	1,600	3,200
-37A	T	13.4	8	1,198.4	57.5	76-05-06	--	10,000	6,970	130	360	46	1,800	160	310	0	2,500	1,800

Table 17. -- Water-quality data (Continued)

[Analyses were performed at U.S. Geological Survey Central Laboratories, except as noted]

Well number	Well designation (see text)	Sampling depth below land surface (m)[1]	Sampling depth below water table (m)[1]	Altitude of sampling point (m)[1]	Water temperature (°C)[2]	Date of sample	pH	Specific conductance[3] (micromhos)	Dissolved solids (mg/L)	Silica, dissolved (mg/L as SiO_2)	Calcium, dissolved (mg/L as Ca)	Magnesium, dissolved (mg/L as Mg)	Sodium, dissolved (mg/L as Na)	Potassium, dissolved (mg/L as K)	Bicarbonate (mg/L as HCO_3)[3]	Carbonate (mg/L as CO_3)[3]	Sulfate, dissolved (mg/L as SO_4)	Chloride, dissolved (mg/L as Cl)
U.S. Geological Survey test wells																		
DH-41A	M	42.4	33	1,165.8	21.0	76-05-20	--	3,920	2,210	70	18	5.0	750	60	310	3	39	1,100
						80-04-03	8.28	3,890	2.070	78	18	5.4	730	57	310	0	20	1,000
AH-46D	M	16.3	15	1,172.9	16.5	78-11-09	8.33	1,090	694	38	.9	4	250	6.0	350	1	110	110
DH-48A	M	31.2	29	1,158.6	26.5	78-11-06	8.08	3,300	1,900	49	11	4.2	680	25	390	2	110	820
-48B	U	4.3	2	1,185.5	16.5	78-11-20	8.15	5,820	3,450	39	10	5.0	1,300	45	470	3	110	1,700
-49A	M	31.8	--	1,152.8	18.0	78-11-07	8.20	2,710	1,570	43	3.1	1.1	580	12	460	4	130	560
-50A	M	19.8	17	1,170.4	15.5	78-11-07	8.11	2,860	1,580	43	11	7.3	560	30	390	3	34	690
-51A	L	44.1	32	1,158.8	18.5	78-11-06	8.10	4,970	2,770	37	30	16	1,000	49	370	2	42	1,400
-52A	M	45.3	28	1,161.7	21.0	78-11-21	8.11	1,400	785	41	4.4	6	290	9.5	420	3	19	210
-53A	L	42.2	106	1,157.1	24.5	78-11-06	7.90	6,670	3,600	51	20	11	1,300	46	460	7	47	1,900
AH-56C	U	23.0	20	1,162.9	18.0	78-11-08	7.85	8,420	4,690	38	55	19	1,700	61	300	0	250	2,400
DH-58B	U	2.9	2	1,180.1	16.0	78-11-20	8.60	51,500	33,000	17	8.8	1.9	13,000	340	810	133	48	19,000
-59A	L	45.3	41	1,147.7	27.5	78-11-08	8.00	5,590	3,160	74	24	12	1,100	38	440	2	76	1,600
AH-59B	U	4.5	0	1,188.5	13.0	78-11-21	7.32	11,800	6,500	27	11	16	2,600	15	100	0	250	3.400
-60C	M	30.4	28	1,154.3	19.5	78-11-08	8.21	4,430	2,570	45	4.8	.7	970	18	530	4	250	1,000
DH-64A	T	243.8	241	946.7	77.5	81-12-18	7.09	11,700	6,640	125	139	17	2,100	110	220	0	320	3,700
						82-06-10	--	11,100	6,930	120	140	19	2,300	120	210	0	330	3,800
U.S Bureau of Reclamation test wells																		
DH-13C	M	66.6	62	1,150.2	20.0	76-05-04	--	2,030	1,280	18	71	9.1	320	33	100	2	500	270
						80-04-02	--	--	--	--	--	--	340	43	--	--	430	270
-14A[8]	T	159.0	153	1,054.2	144.5	76-07-27	--	8,960	4,990	170	170	.8	1,650	50	110	0	68	2,800
Kennametals private test well																		
----	T	174	160	1,033	36	78-12-12	7.41	9,340	5,550	83	80	23	1,900	120	350	0	240	3,000
Chevron Resources Co. private well																		
1-29	T	286	279	927	186	81-12-18	4.6	6,880	3,780	220	58	36	1,200	130	29	0	62	2,200

Table 17. -- Water-quality data (Continued)

[Analyses were performed at U.S. Geological Survey Central Laboratories, except as noted]

Well number	Date of sample	Fluoride, dissolved (mg/L as F)	Bromide, dissolved (mg/L as Br)	Sulfide, dissolved (mg/L as S)	Nitrogen, ammonia dissolved (mg/L as N)	Nitrogen, nitrite dissolved (mg/L as N)	Nitrogen, nitrate dissolved (mg/L as N)	Arsenic, dissolved (µg/L as As)	Barium, dissolved (µg/L as Ba)[4]	Boron, dissolved (µg/L as B)[4]	Lithium, dissolved (µg/L as Li)	Manganese, dissolved (µg/L as Mn)	Mercury, dissolved (µg/L as Hg)	Rubidium, dissolved (µg/L as Rb)[5]	Strontium, dissolved (µg/L as Sr)[4]	δ^D (per mil)[6]	$\delta^{18}O$ (per mil)[7]
U.S. Geological Survey test wells																	
AH-2A	76-05-06	.8	3.8	--	2.1	.00	.04	37	250	6,400	1,700	--	--	120	980	-109.7	-12.7
-3A	76-05-20	1.6	1.0	--	.56	.01	.00	35	--	3,000	510	--	--	<10	--	-109.9	-15.4
-4A	73-06-27	.5	--	--	--	.00	.01	7	--	3,600	70	--	--	--	--	--	--
	76-05-04	--	2.4	--	2.3	--	--	--	--	3,700	--	--	--	20	--	--	--
-8A	73-06-27	.3	--	--	--	.00	.00	12	--	230	10	--	--	--	--	--	--
	76-04-22	--	.8	--	.73	--	--	--	--	230	--	--	--	10	--	-113.0	-14.4
	80-03-26	.2	--	.0	--	--	--	--	--	230	20	20	.3	--	--	--	--
-9A	73-06-27	2.2	--	--	--	.00	.00	39	--	4,900	340	--	--	--	--	--	--
	76-05-20	2.5	3.3	--	.92	--	--	40	--	4,800	--	--	--	10	--	-111.3	-13.7
-10A	78-11-09	.2	--	--	--	--	--	--	--	13,000	50	--	--	--	--	-110	-13.6
-12A	76-05-20	1.0	8.2	--	3.3	--	.00	6	--	9,100	2,400	--	--	20	--	--	--
	78-11-21	.9	--	--	--	--	--	--	--	8,700	2,600	--	--	--	--	-107	-12.7
-13A	78-11-09	1.4	--	--	--	--	--	--	--	16,000	1,800	--	--	--	--	--	--
-18A[8]	76-07-27	.2	--	--	--	--	--	--	--	350	50	--	--	<20	--	-111.3	-14.6
DH-29A	76-04-02	.6	3.5	--	1.3	.02	.00	2	260	4,200	860	--	--	120	710	-110.8	-13.2
	80-04-02	.5.	--	.1	--	--	--	--	--	4,200	870	20	.4	--	--	--	--
-30A	76-05-04	.6	4.5	--	1.3	.01	.00	30	120	5,800	1,700	--	--	220	2,200	-110.1	-13.7
	80-03-28	.7	--	2.1	--	--	--	--	--	5,900	1,600	130	.3	---	--	--	--
-31A	76-05-05	1.0	4.2	--	.61	.00	.02	1	270	5,900	1,600	--	--	200	1,900	-107.8	-12.8
-32A	76-05-06	.5	8.0	--	1.2	.00	.06	2	240	6,600	2,300	--	--	320	3,300	-107.4	-12.5
	80-03-31	.4	--	.2	--	--	--	--	--	6,300	2,400	10	.3	--	--	--	--
AH-36A	76-05-06	.6	12	--	2.2	.00	.03	5	70	11,900	3,300	--	--	1,000	12,000	-104.3	-12.0
	80-04-01	.6	--	.0	--	--	--	--	--	11,000	2,800	980	.4	--	--	--	--
-37A	76-05-06	.6	6.8	--	1.5	.00	.02	6	70	10,300	2,000	--	--	600	7,300	-102.7	-12.3

Table 17. -- Water-quality data (Continued)

[Analyses were performed at U.S. Geological Survey Central Laboratories, except as noted]

Well number	Date of sample	Fluoride, dissolved (mg/L as F)	Bromide, dissolved (mg/L as Br)	Sulfide, dissolved (mg/L as S)	Nitrogen, ammonia dissolved (mg/L as N)	Nitrogen, nitrite dissolved (mg/L as N)	Nitrogen, nitrate dissolved (mg/L as N)	Arsenic, dissolved (µg/L as As)	Barium, dissolved (µg/L as Ba)[4]	Boron, dissolved (µg/L as B)[4]	Lithium, dissolved (µg/L as Li)	Manganese, dissolved (µg/L as Mn)	Mercury, dissolved (µg/L as Hg)	Rubidium, dissolved (µg/L as Rb)[5]	Strontium, dissolved (µg/L as Sr)[4]	δD (per mil)[6]	$\delta^{18}O$ (per mil)[7]
U.S. Geological Survey test wells																	
DH-41A	76-04-03	1.1	3.8	--	1.9	.02	.01	5	180	5,100	1,300	--	--	60	630	-110.6	-13.3
	80-04-03	1.1	--	.0	--	--	--	--	--	5,300	1,300	70	.1	--	--	--	--
AH-46D	78-11-09	1.2	--	--	--	--	--	--	--	2,300	10	--	--	--	--	-111	-14.6
DH-48A	78-11-06	.5	--	--	--	--	--	--	--	7,200	440	--	--	--	--	-110	-13.9
-48B	78-11-20	3.0	--	--	--	--	--	--	--	8,000	110	--	--	--	--	-108	-13.0
-49A	78-11-07	1.2	--	--	--	--	--	--	--	6,200	30	--	--	--	--	-113	-14.3
-50A	78-11-07	1.3	--	--	--	--	--	--	--	3,900	490	--	--	--	--	-110	-13.9
-51A	78-11-06	.9	--	--	--	--	--	--	--	7,000	1,300	--	--	--	--	-109	-13.3
-52A	78-11-21	1.8	--	--	--	--	--	--	--	2,100	20	--	--	--	--	-111	-14.7
-53A	78-11-06	.4	--	--	--	--	--	--	--	10,000	1,600	--	--	--	--	-108	-12.8
AH-56C	78-11-08	.3	--	--	--	--	--	--	--	13,000	370	--	--	--	--	-102	-11.4
DH-58B	78-11-20	1.6	--	--	--	--	--	--	--	44,000	410	--	--	--	--	- 89	- 8.3
-59A	78-11-08	.2	--	--	--	--	--	--	--	10,000	650	--	--	--	--	-110	-13.4
AH-59B	78-11-21	1.4	--	--	--	--	--	--	--	720	190	--	--	--	--	-106	-12.8
-60C	78-11-08	.5	--	--	--	--	--	--	--	13,000	80	--	--	--	--	-109	-13.3
DH-64A	81-12-18	2.3	--	--	--	--	--	19	--	15,000	1,900	150	1.1	--	--	- 91.5	- 9.1
	82-06-10	2.7	--	--	--	--	--	--	--	--	2,100	140	--	--	--	- 89.5	- 9.5
U.S. Bureau of Reclamation test wells																	
DH-13C	76-05-04	.2	1.2	--	1.0	.01	.02	8	130	570	130	--	--	20	1,100	-112.3	-14.3
	80-04-02	.2	--	.0	--	--	--	--	--	590	150	5	.2	--	--	--	--
-14A[8]	76-07-27	1.9	10	--	--	--	--	150	--	13,500	3,000	170	--	220	--	-107.2	-11.4
Kennametals private test well																	
----	78-12-12	1.3	--	--	--	--	--	--	--	580	1,700	--	--	--	--	-101	-11.5
Chevron Resources Co. private well																	
1-29	81-12-18	1.3	--	--	--	--	--	54	--	9,300	2,300	30	.1	--	--	-108	-11.9

Table 17. -- Water-quality data (Continued)

[Analyses were performed at U.S. Geological Survey Central Laboratories, except as noted]

1/ Indicated sampling depth is mid-point of producing interval.

2/ Indicated wster temperatures were measured at the sampling depth with a down-hole temperature probe, except those for the Kennametals and Chevron Resources wells, which were well-head temperatures.

3/ Specific-conductance, bicarbonate, and carbonate determinations for samples collected in 1973 and 1976 are laboratory values except at well AH-18A.

4/ Barium, boron, and strontium determinations for samples collected in 1976 are from E. A. Jenne (U.S. Geological Survey, written commun., 1977).

5/ Rubidium determinations from R. H. Mariner (U.S. Geological Survey, written commun., 1976).

6/ Data for samples collected in 1976 from Merlivat Laboratories, France. Data for subsequent samples from Nucleares de Saclay, Department of Research and Analysis, Roissy, France.

7/ Data from Geochron Laboaratories, Cambridge, Mass.

8/ Samples were collected by R. H. Mariner, U.S. Geological Survey, and processed in the same manner described by Mariner and others (1975).